Mathematische Modelle zum Parasitenerwerb bei der Onchozerkose des Menschen

Dissertation

der Fakultät für Biologie
der Eberhard Karls Universität Tübingen

zur Erlangung des Grades eines Doktors
der Naturwissenschaften

vorgelegt von

Hans-Peter Dürr
aus Calw
2002

Tag der mündlichen Prüfung: 20. März 2002

Dekan: Prof. Dr. H. - U. Schnitzler

1. Berichterstatter:	Prof. Dr. K. Dietz
	Prof. Dr. H. Schulz-Key
2. Berichterstatter:	Prof. Dr. D. Ammermann
	Prof. Dr. K. - P. Hadeler

INHALT

Teil A1

Teil A2

Teil B1

Teil B2

Mathematische Modelle zum Parasitenerwerb bei der Onchozerkose des Menschen

Einleitung

Die vorliegende Dissertation beschäftigt sich mit der Modellierung, Auswertung und Interpretation von Querschnittsdaten zur Onchozerkose, die vor über 20 Jahren in den afrikanischen Ländern Burkina Faso und Liberia erhoben wurden. Onchozerkose (Flussblindheit) ist die Folge einer Infektion mit dem Parasiten *Onchocerca volvulus*, der wegen einer ausgeprägten Reproduktionsbiologie den Menschen mit einer immensen Zahl von Nachkommenstadien (Mikrofilarien) belastet, starke Hautveränderungen hervorrufen kann und im schlimmsten Fall zur Erblindung des Menschen führt. Die Infektion wird von blutsaugenden Mücken übertragen und die Parasit-Wirt-Beziehung zeigt eine für Parasitosen mit Wirtswechsel typische Komplexität in den Regulationsmechanismen, die auf den Erhalt des Parasiten in der menschlichen Bevölkerung ausgerichtet sind.

Die hier untersuchten Daten entstammen zweier Nodulektomie-Kampagnen, innerhalb derer die in der Haut infizierter Menschen abgekapselnden Parasiten operativ entfernt wurden und somit Schätzwerte für die Parasitenbelastung in der Bevölkerung gewonnen wurden. Eine damalige Hoffnung, die Übertragung der Infektion durch eine einmalige Entfernung des Parasiten aus der menschlichen Population unterbrechen zu können, konnte sich nicht erfüllen, denn man musste feststellen, dass die Fähigkeit des Parasiten, sich durch regulatorische Strategien stabil in seiner Wirtspopulation zu verankern, bei weitem größer ist, als bis dahin angenommen wurde. Dieser Versuch einer Intervention hat jedoch zu einem einzigartigen Datensatz geführt, der durch eine sorgfältige Erfassung der Parasitenlasten Auskunft über die Wechselwirkungen zwischen Parasit und Mensch geben kann.

Ziel dieser Dissertation ist es, durch Anpassung mathematischer Modelle Erkenntnisse über die Parasit-Wirt-Beziehung aus diesem Datensatz zu gewinnen, unter besonderer Beachtung von dichteabhängigen Regulationsmechanismen. Wie in den späteren Kapiteln dargelegt, ist eine Haupterkenntnis dieser Arbeit, dass der Parasitenerwerb entgegen bisheriger Annahmen nicht als konstant, d.h. unabhängig vom Alter und der Parasitenlast des Menschen gesehen werden kann. Vielmehr ist anzunehmen, dass aufgrund einer vom Parasiten induzierten Immunsuppression beim Menschen die Infektionsrate mit zunehmender Parasitenbelastung und daher mit zunehmendem Alter steigt. Diese Art der Dichteabhängigkeit verändert Prognosen zur Stabilität des infektionsfreien Zustandes und wird eine Überarbeitung von Übertragungsmodellen erforderlich machen, die bisher zur Evaluation von Interventionsmaßnahmen bei der Onchozerkose eingesetzt wurden.

Im Folgenden seien zunächst die Eigenschaften der Erkrankung, der Lebenszyklus des Parasiten und klinisches und epidemiologisches Wissen zusammengefasst:

Onchozerkose

Die Onchozerkose des Menschen (Flussblindheit) gehört zu den Filariosen, die durch Fadenwürmer hervorgerufen werden und in tropischen Gebieten große medizinische und sozioökonomische Bedeutung haben (Benton 1998; Burnham 1998). Onchozerkose und die lymphatische Filariose (Elephantiasis) sind die beiden Wurmerkrankungen mit den schwerwiegendsten Folgen für die menschliche Bevölkerung in endemischen Gebieten. Die Weltgesundheitsorganisation zählt die Filariosen zu den sechs wichtigsten parasitären Erkrankungen, deren Erforschung und Bekämpfung Vorrang hat. Filariosen verlaufen chronisch. Bei der Onchozerkose führt die Infektion nicht nur häufig zu Erblindung, sondern durch eine starke Immunsuppression und durch schwerste Onchodermatitiden zu einem schlechten Allgemeinzustand, wodurch die ohnehin niedrige Lebenserwartung in den betroffenen Ländern um durchschnittlich 10 Jahre reduziert wird (Duke 1990; WHO 1995). Wegen der besonderen Brutbiologie können sich die Larven der Überträgermücken nur in schnell fließenden Gewässern entwickeln. Die Parasitose kommt daher entlang der landwirtschaftlich nutzbaren Flussläufe vor, was die wirtschaftliche Entwicklung in den trockenen Savannenländern stark behindert hat. Nach Einschätzung der WHO ist die Onchozerkose der wichtigste Faktor, der einer erfolgreichen Entwicklung der Landwirtschaft entgegensteht.

Geografische Verbreitung

Onchozerkose ist in 26 Staaten Afrikas und in 6 Regionen Lateinamerikas endemisch (Abb. 1) und die Zahl der Menschen, die dem Infektionsrisiko ausgesetzt sind, beläuft sich weltweit auf ca. 120 Millionen. Die Zahl der mit dem Parasiten infizierten Menschen wird auf ca. 17.7 Millionen geschätzt, 99% davon leben allein in Afrika. Die Zahl der durch Onchozerkose Erblindeten wird auf 270 000 geschätzt und weitere 500 000 leiden unter einer starken Beeinträchtigung der Sehfähigkeit. Diese Zahlen unterschätzen nach Angaben der WHO jedoch das wahre Ausmaß noch, da es sich nur um die offiziell gemeldeten Fälle handelt (WHO 1995).

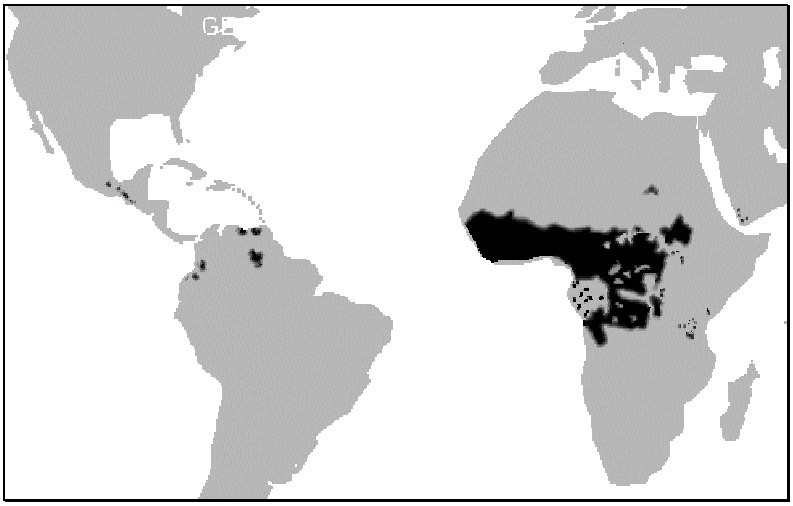

Abb. 1: Geografische Verbreitung der Onchozerkose

Der Lebenszyklus des Parasiten *Onchocerca volvulus*

Die adulten Weibchen des Parasiten *O. volvulus* sind 20-50 cm lang bei einem Durchmesser von ca. 0.4 mm. Sie knäueln sich bevorzugt im Unterhautbindegewebe des Menschen auf und bilden einen Knoten, das Onchozerkom, das von einer Kapsel mit wirtseigenem Bindegewebe umgeben ist. Knoten können sich auch in tieferen Gewebsschichten befinden, in seltenen Fällen liegen sie sogar dem Knochengewebe auf. Es können sich mehrere Weibchen in einem Knoten zusammenlagern, der dann die Größe einer Walnuss erreichen und äußerlich ertastbar (palpierbar) sein kann. Weibliche *O. volvulus* haben eine Lebenserwartung von 9-14 Jahren und produzieren Millionen von Mikrofilarien, die in die oberflächlichen Schichten der Haut auswandern, ca. ein Jahr lebensfähig sind und von der blutsaugenden Mücke aufgenommen werden. Die Männchen sind sehr viel kleiner (2.5-5 cm lang, 0.15 mm dick), haben eine Lebenserwartung von ein bis zwei Jahren und können, im Gegensatz zu den sessilen Weibchen, zwischen den Knoten wandern (Schulz-Key, 1990).

Zwischenwirte sind ausschließlich Mücken der Gattung *Simulium* (Kriebelmücken). Durch eine Blutmahlzeit nehmen sie Mikrofilarien aus der Haut auf; diese durchbrechen nach der Ingestion die Darmwand der Mücke und wandern von deren Hinterleib über den Thorax in die Kopfkapsel ein. Die Entwicklung in der Mücke ist mit drei Häutungen verbunden (Larvenstadien L1, L2, L3) und nach sechs bis sieben Tagen abgeschlossen. Die in der Kopfkapsel angekommenen infektiösen Larven (L3) können bei der nächsten Blutmahlzeit der Mücke auf einen Menschen übertragen werden. In diesem entwickelt sich nach einer erneuten Häutung zur vierten Larve (L4) im Laufe eines Jahres wieder ein adulter Parasit heran.

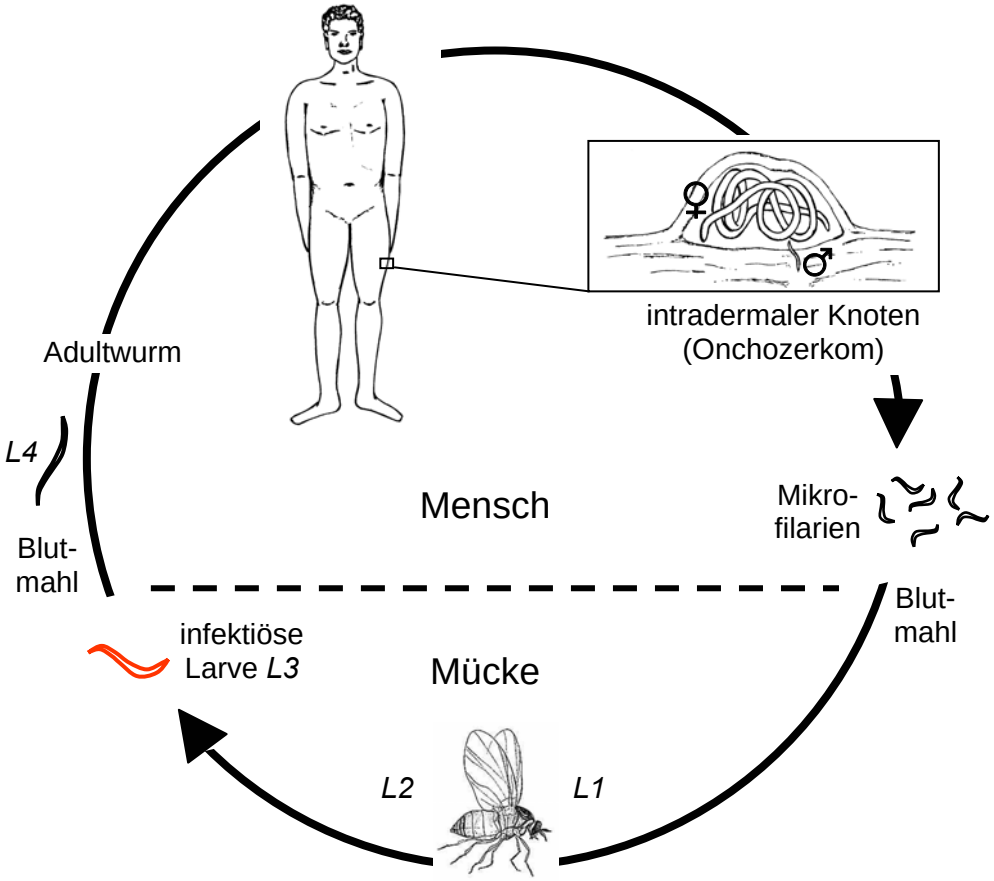

Abb. 2: Der Lebenszyklus des Parasiten *Onchocerca volvulus*

Klinische Aspekte

Onchozerkose beeinträchtigt den Menschen in erster Linie durch die vom adulten Weibchen in Massen produzierten Mikrofilarien, die aus den Knoten in die Haut ausschwärmen. Bei sehr starkem Befall sind Mikrofilarien auch in tiefer gelegenen Gewebsschichten oder Organen, selten auch im Blut zu finden. Die Pathologie ist eng verknüpft mit dem Absterben der Mikrofilarien und dem Ausmaß der menschlichen Immunreaktion. Demnach werden drei Reaktionstypen unterschieden (Maizels & Lawrence 1991; Ottesen 1984), wenngleich die Übergänge auch fließend sein können: Den Fällen mit starker Pathologie liegt meist eine ausgeprägte Immunabwehr zugrunde, infolge derer es zu Entzündungsreaktionen in der Haut kommt. Dies führt bei den Betroffenen zu oft unerträglichem Juckreiz, zur Degeneration und Depigmentierung der Haut. In den meisten Patienten ist die Immunantwort jedoch vermindert, es

entwickelt sich eine Art Toleranz gegenüber dem Parasiten, die anfänglich mit einer verminderten Pathologie, jedoch oft hohen Mikrofilariendichten einhergeht. Beim dritten, jedoch sehr seltenen Reaktionstyp finden sich weder hohe Mikrofilariendichten noch eine ausgeprägte Pathologie. Diese sog. putativ Immune (Ward et al. 1988), die es auch in stark endemischen Gebieten gibt, weisen eine noch nicht verstandene Resistenz gegenüber der Infektion auf. Die schlimmste Komplikation bei der Onchozerkose ist Erblindung, verursacht durch Mikrofilarien, die in den Augenapparat einwandern und infolge des Absterbens entweder die Augenlinse trüben oder zu Augenläsionen führen. In stark endemischen (hyperendemischen) Regionen kann der Anteil der Erblindeten 10-20% der Bevölkerung betragen und vereinzelt wurden Dörfer gefunden, in denen 50% der über 30-jährigen erblindet waren.

Immunepidemiologie

Immunepidemiologisch relevante Variablen der Onchozerkose sind Prämunität, Crowding und Immunopriming. Ein entscheidender immunologischer Faktor für die Regulierung der Adultwurmlast ist eine Prämunität (concomitant immunity). Sie erschwert oder unterbindet eine Entwicklung von Larven, die auf einen bereits infizierten Wirt treffen (Barthold & Wenk 1992; Geiger et al. 1996). Ein zu starker Befall mit adulten Filarien, der sowohl dem Parasiten als auch dem Wirt schaden würde, wird durch diese Prämunität vermieden. Mechanismen der Regulierung der Dichte der Mikrofilarien in der Haut, die durch die Weibchen freigesetzt werden, sind bisher unzureichend bekannt. Für die Ausbildung der Mikrofilarien in den Uteri der Weibchen und deren Freisetzung gibt es Rückkopplungsmechanismen und Kompensationen bei niedriger oder sehr hoher Adultwurmlast, wie dies u.a. beim Crowding deutlich wird (Schulz-Key 1990). Der Parasit kann das Überleben der Mikrofilarien in der Wirtspopulation auch dadurch sichern, dass Mikrofilarien diaplazentar auf Embryos übergehen. Im Embryo werden die Antigene als "körpereigen" definiert, weil sich das Immunsystem in der Prägungsphase befindet. Dieses Immunopriming induziert eine Art Toleranz, die während späterer Infektionen im Kindes- und Erwachsenenalter zu einer verminderten Abwehr gegen Mikrofilarien führt (Soboslay et al. 1999). Die "Ivermectin-facilitated immunity" ist ein Phänomen, das nach Behandlung mit dem Medikament Ivermectin auftritt: infolge der reduzierten Parasitenlast, wird die immunologische, zelluläre Anergie allmählich umgekehrt und die Immunkompetenz des Menschen verbessert (Schulz-Key et al. 1992; Soboslay et al. 1994). Dies weist auf eine durch den Parasiten induzierte Immunsuppression hin, die hinsichtlich der Pathologie sogar von Vorteil für den Wirt sein kann (s.o.).

Bekämpfung der Onchozerkose

Seit 1974 gibt es ein von der WHO ins Leben gerufenes und von der Weltbank finanziertes Bekämpfungsprojekt in Westafrika, das Onchocerciasis Control Programme (OCP[1]). Erklärtes Ziel dieser Maßnahme war es, die Übertragung des Parasiten durch regelmäßiges Einleiten von Insektiziden in die Brutplätze der Überträgermücken in den Flüssen so lange zu unterbinden, bis die Parasitenpopulation überaltert und ausgestorben sein würde. Diese Intervention, die aufgrund der Langlebigkeit der Parasiten (9-14 Jahre) zunächst auf eine Dauer von 20 Jahren angesetzt war, ist sehr erfolgreich verlaufen (Hougard et al. 1997). Wegen des großen logistischen Aufwandes und der hohen Kosten wird die Organisation des Fortführungsprogrammes APOC[2] (African Programme for Onchocerciasis Control) derzeit den lokalen Behörden in Afrika übertragen. Damit verbunden ist auch die Umstellung auf eine neue, einfachere Bekämpfungsstrategie, die durch das in den 80er Jahren für die Behandlung der Onchozerkose freigegebene Medikament Ivermectin möglich wird. Ivermectin tötet die Mikrofilarien sehr effektiv ab, wobei eine ein- bis zweimalige Einnahme pro Jahr ausreicht (Awadzi et al. 1985; Ette et al. 1990).

Obwohl die Elimination der Onchozerkose in über elf Ländern Afrikas erreicht wurde (Hougard et al. 1997), gibt es immer noch Regionen, in denen Onchozerkose aufgrund von geografischer Unzugänglichkeit, Bürgerkriegsunruhen o.a. Ursachen unbekämpft blieb und weiterhin endemisch ist. Aus diesen Regionen kann die Infektion wieder importiert werden, sei es durch Wanderarbeiter oder durch die Überträgermücken, die weite Strecken überwinden oder passiv mit dem Wind verdriftet werden können. Dadurch entsteht die Frage, wie stabil der infektionsfreie Zustand in der post-Interventionszeit ist, bzw. wieviel importierte Infektion er verkraften kann, ohne in den ursprünglichen Grad der Endemizität zurückzufallen. Da nicht alle Regionen medizinisch versorgbar sind und es in Entwicklungsländern schwierig ist, alle Personen für Medikations-Kampagnen zu erfassen, wird auch die Beteiligungsquote (Anteil der Bevölkerung, der von der Behandlung mit Ivermectin erreicht wird) eine entscheidende Rolle für die zukünftigen Erfolge bei der Bekämpfung der Onchozerkose spielen. Mathematische Modelle, welche die Infektions- und Übertragungsdynamik zu beschreiben vermögen, können hier helfen, zukünftige Entwicklungen oder Gefahren vorherzusagen und effiziente Bekämpfungsstrategien zu planen.

[1] http://www.who.int/ocp/index.htm

[2] http://www.who.int/ocp/apoc/

Mathematische Modelle zur Onchozerkose

Das erste auf Daten basierte Onchozerkosemodell wurde von Dietz (1982) entwickelt. Die Modellanpassung erforderte Annahmen über dichteabhängige Regulationen sowohl im Vektor als auch im menschlichen Wirt. Das Modell ist nach Wirtsalter strukturiert und erlaubt es, den Effekt der damals einzig verfügbaren Kontrollmaßnahme, nämlich der Vektorkontrolle, zu evaluieren. Das Modell sagte voraus, dass unterhalb einer annual biting rate (ABR, jährliche Zahl von Mückenbissen pro Mensch) von etwa 300 keine stabile Übertragung der Onchozerkose möglich ist. Vom OCP wurde später ein stochastisches Simulationsmodell in Auftrag gegeben, das von J.D.F. Habbema et al. unter dem Namen ONCHOSIM veröffentlicht wurde (Habbema et al. 1992; Plaisier et al. 1990). Die dichteabhängige Regulation der Parasitenpopulation wird hier jedoch ganz auf die Phase im Übertragungsvektor beschränkt. Weitere Transmissionsmodelle zur Onchozerkose sind in der Arbeit von Basáñez & Ricardez-Esquinca (2001) zusammengefasst.

ERGEBNISSE DER DISSERTATION

Die Ergebnisse dieser Dissertation sind in Form von vier Manuskripten zusammengefasst, von denen die ersten beiden bereits veröffentlicht und die letzten beiden zur Veröffentlichung eingereicht sind. Die Arbeiten sind thematisch in die Teile A und B gegliedert, wobei das jeweils zuerst aufgeführte Manuskript (A1, B1) das zugrunde liegende mathematische Modell bzw. die Methodik beschreibt und das jeweils nachfolgende Manuskript (A2, B2) die biologische Anwendung mit den aus dem Datensatz gewonnenen Erkenntnissen. Diese Reihenfolge entspricht auch der chronologischen Entstehung, woraus sich der biologische Zusammenhang aller vier Arbeiten wie folgt ergibt:

Wie im vorhergehenden Kapitel "Der Lebenszyklus des Parasiten *O. volvulus*" beschrieben, kapselt sich der weibliche Parasit bevorzugt im Unterhautbindegewebe ab, wobei sich mehrere Weibchen in einem solchen Knoten (Onchozerkom) zusammenfinden können. Es wird angenommen, dass die Zahl der durch Palpation (Tastuntersuchung) feststellbaren Onchozerkome die wahre Zahl der Onchozerkome, also einschließlich der in tieferen Gewebsschichten unerkannt gebliebenen Onchozerkome, zu repräsentieren vermag. Da einerseits die Zahl adulter Weibchen pro Wirt die Zielgröße der späteren Untersuchungen ist und andererseits der Datensatz aufgrund des Palpationsbefundes Verzerrungen enthält (s. B2), müssen zunächst Verteilungen für die Zahl der Knoten pro Wirt und für die Zahl adulter Weibchen pro Knoten ermittelt werden. Dies ist das Hauptanliegen der Veröffentlichung A1, wo ein auf Partitionen basierendes Gruppierungsmodell entwickelt wird. Dieses wird in der Veröffentlichung A2 dazu verwendet, den Knotenbildungsprozess von *O. volvulus* zu beschreiben und artspezifische Schätzwerte für das Gruppierungsverhalten des Parasiten zu ermitteln.

Die Vorarbeiten der erstgenannten Veröffentlichungen gehen ein in das Manuskript B2, das den biologischen Schwerpunkt der Dissertation bildet: anhand von Computer-Simulationen wird die Studie und damit die Entstehung der Daten inklusive der zuvor erwähnten Verzerrungen nachgestellt. Es kann auf diese Weise gezeigt werden, dass für den Parasitenerwerb bei der Onchozerkose dichteabhängige Regulationsprozesse gefordert werden müssen. Dieses Resultat ergibt sich aus der Falsifizierung anderer, in Frage kommender Prozesse, die den Parasitenerwerb ebenfalls modulieren können. Eine allgemeine Beschreibung dieser Prozesse und die Gründe für deren Ausscheiden findet sich im Manuskript B1.

Die Inhalte der einzelnen Arbeiten lassen sich wie folgt zusammenfassen:

Teil A1:

Stochastic models for aggregation processes beschreibt stochastische Modelle, wie sie für das Gruppierungsverhalten des Parasiten formuliert werden müssen. Die Modelle bauen hierarchisch auf einem Parameter *q* auf, der die Wahrscheinlichkeit angibt, mit der ein Objekt (ein Parasit) eine neue Gruppe (ein Onchozerkom) bildet. Anhand eines Partitionsprozesses lässt sich über diesen Parameter eine binominalverteilte Gruppenanzahl pro Habitat (Anzahl der Knoten pro Mensch) vorhersagen. Es wird daraus eine neue Verteilung für die Zahl der Objekte pro Gruppe (Zahl der Parasiten pro Knoten) hergeleitet und gezeigt, dass sie gegen eine geometrische Verteilung konvergiert, wenn die Zahl der Objekte im Habitat gegen Unendlich strebt. Im Hinblick auf die Datenanpassung sind varianzerhöhende Annahmen erforderlich, so dass das Modell durch zwei Varianten erweitert wird. Einerseits lässt sich annehmen, dass die Bildungswahrscheinlichkeit *q* zwischen den Wirten gemäß einer Betaverteilung streut, andererseits könnte es auch möglich sein, dass *q* von der Gruppengröße abhängt. Trotz der Unterschiedlichkeit dieser Annahmen konvergieren beide Modelle zu einer Waring-Verteilung für die Zahl der Objekte pro Gruppe, wenn die Zahl der Objekte im Habitat gegen Unendlich strebt. Theoretisch ist also aufgrund einer zu fordernden, zusätzlichen Variabilität nicht entscheidbar, ob die Varianz durch eine gewichtete Gruppenattraktivität oder durch eine streuende Bildungswahrscheinlichkeit erklärt werden muss.

Teil A2:

A stochastic model for the aggregation of Onchocerca volvulus in nodules ist die Anwendung des in A1 beschriebenen Modells auf den Knotenbildungsprozess von *O. volvulus*. Die aus den Daten geschätzte mittlere Bildungswahrscheinlichkeit von μ_q=0.4 lässt darauf schließen, dass eine weibliche Larve 4 (L4) während ihrer etwa einjährigen Entwicklung zum adulten Parasiten eher dazu tendiert, in ein bereits bestehendes Onchozerkom einzuwandern als ein neues Onchozerkom zu bilden. Die biologische Begründung hierfür ist unklar und wirft die Frage auf, ob der weibliche Parasit durch die Tendenz zur Aggregation einen Vorteil erlangt. Das Modell wird basierend auf einer heterogenen Bildungswahrscheinlichkeit angepasst und es ist nicht entscheidbar, ob die alternative Erklärung, gegeben durch eine mit der Knotengröße zunehmende Attraktivität gegenüber einer L4 (s.o.), nicht auch zutreffen kann. Ungeachtet dieses verbleibenden Erklärungsbedarfs sind damit die Verteilungen für die Zahl der Knoten pro Wirt und für die Zahl adulter weiblicher Parasiten pro Knoten charakterisiert und können in der unter B2 dargestellten simulationsbasierten Schätzung des Parasitenerwerbs implementiert werden. Wichtige Anwendungen findet das für den Knotenbildungsprozess von *O. volvulus* entwickelte Modell in der Diagnostik und der retrospektiven Auswertung von Palpationsdaten, da nun von der Zahl palpierter

Knoten auf die zu erwartenden Verteilungen der Parasitenlasten geschlossen werden kann. Diese Möglichkeit zur Extrapolation wird ein wichtiges Werkzeug für die Auswertung weiterer Palpationsdatensätze werden, deren Informationsgehalt bislang, trotz oft großer Stichprobenumfänge, nur selten ausgeschöpft wird (s. Ausblick).

Teil B1:

The interpretation of age-intensity profiles and dispersion patterns in parasitological surveys ist eine Übersicht zu Regulationsmechanismen und deren Einfluss auf die Verteilungen von Parasitenlasten, wie man sie aus Querschnittsuntersuchungen erhält. Im Einzelnen handelt es sich um die Darstellung der Prozesse i) altersabhängige Exposition, ii) parasiten-induzierte Wirtsmortalität, iii) Heterogenität in der Wirtspopulation, iv) "geklumpte" Infektion, v) dichteabhängige Parasitensterblichkeit und vi) dichteabhängiger Parasitenerwerb, wie er in B2 modelliert wird. Die Arbeit liefert einen Beitrag zu den in den letzten Jahren aufgekommenen Bestrebungen, von aus Querschnittsdaten erhaltenen Streuungsmustern in den Parasitenlasten auf zugrunde liegende Regulationsmechanismen schließen zu wollen. Die für die einzelnen Mechanismen charakteristischen Querschnittsprofile werden gezeigt, gleichwohl wird darauf hingewiesen, dass die Mehrdeutigkeit in der Interpretierbarkeit dieser Profile stark zunimmt, wenn unterschiedliche Mechanismen zusammenwirken. Zur Überprüfbarkeit entsprechender Hypothesen wird ein Computerprogramm bereitgestellt, das Querschnittsprofile für eine beliebige Kombination von Prozessen bei frei zu wählenden Parameterwerten und Stichprobengrößen simulieren kann. Wichtige Erkenntnisse dieser Arbeit betreffen den Mechanismus der parasiten-induzierten Wirtsmortalität. Es wird gezeigt, dass diese, entgegen der Behauptung mancher Feldstudien, praktisch nicht in Querschnittsdaten entdeckt werden kann, es sei denn, es liegt eine ausgeprägte Heterogenität in der Wirtspopulation vor. Die vergleichende Darstellung aller sechs Prozesse zusammen mit dem Computerprogramm sollen den praktisch arbeitenden Parasitologen darin unterstützen, *a priori* Wissen und Hypothesen an vorliegenden Daten messen zu können. Die Arbeit zeigt ferner auf, dass für die Erklärung der im nachfolgenden Manuskript gezeigten Daten keiner der fünf bislang bekannten Mechanismen geeignet ist. Die Tendenz der mittleren Parasitenlast ließe sich nur erklären, wenn eine unrealistische Form der altersabhängigen Exposition angenommen wird. Der alternativ in dieser Arbeit erstmals vorgestellte Prozess des dichteabhängigen Parasitenerwerbs mit positiver Rückkoppelung erklärt darüber hinaus die vorliegenden Streuungsmuster optimal, vor allem das Auftreten sehr geringer Parasitenlasten in älteren Patienten.

Teil B2:

Density-dependent parasite establishment suggests infection-associated immunosuppression as an important mechanism for parasite density regulation in onchocerciasis inkorporiert die Ergebnisse der zuvor verfassten Arbeiten und beschreibt die biologisch wichtigste Erkenntnis der Dissertation. Die hier geschilderten Ergebnisse werden durch eine Methodik erhalten, die bislang nur in ihrer theoretischen Machbarkeit vorgestellt wurde. Hierbei handelt es sich um die simulationsbasierte Maximum-Likelihood Schätzung, die eine äußerst flexible Modellanpassung ermöglicht. Diese wird darüber hinaus optimiert, indem nicht nur die theoretische Entstehung der Querschnittsdaten sondern auch die Eigenheiten und Verzerrungen des Studiendesigns simuliert werden. Die entsprechende Vorgehensweise ist im Appendix zu B2 erklärt. Die altersabhängigen Verteilungen der Parasitenlasten, wie sie in den Nodulektomie-Kampagnen in Burkina Faso und Liberia gefunden wurden, verlangen die Annahme eines mit dem Alter zunehmenden Parasitenerwerbs. Üblicherweise wird dies durch eine mit dem Alter zunehmende Exposition erklärt (s. B1). Eine unter dieser Hypothese zuerst durchgeführte Schätzung anhand der Daten ergab jedoch, dass die Exposition linear mit dem Alter zunehmen müsse - ein Ergebnis, das der Beobachtung widerspricht.

Die Lösung dieses Problems besteht in der Annahme, dass die Zahl der pro Zeit erworbenen Parasiten nicht mit dem Alter, sondern mit der Parasitenlast selbst, zunimmt. Dies stellt einen autokatalytischen Prozess dar, der aufgrund seiner positiven Rückkopplung in biologischer Hinsicht nicht nahe liegend ist, vor allem nicht, weil im klassischen Ansatz eher mit zunehmender Resistenz als mit zunehmender Suszeptibilität gegenüber dem Erreger gerechnet wird. Im Fall der Onchozerkose jedoch ist die biologische Ursache für einen solchen autokatalytischen Prozess durch experimentelle Arbeiten bekannt, die eine infolge der Parasitenbelastung abnehmende Resistenz des Wirtes gefunden haben. Ein derartig dichteabhängiger Parasitenerwerb kann hinsichtlich seines Einflusses bei bestehenden Interventionskampagnen in endemischen Ländern Afrikas von den bisherigen Modellen oder Simulationsprogrammen zur Übertragung und Bekämpfung von Onchozerkose nicht evaluiert werden. Es ist jedoch anzunehmen, dass dieser Mechanismus die Bekämpfung des Parasiten erleichtert, weil die interventionsbedingte Steigerung der Immunkompetenz in der Bevölkerung unterstützend wirkt. Zukünftige Modelle sollten hier untersuchen, ob der Einfluss des dichteabhängigen Parasitenerwerbs wieder Anlass zur Hoffnung gibt, dass Onchozerkose eine eliminierbare und nicht nur kontrollierbare Erkrankung ist (s. Ausblick).

DISKUSSION ZUR GESAMTEN ARBEIT

Die in Kapitel B2 zusammengefassten Ergebnisse zeigen, dass die bisherige Annahme eines im Lauf des Lebens konstant bleibenden Parasitenerwerbs bei der Onchozerkose nicht aufrecht erhalten werden kann. Ein konstanter Parasitenerwerb würde die Parasitenlast von Kindern stark überschätzen und das Gleichgewicht würde sich, ebenfalls entgegen der Beobachtung, schon ab einem Wirtsalter von etwa 20 Jahren einstellen (s. auch B1). Die Erklärung der Daten erfordert also einen regulatorischen Einfluss, der zu einem *verzögerten* Parasitenerwerb, und so zu einer nur langsam über das Alter ansteigenden Parasitenlast führt. Es sind nur drei Prozesse bekannt, die einen solchen verzögernden Einfluss bereitstellen können, diese lauten i) eine mit dem Alter zunehmende *Exposition*, ii) eine mit dem *Alter* abnehmende Fähigkeit, den Parasiten immunologisch zu kontrollieren (hohe Resistenz in Kindern) oder iii) eine mit der *Parasitenlast* abnehmende Fähigkeit, den Parasiten immunologisch zu kontrollieren (hohe Resistenz in Nichtinfizierten). Von diesen Prozessen scheidet die altersabhängige Exposition (i) aus, weil die Datenanpassung sie als linear mit dem Alter zunehmend fordert - eine Annahme, die aus praktischer Sicht verworfen werden muss. Für eine sich allein infolge des Älterwerdens veringernde Resistenz (ii) gibt es keine experimentellen Befunde. Demgegenüber stehen viele Arbeiten zum immunsuppressiven Einfluss des Parasiten, was zu einer mit der Parasitendichte abnehmenden Immunkompetenz führt (iii) (zusammengefasst in Maizels & Lawrence 1991). Parasiteninduzierte Immunsuppression wurde nicht nur bei der Onchozerkose (Cooper et al. 2001; Elkhalifa et al. 1991; Soboslay et al. 1994), sondern auch auch bei der lymphatischen Filariose nachgewiesen (Piessens et al. 1980) und es wird diskutiert, ob es sich dabei um eine Eigenschaft der meisten Nematoden handeln könnte (Allen & MacDonald 1998).

Im hier verwendeten Modell zum Parasitenerwerb bei der Onchozerkose wird die Dichteabhängigkeit aus der Zahl adulter, weiblicher *O. volvulus* abgeleitet. Dies entspricht der Annahme, dass Immunsuppression allein durch dieses Parasitenstadium induziert werden kann. Beim gegenwärtigen Kenntnisstand kann nicht entschieden werden, zu welchem Anteil dei anderen Parasitenstadien zur Immunsuppression beitragen. Die "Ivermectin-facilitated immunity" (Schulz-Key et al. 1992; Soboslay et al. 1994) weist auf einen Zusammenhang mit den Mikrofilarien hin, andererseits ist aus dem Tiermodell bekannt, dass ein einziger Adultparasit ausreichen kann, um resistente Tiere suszeptibel zu machen (Hoffmann et al. 2001). Das mathematische Modell repräsentiert beide Annahmen gleichermaßen, wenn angenommen wird, dass die Mikrofilariendichte proportional der Dichte adulter Parasiten ist und sich der Einfluss daher nur durch einen Proprotionalitätsfaktor unterscheidet.

Eine überraschende Feststellung bei der Datenschätzung ist, dass der Parasitenerwerb im hyperendemischen Bereich nahezu unabhängig vom

Übertragungsdruck (ATP, annual transmission potential) ist (das ATP beziffert die durch Mücken jährlich übertragene Zahl infektiöser Larven). Es bedarf offenbar nur eines geringen Übertragungsdrucks, um die Infektion endemisch zu halten; ein darüber hinausgehender Übertragungsdruck steigert die Endemizität nicht und die Übertragungsdynamik wäre folglich nicht proportional dem ATP. Dieser Befund steht im Einklang mit dem Konzept der "concomitant immunity" (Immunität gegenüber den invasiven Stadien eines Parasiten, hier die infektiöse Larve L3), die auch für Filariosen nachgewiesen wurde (Barthold & Wenk 1992; Day et al. 1991). Diese Immunität muss jedoch als kurzlebig angenommen werden, damit höhere Parasitenlasten erklärbar sind. Wichtig ist auch, zu bemerken, dass den ATP-Werten von hunderten oder sogar tausenden infektiösen Larven pro Jahr und Mensch eine Erwerbsrate von maximal fünf adulten Parasiten pro Jahr gegenübersteht. Der Mensch ist also in der Lage, den größten Teil der ihn bedrohenden Infektiosität neutralisieren zu können.

Die beobachteten, altersabhängigen Parasitenlasten müssen demnach wie folgt interpretiert werden: Der Mensch besitzt - natürlicherweise oder erworbenerweise - eine ausgeprägte immunologische Kompetenz zur Abwehr des Parasiten. Nur dies kann die im Mittel sehr geringen Parasitenlasten in Kindern und Jugendlichen begründen. Kann sich jedoch (während der ersten Lebensjahre) ein Parasit erfolgreich im Menschen etablieren, so wird diese Immunkompetenz geschwächt und es verkürzt sich infolgedessen die Zeit bis zur nächsten Infektion. Diese nur graduelle Zunahme im Parasitenerwerb pro Zeiteinheit führt zu einem Verzögerungsprozess, so dass die Parasitenlast über das Alter nur langsam zunimmt. Bei der Waldform der Onchozerkose (Liberia) stellt sich kein Gleichgewicht ein, während dies bei der Savannenform (Burkina Faso) ab einem Wirtsalter von ca. 50 Jahren erkennbar ist.

Dichteabhängiger Parasitenerwerb infolge von parasiteninduzierter Immunsuppression sollte den Erfolg von Interventionsmaßnahmen nachhaltig unterstützen. Wie im Fall der "Ivermectin-facilitated immunity" (s.o.) sollte die interventionsbedingte Reduzierung der Parasitenlast zu einer verbesserten Immunkompetenz in der Bevölkerung führen und das Risiko von Re-Infektionen verringern. Das Onchocerciasis Control Program (OCP, s.o.) hat bereits zu Beobachtungen geführt, die durch diesen Regulationsmechanismus erklärt werden können. Dies betrifft z.B. die unerwartet schnelle Abnahme in den Mikrofilariendichten in der Bevölkerung (Remme et al. 1990) ebenso wie den stabil infektionsfreien Zustand nach einer Interventionskampagne (Hougard et al. 2001). Darüberhinaus ist es auch möglich, dass ein verbesserter Immunstatus dem Menschen hilft, noch vorhandene Parasiten schneller zu eliminieren (Soboslay et al. 1997) oder deren Reproduktivität zu schwächen (Karam et al. 1987).

AUSBLICK

Das Vorliegen eines dichteabhängigen Parasitenerwerbs bei der Onchozerkose lässt neue Fragen hinsichtlich der immunologischen Vorgänge im Menschen aufkommen und erfordert ein Überarbeiten der bisherigen Modelle zur Evaluation von Bekämpfungsmaßnahmen bei der Onchozerkose. Die in Kindern bzw. Nichtinfizierten zu findenden, niedrigen Parasitenlasten offenbaren das große Potential an immunologischer Kompetenz des Menschen gegenüber dem Parasiten und es sollte weiter untersucht werden, ob dieser Abwehrmechanismus auf einer angeborenen oder erworbenen Immunität beruht. Vor allem die Rolle und Tragfähigkeit der "concomitant immunity" könnte zu einem Schlüssel in der Bekämpfung der Onchozerkose werden. Die hier dargestellten Ergebnisse zeigen auch, dass die Erforschung von dichteabhängigen Regulationsprozessen eine große Voraussetzung für das Verständnis der Parasit-Wirt-Interaktion ist. In Ergänzung zu dieser Arbeit ist der wichtigste, nächste Schritt die Untersuchung von Dichteabhängigkeiten im Reproduktionsverhalten von *O. volvulus*. Diese kann sich sehr negativ auf den Erfolg von Interventionskampagnen auswirken, wenn bereits geringe Anzahlen adulter Parasiten ausreichen, um hohe Mikrofilariendichten im Menschen herbeizuführen.

Diese Art der Dichteabhängigkeit ist im vorliegenden Datensatz bereits erkennbar; zur geplanten Untersuchung dieser Hypothese ist jedoch die Hinzunahme weiterer Datensätze erforderlich. Die in A2 gewonnen Erkenntnisse sollen in Zukunft dazu verwendet werden, die in großen Stichprobenumfängen verfügbaren Palpationsdatensätze in solche Analysen einbinden zu können. Für den dichteabhängigen Parasitenerwerb haben Vorarbeiten an einem deterministischen Transmissionsmodell ergeben, dass dieser Prozess zu Schwellenphänomenen in der Übertragung der Onchozerkose führt. Demnach sollten sich für die einzelnen Variablen im Übertragungszyklus - also z.B. für das ATP oder für die Mückendichten - Schwellenwerte bestimmen lassen, unterhalb derer die Übertragungsdynamik der Infektion zusammenbricht. Im Rahmen einer Fortsetzung des Projektes ist daher geplant, solche Schwellen zu quantifizieren und weitergehende Untersuchungen durchzuführen mit dem Ziel, den bisherigen Erfolg bei der Bekämpfung der Onchozerkose mit mathematischen Modellen und daraus abgeleiteten Empfehlungen und Prognosen zu stützen.

Stellungnahme zum Eigenanteil an den vorgelegten Publikationen/Manuskripten:

Die Ergebnisse der vorliegenden vier Arbeiten wurden von Hans-Peter Dürr selbstständig erarbeitet und zusammengefasst, unter Anleitung von Prof. Dr. K. Dietz (Institut für Medizinische Biometrie, Universität Tübingen), Prof. Dr. H. Schulz-Key (Institut für Tropenmedizin, Universität Tübingen) und Dr. M. Eichner (Institut für Medizinische Biometrie, Universität Tübingen).

LITERATUR

Allen, J. E. & MacDonald, A. S. 1998 Profound suppression of cellular proliferation mediated by the secretions of nematodes. *Parasite Immunol* **20**, 241-247.

Awadzi, K., Dadzie, K. Y., Schulz-Key, H., Haddock, D. R., Gilles, H. M. & Aziz, M. A. 1985 The chemotherapy of onchocerciasis. X. An assessment of four single dose treatment regimes of MK-933 (ivermectin) in human onchocerciasis. *Ann Trop Med Parasitol* **79**, 63-78.

Barthold, E. & Wenk, P. 1992 Dose-dependent recovery of adult *Acanthocheilonema viteae* (Nematoda: Filarioidea) after single and trickle inoculations in jirds. *Parasitol Res* **78**, 229-234.

Basáñez, M. G. & Ricardez-Esquinca, J. 2001 Models for the population biology and control of human onchocerciasis. *Trends Parasitol* **17**, 430-438.

Benton, B. 1998 Economic impact of onchocerciasis control through the African Programme for Onchocerciasis Control: an overview. *Ann Trop Med Parasitol* **92 Suppl 1**, 33-39.

Burnham, G. 1998 Onchocerciasis. *Lancet* **351**, 1341-1346.

Cooper, P. J., Mancero, T., Espinel, M., Sandoval, C., Lovato, R., Guderian, R. H. & Nutman, T. B. 2001 Early human infection with *Onchocerca volvulus* is associated with an enhanced parasite-specific cellular immune response. *J Infect Dis* **183**, 1662-1668.

Day, K. P., Gregory, W. F. & Maizels, R. M. 1991 Age-specific acquisition of immunity to infective larvae in a bancroftian filariasis endemic area of Papua New Guinea. *Parasite Immunol* **13**, 277-290.

Dietz, K. 1982 The population dynamics of onchocerciasis. In *The population dynamics of infectious diseases: theory and applications* (ed. R. M. Anderson), pp. 209-241. London, New York: Chapman and Hall.

Duke, B. O. 1990 Human onchocerciasis - an overview of the disease. *Acta Leiden* **59**, 9-24.

Elkhalifa, M. Y., Ghalib, H. W., Dafa'Alla, T. & Williams, J. F. 1991 Suppression of human lymphocyte responses to specific and non-specific stimuli in human onchocerciasis. *Clin Exp Immunol* **86**, 433-439.

Ette, E. I., Thomas, W. O. & Achumba, J. I. 1990 Ivermectin: a long-acting microfilaricidal agent. *Dicp* **24**, 426-433.

Geiger, S. M., Hoffmann, W., Rapp, J., Schulz-Key, H. & Eisenbeiss, W. F. 1996 Filariidae: cross-protection in filarial infections. *Exp Parasitol* **83**, 352-356.

Habbema, J. D., Alley, E. S., Plaisier, A. P., van Oortmarssen, G. J. & Remme, J. 1992 Epidemiological modelling for Onchocerciasis control. *Parasitol Today* **8**, 99-103.

Hoffmann, W. H., Pfaff, A. W., Schulz-Key, H. & Soboslay, P. T. 2001 Determinants for resistance and susceptibility to microfilaraemia in *Litomosoides sigmodontis* filariasis. *Parasitology* **122**, 641-649.

Hougard, J. M., Alley, E. S., Yameogo, L., Dadzie, K. Y. & Boatin, B. A. 2001 Eliminating onchocerciasis after 14 years of vector control: a proved strategy. *J Infect Dis* **184**, 497-503.

Hougard, J. M., Yameogo, L., Seketeli, B., Boatin, B. A. & Dadzie, K. Y. 1997 Twenty-two years of blackfly control in the Onchocerciasis Control Programme in West Africa. *Trends Parasitol* **13**, 425-431.

Karam, M., Schulz-Key, H. & Remme, J. 1987 Population dynamics of *Onchocerca volvulus* after 7 to 8 years of vector control in West Africa. *Acta Trop* **44**, 445-457.

Maizels, R. M. & Lawrence, R. A. 1991 Immunological tolerance: the key feature in human filariasis? *Parasitol Today* **7**, 271-276.

Ottesen, E. A. 1984 Immunological aspects of lymphatic filariasis and onchocerciasis in man. *Trans R Soc Trop Med Hyg* **78**, 9-18.

Piessens, W. F., Ratiwayanto, S., Tuti, S., Palmieri, J. H., Piessens, P. W., Koiman, I. & Dennis, D. T. 1980 Antigen-specific suppressor cells and suppressor factors in human filariasis with *Brugia malayi*. *N Engl J Med* **302**, 833-837.

Plaisier, A. P., van Oortmarssen, G. J., Habbema, J. D., Remme, J. & Alley, E. S. 1990 ONCHOSIM: a model and computer simulation program for the transmission and control of onchocerciasis. *Comput Methods Programs Biomed* **31**, 43-56.

Remme, J., De Sole, G. & van Oortmarssen, G. J. 1990 The predicted and observed decline in onchocerciasis infection during 14 years of successful control of *Simulium* spp. in West Africa. *Bull World Health Organ* **68**, 331-339.

Schulz-Key, H. 1990 Observations on the reproductive biology of Onchocerca volvulus. *Acta Leiden* **59**, 27-44.

Schulz-Key, H., Soboslay, P. T. & Hoffmann, W. H. 1992 Ivermectin-facilitated immunity. *Parasitol Today* **8**, 152-153.

Soboslay, P. T., Geiger, S. M., Drabner, B., Banla, M., Batchassi, E., Kowu, L. A., Stadler, A. & Schulz-Key, H. 1999 Prenatal immune priming in onchocerciasis - *Onchocerca volvulus*-specific cellular responsiveness and cytokine production in newborns from infected mothers. *Clin Exp Immunol* **117**, 130-137.

Soboslay, P. T., Geiger, S. M., Weiss, N., Banla, M., Lüder, C. G., Dreweck, C. M., Batchassi, E., Boatin, B. A., Stadler, A. & Schulz-Key, H. 1997 The diverse expression of immunity in humans at distinct states of *Onchocerca volvulus* infection. *Immunology* **90**, 592-599.

Soboslay, P. T., Lüder, C. G., Hoffmann, W. H., Michaelis, I., Helling, G., Heuschkel, C., Dreweck, C. M., Blanke, C. H., Pritze, S., Banla, M. & Schulz-Key, H. 1994 Ivermectin-facilitated immunity in onchocerciasis; activation of parasite-specific Th1-type responses with subclinical *Onchocerca volvulus* infection. *Clin Exp Immunol* **96**, 238-244.

Ward, D. J., Nutman, T. B., Zea-Flores, G., Portocarrero, C., Lujan, A. & Ottesen, E. A. 1988 Onchocerciasis and immunity in humans: enhanced T cell responsiveness to parasite antigen in putatively immune individuals. *J Infect Dis* **157**, 536-543.

WHO. 1995 Onchocerciasis and its Control, WHO Technical Report Series 852. Geneva.

Stochastic models for aggregation processes[1]

ABSTRACT

Three models are presented, which describe the aggregation of objects into groups and the distributions of group sizes and group numbers within habitats. The processes regarded are pure accumulation processes which involve only formation and invasion of groups. Invasion represents the special case of fusion when only single objects - and not groups - join a group of certain size. The basic model is derived by a single parameter, the formation probability *q,* which represents the probability of an object to form a new group. A novel, discrete and finite distribution that results for the goup sizes is deduced from this aggregation process and it is shown that it converges to a geometric distribution if the number of objects tends to infinity. Two extensions of this model, which both converge to the Waring distribution, are added: the model can be extended either with a beta distributed formation probability or with the assumption that the invasion probability depends on the group size. Relationships between the limiting distributions involved are discussed.

INTRODUCTION

Grouping is a general phenomenon in biology and ecology where organisms form swarms, flocks and herds [1]. The dynamics of these systems are driven by group formation, fusion and fission [2]. Discrete and stochastic processes in such models were traditionally treated with approximations by continuous, deterministic models. Most of the literature concerning this topic originated from research activities in physical chemistry, mainly from the Smoluchowski coagulation equation (1916) and its continuous analogue, which were used to describe fusion processes of particles in colloides or aerosols. Recent developments treat coalescence stochastically, taking also into account the convergence of the behaviour of an infinite number of particles and the existence of solutions [3]. In contrast to these approaches in theoretical probability, recent progresses have been made in the field of applied probability: stochastic models have been adjusted to finite particle systems, exact solutions for the group size distributions were given and Monte-Carlo simulations were compared with continuous and deterministic models [4].

Stimulated by a parasitological example, where parasites (objects) form nodules (groups) and accumulate in the host (habitat), a model was required that describes the parasites' distribution per group. In contrast to published

---

[1] H.P. Duerr & K. Dietz, 2000. Stochastic models for aggregation processes. Mathematical Biosciences 165: 135-145.

approaches, the required model had to have the joint properties: (1) to generate a discrete and finite distribution *and* (2) to describe stochastically the accumulation via the processes of formation and fusion (invasion). The hierarchy of grouping is represented by the order of the terms object, group and habitat. The basic **S**tochastic **A**ggregation **M**odel, SAM(0,*q*,0), is based on a single parameter *q*, the probability of an object to form a new group, and *p*=1-*q*, the invasion probability, which is independent of the group size and independent of the total number of objects. The second model, SAM(α,β,0), assumes that *q* is beta distributed with parameters α and β and can thus account for varying properties between habitats, i.e. their individual behavior with respect to the formation process. The third model, SAM(0,*q*,*r*), is deduced from a denumerable Markov process with continuous time and assumes that *p* depends on present group sizes according to a weighting parameter *r* between 0 and 1. Although the approaches differ methodically, both extended models lead to an identical distribution of group sizes and they can be applied to compare the underlying mechanisms of such aggregation processes.

MODEL I: THE STOCHASTIC AGGREGATION MODEL (SAM(0,*q*,0))

The distribution of the number of groups per habitat (group distribution)

A basic tool to derive the distribution of the number of groups per habitat are partitions. Partitions of the natural number *N* are the possible combinations of integers which sum up to *N*, without regarding order [5]. For example the partitions of four are 1^4, $1^2 2^1$, $1^1 3^1$, 2^2 and 4^1, where superscripts indicate the number of each base respectively. In this context the base will be the group size, i.e. the number of objects per group.

Fig. 1 illustrates the way to a binomial distribution of the number of groups per habitat ("group distribution"). The probability for an object to form a new group of size one, or to join a group is denoted by the formation probability *q* and the invasion probability *p*=1-*q*, respectively. It is assumed that both events occur independently of (1) the number of objects per habitat (*N*) and (2) the group size. The ordinary binomial process continues only up to *N*=3. From there on the event of invasion branches as partitions become inhomogeneous (see partition $1^1 2^1$; *N*=3). According to assumption (2) the invasion probability for each group in the partition is *p/m*, with *m*=number of groups per partition. Different partitions can lead to the same number of groups as shown for *N*=4: the partitions $1^2 2^1$ and 2^2 consist both of two groups, leading to a binomial distribution of the number of groups per habitat.

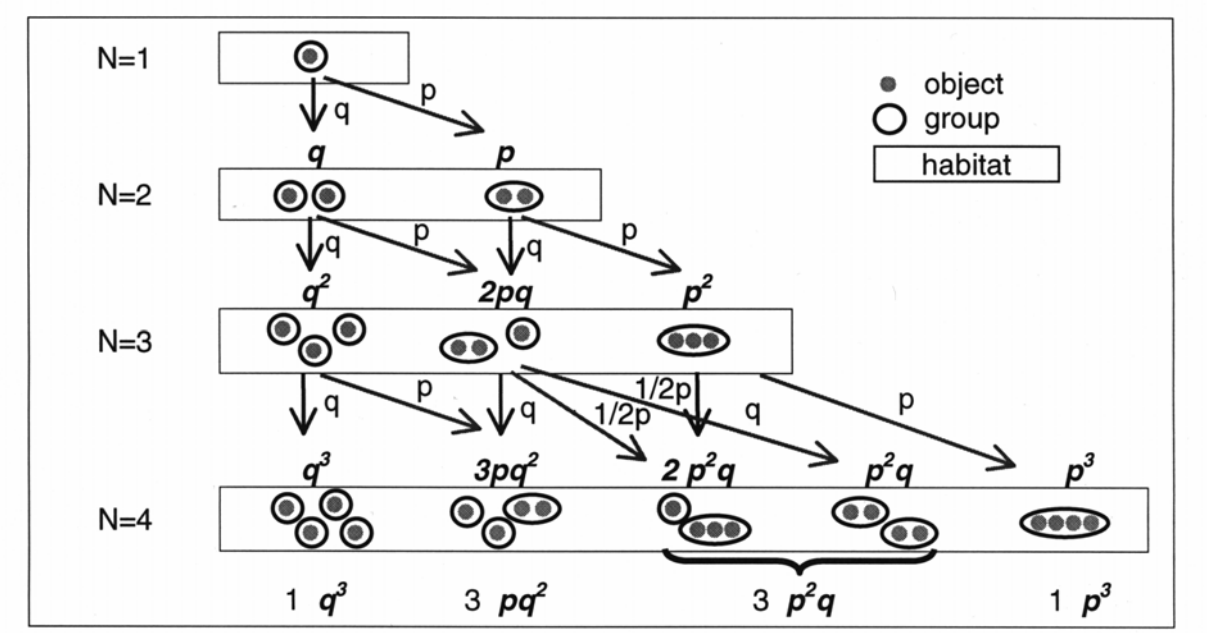

Fig 1: probability tree for a partition process. Formation probability: *q*. Invasion probability: *p*.

Table 1 gives an overview for the further partitions of *N*=5 to *N*=7. The partition number $z_{k,w}$ accounts for the absolute frequency of a partition within a class, that contains identical group numbers. Since the group numbers are binomially distributed the partition numbers of a class sum up to the binomial coefficient. The absolute frequency $H_{k,w}$ (the superscript in a partition) accounts for the number of groups of a certain size within a partition.

N=5	1^5	1^32	1^23	12^2	14	23	5
P	q^4	q^3p^1	q^2p^2		q^1p^3		p^4
z	1	4	3	3	2	2	1
BC	1	4	6		4		1

N=6	1^6	1^42	1^33	1^22^2	1^24	123	2^3	15	24	3^2	6
P	q^5	q^4p^1	q^3p^2		q^2p^3			q^1p^4			p^5
z	1	5	4	6	3	6	1	2	2	1	1
BC	1	5	10		10			5			1

N=7	1^7	1^52	1^43	1^32^2	1^34	1^223	12^3	1^25	124	13^2	2^23	16	25	34	7
P	q^6	q^5p	q^4p^2		q^3p^3			q^2p^4				q^1p^5			p^6
z	1	6	5	10	4	12	4	3	6	3	3	2	2	2	1
BC	1	6	15		20			15				6			1

Table 1: partitions for *N=5* to *N=7*. P: powers of the binomial distribution, *z*: partition number, BC: binomial coefficient. Classes are separated by vertical lines. In the partitions superscript $H_{k,w}$ =1 is omitted.

The distribution of objects per group (partition distribution)

The partition distribution is derived via two probability generating functions (pgfs), of which f_N leads to the average number of groups per habitat and g_N represents the frequency of the group size w. Let q_k be the probability that k groups occur and let N be the total number of objects per habitat. Then

$$f_N(x) = \sum_{k=1}^{N} q_k x^k \tag{1}$$

is the pgf for the number of groups per habitat and

$$\mu_K = f_N'(1) = \sum_{k=1}^{N} k\, q_k \tag{2}$$

the corresponding expectation. We define

$$g_N(x) = q_1 x^N + \sum_{k=2}^{N} \binom{N-1}{k-1}^{-1} q_k \sum_{w=1}^{N+1-k} (z_{k,w}\, H_{k,w}\, x^w), \tag{3}$$

where the inner and the outer sum represent all possible group sizes (index w) and the numbers of groups (index k), respectively. The probability q_1 cannot be included within the sum and is therefore added separately. The product of the partition number and the group size frequency ($z_{k,w}H_{k,w}$, see Table 1) divided by the binomial coefficient accounts for the relative frequency of a group size within a class.

Given (2) and (3) the pgf for the group sizes is

$$h_N(x) = \frac{g_N(x)}{\mu_K} \tag{4}$$

and the coefficients of x^w give the probability that w objects per group occur.

The partition matrix

A matrix was found that enables us to determine the product of $z_{k,w}\, H_{k,w}$ directly without executing the process as shown in Fig. 1. Table 2 shows this matrix for N=7. It is obvious that the objects in the main diagonal simply reflect k as it is given by q_k.

q_k \ x^w	x^7	x^6	x^5	x^4	x^3	x^2	x^1
q_1	**1**						
q_2		**2**	2	2	2	2	2
q_3			**3**	6	9	12	15
q_4				**4**	12	24	40
q_5					**5**	20	50
q_6						**6**	30
q_7							**7**

Table 2: Partition matrix for N=7.

Starting from the main diagonal the elements $a_{w,k}$ of the matrix can be calculated through the recursion

$$a_{w-1,k} = a_{w,k}\frac{N-w}{N-w-k+2}. \tag{5a}$$

An element of any partition matrix is given by the solution

$$a_{w,k} = k\binom{N-w-1}{k-2}. \tag{5b}$$

This expression is substituted into (3); thus,

$$g_N(x) = q_1 x^N + \sum_{k=2}^{N}\binom{N-1}{k-1}^{-1} k q_k \sum_{w=1}^{N+1-k}\binom{N-w-1}{k-2}x^w. \tag{6}$$

Let us now recall that q_k, the probability that k groups occur, is binomially distributed with parameters N-1 and q:

$$q_k = P(K=k \mid N,q) = \binom{N-1}{k-1}q^{k-1}(1-q)^{N-k}, \quad k = 1,...N. \tag{7}$$

Expectation and variance are μ_K=1+(N-1)q and σ_K^2=(N-1)q(1-q). Inserted into (6) we obtain the pgf for the group sizes

$$h_N(x) = \frac{(1-q)^{N-1}x^N + \sum_{k=2}^{N} q^{k-1}(1-q)^{N-k} k \sum_{w=1}^{N+1-k}\binom{N-w-1}{k-2}x^w}{1+(N-1)q}. \tag{8a}$$

Expectation and variance of the corresponding distribution can be calculated from this pgf with the relations $\mu_N = h'_N(1)$ and $\sigma_N^2 = h''_N(1) + h'_N(1) - (h'_N(1))^2$.

Convergence of the partition distribution

We show that if N tends to infinity the partition distributions converges to the geometric distribution. Table 3 gives an overview for the deviation between the partition distribution and the geometric distribution. The deviation is calculated as the maximum difference between the two probability functions, conditioning the geometric distribution according to the finite carrier of the partition distribution.

q	0.1	0.2	0.3	0.4	0.5	0.6	0.7	0.8	0.9
N=10	0.1444	0.0510	0.0646	0.0587	0.0450	0.0374	0.0288	0.0195	0.0099
N=50	0.0559	0.0303	0.0197	0.0140	0.0098	0.0079	0.0059	0.0040	0.0020
N=100	0.0320	0.0158	0.0101	0.0071	0.0050	0.0040	0.0030	0.0020	0.0010

Table 3: Maximum deviation between partition distribution functions (N=10, N=50, N=100) and the truncated geometric distribution function for formation probabilities [0.1...0.9].

The proof of the convergence requires to exchange the sums in formula (8a), so that we obtain

$$h_N(x) = \frac{(1-q)^{N-1}x^N + \sum_{w=1}^{N-1} x^w \sum_{k=2}^{N-w+1} k\, q^{k-1}(1-q)^{N-k}\binom{N-w-1}{k-2}}{1+(N-1)q}. \qquad (8b)$$

The evaluation of the inner sum leads to

$$h_N(x) = \frac{(1-q)^{N-1}x^N + \frac{q}{1-q}\sum_{w=1}^{N-1} x^w (1-q)^w (2+q(N-1-w)}{1+(N-1)q}. \qquad (8c)$$

If $N\to\infty$ only the highest powers of N have to be considered, so that (8c) reduces to

$$\lim_{N\to\infty} h_N(x) = qx\sum_{w=0}^{N-2}(x(1-q))^w = \frac{qx}{1-x(1-q)} = \frac{x}{1+(\frac{1}{q}-1)(1-x)}, \qquad (8d)$$

which is the pgf for the zero-truncated geometric distribution.

MODEL II: THE STOCHASTIC AGGREGATION MODEL WITH BETA DISTRIBUTED FORMATION PROBABILITY (SAM(α,β,0))

If the observed variance of *K* groups per habitat is higher than expected by the basic model with binomially distributed *K*s, it can be assumed that *q* varies between habitats according to a beta distribution. Then the number of groups has a beta binomial distribution [6] with parameters *N*-1, α and β:

$$q_k = P(K = k \mid N,\alpha,\beta) = \frac{1}{B(\alpha,\beta)}\binom{N-1}{k-1}B(k-1+\alpha, N-k+\beta),\ k = 1,...N, \qquad (9)$$

where B(ξ_1, ξ_2) is the beta function. With $\pi=\alpha/(\alpha+\beta)$ and $\theta=1/(\alpha+\beta)$ expectation and variance are $\mu_K=1+(N-1)\pi$ and $\sigma_K^2=(N-1)\pi(1-\pi)(1+(N-1)\theta)/(1+\theta)$.

The probabilities of q_k can then be inserted as shown for formula (8a). Since the partition matrix holds also in this case, the compound partition distribution converges to a compound geometric distribution if $N\to\infty$. The parameter of the geometric distribution underlies then a beta distribution, so that according to Kemp and Kemp's classification a zero-truncated generalized hypergeometric distribution of Type IV (gHypIV) is obtained [7]. With

$$P(W = w) = q(1-q)^{w-1}, \qquad w = 1,2,...$$
$$\text{and density } f(q) = \frac{q^{\alpha-1}(1-q)^{\beta-1}}{B(\alpha,\beta)}, \qquad \alpha,\beta > 0 \qquad (10a)$$

the compound distribution is given by

$$P(W = w) = \frac{1}{B(\alpha,\beta)}\int_0^1 q^{\alpha-1}(1-q)^{\beta-1}q(1-q)^{w-1}dq$$
$$= \frac{B(\alpha+1,\beta+w-1)}{B(\alpha,\beta)} = \frac{\alpha\Gamma(\alpha+\beta)\Gamma(\beta+w-1)}{\Gamma(\beta)\Gamma(\alpha+\beta+w)}, \qquad (10b)$$

which is a special case of the gHypIV, a zero-truncated Waring distribution with parameters $b=\alpha$ and $n=\beta$-1 [8] ($\Gamma(\xi)$ is the gamma function). From the corresponding pgf

$$f(x) = \frac{x}{B(\alpha,\beta)}\int_0^1 \frac{q^{\alpha-1}(1-q)^{\beta-1}}{(1+(1/q-1)(1-x))}dq \qquad (10c)$$

expectation and variance can be derived:

$$\mu_W = f'(1) = 1 + \frac{\beta}{\alpha - 1}, \qquad \alpha > 1,$$
$$\sigma^2_W = f''(1) + f'(1) - (f'(1))^2 = \mu_W(\mu_W - 1)\frac{\alpha}{\alpha - 2}, \qquad \alpha > 2 \tag{10d}$$

MODEL III: WEIGHTING THE INVASION PROBABILITY WITH RESPECT TO THE GROUP SIZE (SAM(0,*q*,*r*))

The aggregation process with weighted invasion probability is described by the following system of differential equations which represents a Markov process with continuous time. The parameter *r* represents a weighting factor which balances the process between the limits *r*=1: the invasion probability for an object is proportional to the group size, and *r*=0: the invasion probability is independent of the group size (which is the assumption in the basic model, SAM(0,*q*,0)).

$$\dot{g}_1 = q - \frac{1-q}{(1-r)G + rN} g_1, \tag{11a}$$

$$\dot{g}_w = \frac{(1-q)(1-r+r(w-1))}{(1-r)G + rN} g_{w-1} - \frac{(1-q)(1-r+rw)}{(1-r)G + rN} g_w, \qquad 0 < r < 1, \tag{11b}$$

where g_w= number of groups of size w, $G = \sum g_w$ and $N = \sum w\, g_w$. Defining f_w to be the relative frequency of groups of size w, and using the relation $\dot{G}=q$, we can derive $g_w = f_w G$:

$$\dot{g}_W = \dot{f}_W G + f_W \dot{G} = \dot{f}_W G + f_W q. \tag{12}$$

Inserting (11a) and (11b) into (12) we obtain

$$\dot{f}_1 G = q - \frac{1-q}{(1-r)G + rN} f_1 G - f_1 q, \tag{13a}$$

$$\dot{f}_W G = \frac{(1-q)(1-r+r(w-1))}{(1-r)G + rN}(f_{w-1} G) - \frac{(1-q)(1-r+rw)}{(1-r)G + rN} f_W G - f_W q. \tag{13b}$$

G and N can be replaced by q due to the definition of the formation probability $q=G/N$.

Since the transition probabilities of denumerable Markov processes approach their equilibrium values with an exponential convergence rate [9], their derivatives decrease faster than the linearly increasing G. Thus, the steady-state distribution of group sizes exists and it is reached when:

$$\begin{aligned} \dot{f}_1 G &= 0, \\ \dot{f}_w G &= 0. \end{aligned} \tag{14}$$

Formulas (13a, b) can then be solved for f_1 and f_w:

$$f_1 = \frac{q + r(1-q)}{1 + r(1-q)}, \tag{15a}$$

$$f_w = \frac{(1-q)(1+r(w-2))}{(1-q)(1+rw)+q} f_{w-1}. \tag{15b}$$

The solution of this recursion leads to

$$\begin{aligned} f_w &= \frac{(q + r(1-q))(1-q)^{w-1}}{1+r(1-q)} \prod_{k=2}^{w} \frac{1+r(k-2)}{1+kr(1-q)} \\ &= \frac{(q + r(1-q))\Gamma\left(2 + \frac{1}{r(1-q)}\right)}{(1+r(1-q))\Gamma\left(\frac{1}{r}\right)} \frac{\Gamma\left(w + \frac{1}{r} - 1\right)}{\Gamma\left(w + \frac{1}{r(1-q)} + 1\right)} \end{aligned} \tag{16}$$

which is a zero-truncated Waring distribution [8] with parameters $b=1+q/(r(1-q))$ and $n=(1/r)-1$. Mean and variance are $\mu=1/q$ and $\sigma^2=\mu^2((1-q)(q+r(1-q))/(q-r(1-q))$, respectively, and the variance is defined only when $q>r/(1+r)$; the latter corresponds exactly to the condition $\alpha>2$ for the variance of SAM($\alpha,\beta,0$).

Special cases of this distribution are the geometric distribution as $r\to 0$ and the Yule distribution for $r=1/2$.

CONCLUSIONS

The Stochastic Aggregation Models (SAM) presented above provide, as special cases of coagulation-fragmentation processes, a new derivation for the zero-truncated geometric distribution and for the zero-truncated Waring distribution. The distributions can be generated by an accumulation process, using partitions to enable stochastic modelling of a finite number of objects. Finite partition distributions for SAM(0,*q*,0) and SAM(α,β,0) are derived and they can be used to describe group size frequencies in cases where the approximation to an infinite number of objects is not appropriate.

Fig. 2 summarizes the three models, their parameters and transitions between them. The basic model, SAM(0,*q*,0), assumes that the formation probability *q* and its counterpart, the invasion probability *p*=1-*q* are constant, i.e. they are independent of the number of existing objects (*N*) and the size of existing groups. The accumulation process converges to a zero-truncated geometric distribution of group sizes if *N* tends to infinity. If the parameter *q* underlies a beta distribution with parameters α and β, which accounts for variability between habitats, then the process converges to a zero-truncated Waring distribution and group sizes are more dispersed than in the basic model. With growing α and β the variance of the beta distribution decreases and in the limiting case both parameters merge into the mean of the distribution, which again equals *q* as in the basic model.

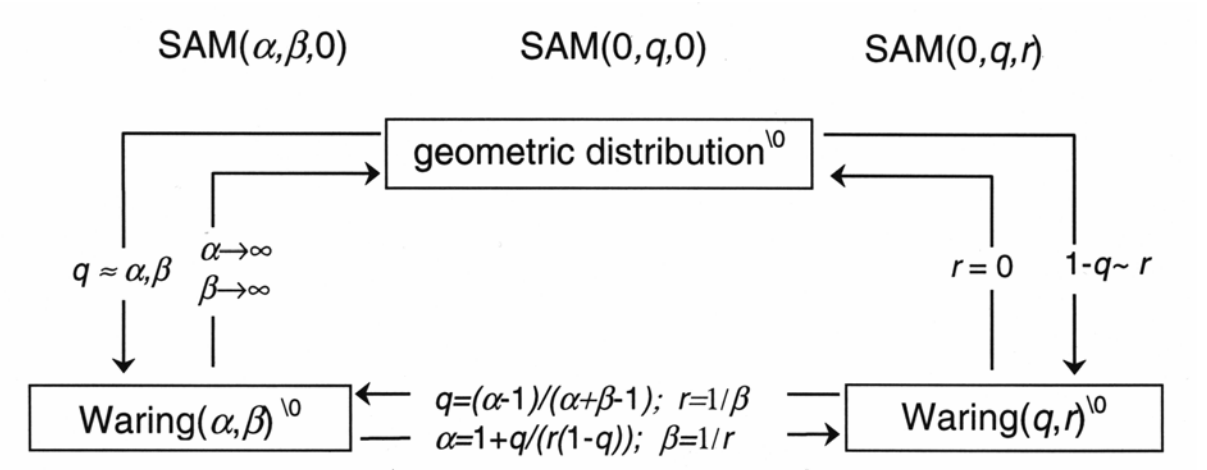

Fig. 2: Relations and transitions between the models. α, β: parameters of the beta distribution; *r*: weighting parameter; \0 indicates the zero-truncated type of the distribution.

The SAM(0,*q*,*r*) describes an aggregation process in which the invasion probability depends on the size of existing groups. If *N* tends to infinity, the underlying Markov process leads, like SAM(α,β,0), to a zero-truncated Waring distribution. Special cases of this model are (1) *r*=0, which means "no

dependence", leading again to the geometric distribution, (2) r=1/2: leads to the Yule distribution and means "balanced dependence", i.e. objects form a new group to the same extent as they are attracted by the groups, proportional to their size and (3) r=1: "total dependence" on the group size, i.e. there is no other factor than the group size influencing the aggregation process. The special case r=1 was already investigated by Simon [10], who described word frequencies by a class of distribution functions given by $f(w)=A\ B(w, \rho+1)$ where A and ρ are constants and $B(w, \rho+1)$ is the beta function. This model corresponds to SAM(0,q,r) (formula (16)) if $A=\rho=1/(1-q)$.

The transitions between both models (see Fig. 2) show that for the complete domain of the parameters ($\alpha,\beta>1$ and $0<r<1$), reparametrization makes both distributions indistinguishable, although the underlying aggregation processes differ considerably. A super model, SAM(α,β,r), which could be developed either by beta mixing q in SAM(0,q,r) or by introducing r in SAM(α,β,0), could therefore not resolve whether the extra variability in the group size distribution has to be attributed to stochastic heterogeneity in habitats or to a weighted attractivity of group sizes. Thus, modelling of such aggregation processes requires the decision, which of the two assumptions is relevant for the investigation of the process.

The geometric distribution can be generated by other grouping models. Referring to [1] it can even result from a grouping process in which fission of groups is possible, assuming that the rates of fusion (by groups of size one) and fission increase linearly with group size. The same holds for the special case of constant rates as well. In [1], it is also shown that from a viewpoint of 'maximum entropy' a group size distribution is geometric if the average group size is constant. Our results give further a discrete and stochastic analogue to investigations of Gueron and Levin [2] on grouping processes with deterministic, continuous models. They showed that a fusion process which occurs independently of the group size leads to an exponential distribution, which is the continuous equivalent to the geometric distribution. This result was generalized in the sense that grouping, which is based on any nondecreasing association between the group size and the probability of fusion, leads to a monotonously decreasing distribution of group sizes.

Recent papers have focussed on the stochastic modelling of related processes, subsumed under the term 'coalescence' [3,11]. Partitions were used to establish a discrete and finite-state Markov process (Marcus-Lushnikov model). Since the rates or group sizes are not restricted in this model, it is most appropriate for the theoretical description of such problems. Furthermore, applied probabilistic studies have been published: stationary groupsize distributions for coagulation-fragmentation processes (CFPs) have been derived for specific rates which were defined to depend only on the group sizes, again implementing partitions to enable discrete and finite modelling [4,12]. Inspite of these methodical similarities between these models and SAM(0,q,r), we were

not able to transform these differing approaches into each other and it might be impossible due to the fact that parameter *r* in SAM(0,*q*,*r*) is, strictly spoken, not a rate but a weighting factor. Among the CFPs, the Becker-Döring equation comes closest to our approach, because it describes a CFP where only groups of size one merge with or split from other groups; a theoretical survey of this model is given by Ball et al. [13].

Cohen [14] investigated grouping processes stochastically, choosing an approach that resembles SAM(0*,q,r*) but implementing additionally splitting of groups. With respect to weighted attractiveness of groups, he introduced fusion and splitting as rates, which are linear functions of the group size. This leads either to truncated forms of the Poisson, the binomial or the negative binomial distribution dependent on the offset and the slope of these functions. The difference to SAM(0*,q,r*) is the implication in Cohens model for 'open systems' that those objects which enter the system cannot form a group of size one, instead they are forced to fuse with other groups that harbour at least two objects. In addition, groups of size one inside the system can only emerge by an internal process, the splitting of groups of size two. In contrast to SAM(0*,q,r*), where all incoming objects pass through a given probability tree in the manner specified, this means that single objects in Cohens model behave differently, dependent on their origin.

The pattern of aggregation in animal grouping processes is often described by the variance-to-mean ratio (*VMR*), comparing it to that of the Poisson distribution, for which it is equal to one. *VMR*s greater than one indicate 'overdispersion', i.e. the group distribution shows a greater variance than expected by random group formation. The basic model with the limiting case of the geometric distribution implies that overdispersion occurs for all formation probabilities $q<1/2$, due to the condition $VMR=(1-q)/q>1$. For any finite partition distribution this treshold moves towards smaller *q*s, strongly dependent on *N* (analysis not shown). In other words, overdispersion of the partition distribution increases with the number of objects per habitat. The same holds as well for the extended models, however, due to the higher variance, caused by the beta distributed or weighted formation probability, the *VMR* in this case increases stronger than in the basic model.

The examples above show that the geometric distribution is a very common aggregation pattern in animal grouping, at least in kinds of their limit distributions and preferably, if the models are simple. The application of partitions in the present model enabled a stochastic description of grouping processes because all possible group sizes and their frequencies were taken into account. The comparison with other models implying only slightly different assumptions showed here that grouping processes become very sensitive systems, if additional parameters are introduced. However, this is in contrast to the present investigation, where considerably differing models lead to the same stationary distribution.

Acknowledgement

The authors are grateful to M. Eichner and H.H. Diebner for fruitful collaboration. This work was supported by the *f*ortüne grant no. 528 of the University Hospital, Tübingen, Germany and by a grant from the Deutsche Forschungsgemeinschaft, Graduiertenkolleg Lebensstile, soziale Differenzen und Gesundheitsförderung.

REFERENCES

[1] A. Okubo, Dynamical aspects of animal grouping: swarms, schools, flocks, and herds, Review, Adv. Biophys. 22 (1986) 1-94.

[2] S. Gueron and S.A. Levin, The dynamics of group formation, Math. Biosci. 128 (1995) 243-64.

[3] D.J. Aldous, Deterministic and stochastic models for coalescence (aggregation and coagulation): a review of the mean-field theory for probabilists. Bernoulli 5 (1999), 3-48.

[4] S. Gueron, The steady-state distributions of coagulation-fragmentation processes. J. Math. Biol. 37 (1998) 1-27.

[5] J. Riordan, Partitions, compositions, trees and networks, in: W.A. Shewhart and S.S. Wilks (Ed.), An Introduction in Combinatorial Analysis. New York, John Wiley & Sons, Inc. London, 1958, pp. 107-162.

[6] D.A. Griffiths, Maximum likelihood estimation for the beta-binomial distribution and an application to the household distribution of the total number of cases of a disease. Biometrics 29 (1973) 637-648.

[7] A.W. Kemp, C.D. Kemp, Generalized hypergeometric distributions, J. R. Stat. Soc., Ser. B, 18 (1956) 202-211.

[8] G. Wimmer, G. Altmann. Thesaurus of univariate discrete probability distributions. Stamm, Essen, Germany, 1999.

[9] J.F.C. Kingman, The exponential decay of Markov transition probabilities. Proc. London Math. Soc. (3) 13 (1963) 337-358.

[10] H. A. Simon, On a class of skew distribution functions. Biometrika 42 (1955) 524-440.

[11] D.J. Aldous, Stochastic coalescence, Proc. of the Intern. Congress of Mathematicians, Vol. III, Doc. Math. (1998) 205-211 (electronic).

[12] R. Durrett, B.L. Granovsky, S. Gueron, The equilibrium behavior of reversible coagulation-fragmentation processes. J. Theor. Prob. 12 (1999) 447-474.

[13] J.M. Ball, J. Carr, O. Penrose, The Becker-Döring cluster equations: basic properties and asymptotic behaviour of solutions. Commun. Math. Phys. 104 (1986) 657-692.

[14] J. E. Cohen, Casual groups of monkeys and men, Harvard University Press, Cambridge, Massachusetts, 1971.

A stochastic model for the aggregation of *Onchocerca volvulus* in nodules[1]

SUMMARY

A model is presented which describes the aggregation of female *Onchocerca volvulus* in nodules and their distribution in the human population. The basic model is based on a single parameter, the formation probability *q*, which represents the probability with which incoming larvae form a new nodule. This parameter describes parasite behaviour which cannot easily be recognized in available data without modelling. The estimate for the average formation probability of μ_q=0.39 suggests an attraction of the invading infective larvae to already existing nodules or resident worms with probability 0.61. No significant difference in μ_q was found between the forest and savanna parasite strains. The model can be used inversely to estimate the worm burden of persons from palpation data. The observed variance in the number of nodules per person requires the assumption of a variance-increasing mechanism which was implemented by heterogeneity within the host population (extended model with two parameters). Possible reasons for this heterogeneity are presented and its implications concerning the reproductive biology of the parasite are discussed.

INTRODUCTION

Onchocerciasis is a parasitic infection caused by nematodes of the genus *Onchocerca.* The adult worms (macrofilariae) are mostly located in the subcutaneous tissue of their specific hosts. These comprise ungulates, and, exceptionally, also man. Several species are obligatorily located in a capsule consisting of host tissue so as to form a nodule, the onchocercoma, which is also characteristic for the human parasite, *Onchocerca volvulus*. The onchocercoma seems to be induced predominantly or even exclusively by the female parasite, which remains sessile after settlement. While the intranodular parasite species of animals usually remain solitary in nodules of more or less similar size, the human parasite shows a typical accumulation of worms in the onchocercomata with a considerable range of sizes (Schulz-Key & Albiez, 1977). Young, old and degenerated worms may be found in the same nodule, with the average number of female *O. volvulus* per nodule increasing with total worm burden. Ten female worms per nodule are often found, with some nodules harbouring even more than 40 worms (Albiez, Büttner & Duke, 1988; Büttner, Albiez, von Essen & Erichsen, 1988).

---

[1] H.P. Duerr, K. Dietz, D.W. Büttner, H. Schulz-Key, 2001. A stochastic model for the aggregation of *Onchocerca volvulus* in nodules. Parasitology 123: 193-201.

The biological reason behind this unusual aggregation pattern - atypical for the genus *Onchocerca* - of *O. volvulus* in the human host is not yet known. But the advantage it confers in terms of facilitating the meeting and mating of dioeceous parasites should be obvious. This suggestion is supported by the observation that younger male worms regularly leave the nodules. They migrate freely within the host tissue and visit female worms, which require several inseminations per year at distinct intervals (Schulz-Key & Karam, 1986). The sex-finding mechanism of tissue-dwelling nematodes still needs clarification, but a chemotactic attraction may be suspected, either induced by pheromones of the sessile female worm, by other excretory or secretory parasite products, or by the tissue of the nodule itself. In addition, the composition of the worm burden in big nodules and the observation of satellite nodules with smooth and thin capsules, usually containing young worms, indicates a gradual growth of the nodules that accompanies large worm burdens.

The present investigation describes a model mimicking stochastically the nodule forming process of *O. volvulus* and it seeks to clarify the question if the assumption of an attraction of the incoming larvae to resident worms is required to explain the observed parasite's aggregation pattern.

MATERIALS AND METHODS

Sources of data and parasitological procedures

The data derive from two nodulectomy campaigns in villages of the West African countries of Liberia (rain forest) and Burkina Faso (savanna), conducted, respectively, in 1976/77 and 1977/78. Both regions were hyperendemic for onchocerciasis at the time of nodulectomy. After extirpation, the nodules were digested with collagenase (for parasitological procedures see Schulz-Key, Albiez & Büttner, 1977) so that the number of worms per nodule could be precisely assessed. Descriptive aspects of these data sets, the worm burden, the relation of palpable to impalpable nodules, and the incidence of different worm stages were published elsewhere (Schulz-Key & Albiez, 1977; Albiez, 1983; Albiez, Büttner & Schulz-Key, 1984). The absolute numbers listed in Table 1 may differ slightly from those given in these publications due to the fact that it was impossible to reconstruct the exactly identical subset of persons. The villages included in this analysis are Mauwa, Sungbeta, Wodee, Yeahmeah and Meningee (located east of St. Paul River in southern Bong and in Montserrado counties, Liberia), and Kourougbele, Hemkoa, and Yabar (located south of the Bougouriba River in the region of Gaoua, Burkina Faso). For the present investigation, all individuals operated on and showing at least one female adult worm were included in the analysis. Since male worms seem to play a minor role in the nodule forming process (Collins, Lujan, Figueroa & Campbell, 1982), only female worms of all stages are taken into consideration.

Country (parasite strain)	Liberia (forest)	Burkina Faso (savanna)
No. of villages	5	3
Total no. of persons with at least one adult female worm	200	87
Total no. of excised nodules	1969	809
Total no. of female worms *	5116	2092
Average no. of excised nodules per person	9.8	9.3
Average no. of female worms per person *	25.6	24.0
Average no. of female worms per nodule *	2.6	2.6
Percentage of dead female worms	12.2%	15.2%

Table 1: Summary data for nodulectomy trials of *Onchocerca volvulus* in West African localities (see text for sources of data). * includes both live and dead parasites.

Description of the basic model

The methods by which to generate the distribution of the number of worms per nodule have recently been described in terms of a stochastic aggregation process (Duerr & Dietz, 2000). Fig. 1 depicts the basic idea of the probability tree that enables mathematical handling of the sequential process of infection, and Table 2 explains parameters as used in the following. After infection, developing female larvae form a new nodule with formation probability q or else join an already existing nodule with invasion probability p=1-q. The model assumptions are that both probabilities are independent of: (1) N, the number of female worms per person, and (2) the size of the nodules (measured as the number of females per nodule).

The aggregation process leads to a binomial distribution of the number of nodules K per person. Since the female larvae of the initial (primary) infection invariably form the first nodule, the distribution has parameters q and N-1, with mean and variance

$$\begin{aligned} \mu_K &= 1+(N-1)q, \\ \sigma_K^2 &= (N-1)q(1-q). \end{aligned} \tag{1}$$

Thus, the average number of nodules per person is a linear function of N, and the formation probability of female worms within an individual host i can be estimated by

$$q_i = \frac{K_i - 1}{N_i - 1}. \tag{2}$$

Since this relation is derived from the mean of the binomial distribution, q_i is not only the moment estimator but also the maximum likelihood estimator.

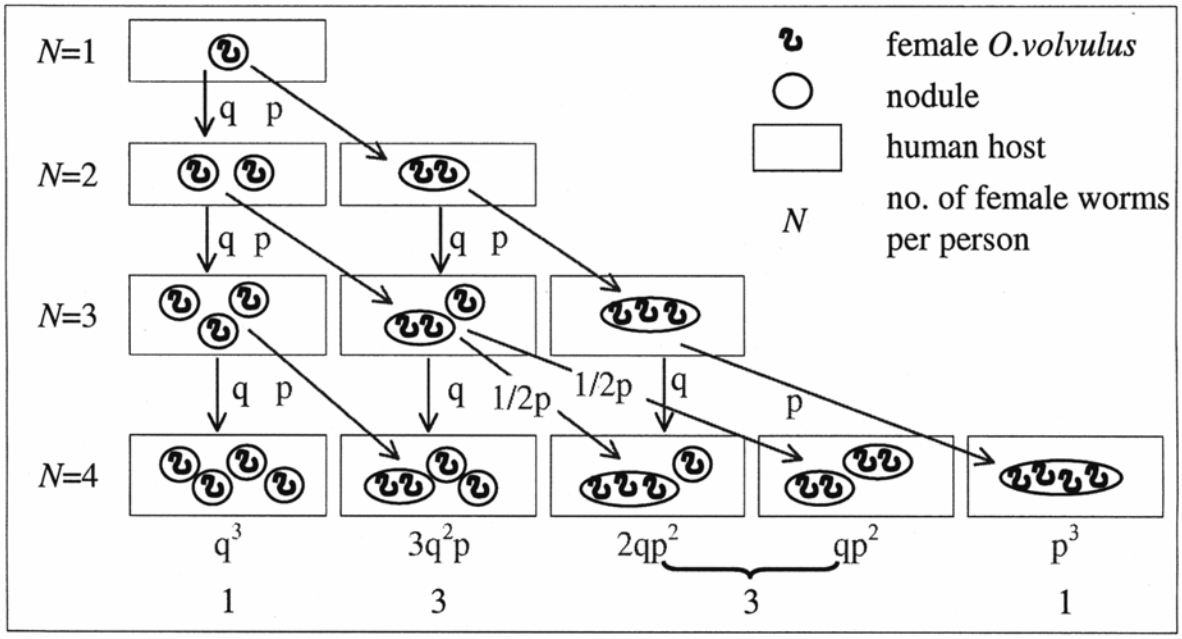

Fig. 1: Representation of the stochastic model describing formation of different nodule sizes after sequential infection with *O. volvulus*. Arrows indicate branches as based on the formation probability q and the invasion probability p=1-q. The last two lines demonstrate that the number of nodules minus one follows a binomial distribution.

Parameter	Definition
q	Probability of formation of a new nodule
p = 1- q	Probability of invasion of an existing nodule
N	No. of adult female worms per person, with N_i as the no. of female worms within the i-th individual host
K	No. of nodules per person, with mean μ_K and variance σ^2_K, and K_i as the no. of nodules within the i-th individual host
α, β	Parameters of the beta distribution of the formation probability with mean μ_q and variance σ_q^2 (see also beta binomial distribution)
m	Parameter of the geometric distribution of the no. of adult female worms per person

Table 2: Parameter notation and definition

Implementation of heterogeneity in the model

As the variance of the binomial distribution is too low to explain the observed variance in the number of nodules per individual, we allow q to vary between individuals, instead of fixing it as in the case of the binomial distribution. This accounts for an assumed variability on the part of hosts to react with differential intensity of encapsulation to the presence of parasites. Defining q to be beta distributed, as described in Duerr & Dietz (2000), the number of nodules per person therefore follows a beta binomial distribution with parameters N-1, α and β:

$$q_k = P(K = k \mid N, \alpha, \beta) = \frac{1}{B(\alpha,\beta)} \binom{N-1}{k-1} B(k-1+\alpha, N-k+\beta), \; k = 1,...N, \tag{3}$$

where $B(\xi_1, \xi_2)$ is the beta function.

The average formation probability and the corresponding variance in this case are

$$\begin{aligned} \mu_q &= \frac{\alpha}{\alpha+\beta}, \\ \sigma_q^2 &= \frac{\alpha+\beta}{(\alpha+\beta)^2(\alpha+\beta+1)}, \end{aligned} \tag{4}$$

and the expected number of nodules and the corresponding variance is given by

$$\begin{aligned} \mu_{K(\alpha,\beta)} &= 1+(N-1)\mu_q, \\ \sigma^2_{K(\alpha,\beta)} &= \frac{(N-1)\mu_q(1-\mu_q)(1+(N-1)/(\alpha+\beta))}{(1+1/(\alpha+\beta))}. \end{aligned} \tag{5}$$

The distribution of nodule sizes

Given the individual worm burden N_i and the probability that k nodules occur, q_k, the probabilities for the expected nodule sizes can be calculated from the probability generating function (pgf) of the partition distribution

$$h_N(x) = \frac{1}{1+(N_i-1)q_k} \left(q_1 x^{N_i} + \sum_{w=1}^{N_i-1} x^w \sum_{k=2}^{N_i-w+1} k q_k \binom{N_i-w-1}{k-2} \Big/ \binom{N_i-1}{k-1} \right). \tag{6a}$$

where x is the dummy variable of the pgf (for details see Duerr & Dietz, 2000). The coefficients of x^w yield then the probability that w female worms per nodule can be found. Fitting these probabilities to data can be done in two ways:

(**A**) In the basic model, with a binomially distributed number of nodule numbers, q_k is replaced by the binomial probabilities

$$q_k = P(K = k \mid N,q) = \binom{N-1}{k-1} q^{k-1}(1-q)^{N-k}, \quad k = 1,...N. \tag{6b}$$

so that we obtain

$$h_N(x) = \frac{(1-q)^{N-1}x^N + \sum_{w=1}^{N-1} x^w \sum_{k=2}^{N-w+1} k\, q^{k-1}(1-q)^{N-k}\binom{N-w-1}{k-2}}{1+(N-1)q}. \tag{6c}$$

Replacing in this stage parameters N and q with the individual parameters (i.e. $N=N_i$, $q=q_i$) results in a fit which is in its parametrization closest to the observations. This fit will be called in the following "individual-based fit".

(**B**) For the extended model with implemented heterogeneity, q_k is given by the beta binomial distribution (eq. (3)) and substituted into eq. (6a). Since these probabilities are based on the population parameters α and β, this fit will be called in the following "parametric fit".

Parameter estimation

Parameters α and β were determined by maximum likelihood estimation, using Powell's algorithm (Press, Teukolsky, Vetterling & Flannery, 1992) in combination with varying initial values. Confidence limits for μ_q were derived from the isolines of the two-dimensional log-likelihood function lnL(α,β): since $\mu_q = 1/(1+\beta/\alpha)$ depends only on the ratio β/α, the slopes of the two tangents to the isoline of lnL(α,β)-5.99/2 determine the lower and upper confidence limits (according to a likelihood ratio test with two degrees of freedom, the 95% quantile is χ^2=5.99).

Predicting the number of female worms from palpation or surgery data

As shown above the number of nodules K_i of individuals with a total worm burden of N_i female worms can be described by the beta binomial distribution with probability P(k_i| N_i = n_i). From this we can inversely calculate the probability that an individual i has n_i female worms given k_i excised nodules. Since this probability is conditioned on K_i, the prediction may not be deduced from the relationship as shown in Fig. 3. Instead, Bayes' theorem must be applied as follows:

$$P(N_i = n_i \mid k_i) = \frac{P(k_i \mid N_i = n_i) \cdot P(n_i)}{\sum_{x=k_i}^{\infty} P(k_i \mid x) \cdot P(x)}, \quad x = 1,2..., \; k_i = 1,2...n_i, \tag{7}$$

where the denominator normalizes the probabilities. P(n_i) is the probability that n_i female worms per person can be found. This can be fitted by the geometric distribution from the population data according to $P(n_i)=(1/m)(1-1/m)^{n_i-1}$ (with parameter estimates m_{forest}=25.6 and $m_{savanna}$=24.0, which are the average number of worms (including live and dead worms) per person as given in Table 1).

Approximation by the Waring distribution

As shown in Duerr & Dietz (2000), the partition distribution of the number of worms per nodule with a beta binomially distributed number of nodules per host converges to a zero-truncated Waring distribution (Wimmer & Altmann, 1999) when $N \to \infty$. The distribution of nodule sizes for heavily infected people can therefore be approximated by the Waring distribution, and the probability that w female worms per nodule are found is given then by

$$P(W = w) = \frac{\alpha \Gamma(\alpha + \beta)\Gamma(\beta + w - 1)}{\Gamma(\beta)\Gamma(\alpha + \beta + w)}, \qquad \alpha > 2, \beta > 0; \qquad w = 1,2,...,N \tag{8}$$

where Γ is the Gamma function and α, β are the parameters of the beta distribution. Mean and variance of this distribution are $\mu_W = 1+\beta/(\alpha-1)$ and $\sigma_W^2 = \mu_W(\mu_W-1)\alpha/(\alpha-2)$, respectively.

RESULTS

Parameter estimates

Table 3 shows the parameter estimates of the beta distributed formation probabilities with corresponding means and variances for the examined individuals in Liberia (forest strain) and Burkina Faso (savanna strain). Overlapping confidence intervals for μ_q indicate that the average formation probabilities of both strains do not differ significantly, so that a common distribution can be assumed. Fig. 2 shows the density functions for these estimates.

Parameter	*O. volvulus* strain		
	Forest (Liberia)	Savanna (Burkina Faso)	Common estimates
α	6.35	11.80	7.60
β	9.47	19.80	11.74
mean μ_q	0.40	0.37	0.39
95% CL (μ_q)	0.37-0.43	0.32-0.41	0.37-0.42
variance σ_q^2	0.014	0.007	0.012

Table 3: Estimates for the parameters of the beta distributed formation probabilities with corresponding means and variances

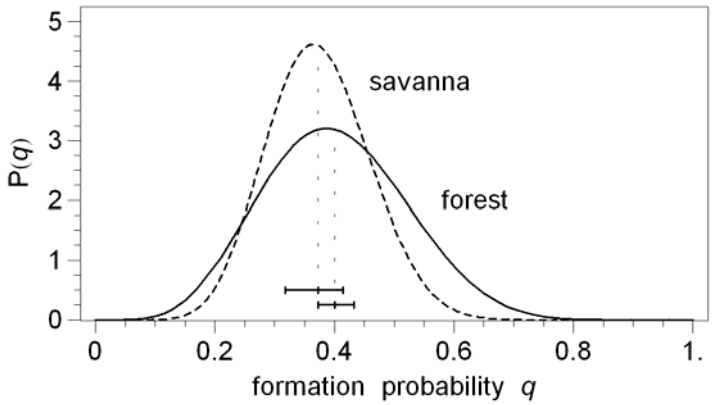

Fig. 2: The beta-distributions of the formation probability *q*; 95%-confidence limits of the mean μ_q are illustrated as bars above the *q*-axis.

Fig. 3 shows the observed numbers of female worms and nodules for individuals in villages of Liberia (forest strain) and Burkina Faso (savanna strain) with the average number of nodules as a function of the total female worm burden. The 95% regions of tolerance cover, respectively, 96% and 94% of the obser-

vations in Liberia and Burkina Faso, and therefore explain the observed variability very well.

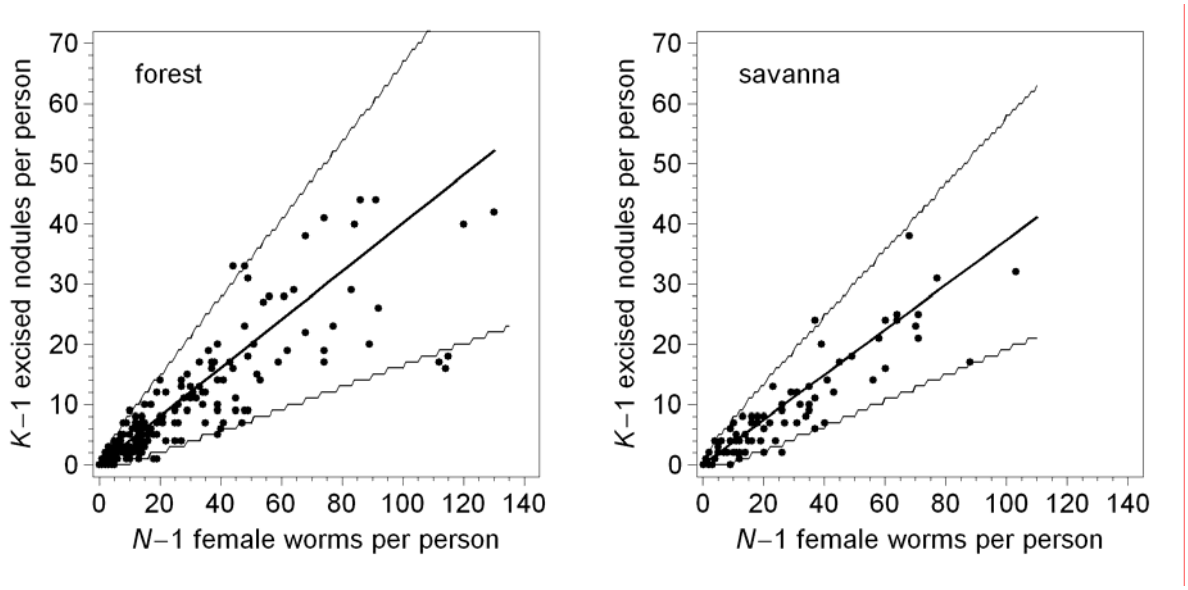

Fig. 3: Comparison between observed data and model prediction. Each point represents the number of female worms and nodules per person. Bold line: mean $\mu_{K(\alpha,\beta)}$ according to the beta binomial distribution; thin line: discrete 95% region of tolerance.

Validation of the model

Since the model makes use of distributions based on the finite support *N,* individual hosts contribute specifically to the distribution of nodules per person in the host population (dependent on their total female worm burden N_i). Accordingly, the host population must be described in terms of the mixture of these individual distributions. In practical terms this means that all theoretical, individual-specific distributions of the number of excised nodules per person were summed up, resulting in the expected distribution for the population. This was done analogously for the distribution of the number of worms per nodule, either using the individual-specific values for N_i and q_i (individual-based fit, see above) or using N_i in combination with the parametric formation probability based on the population parameters α and β (parametric fit).

As shown in Fig. 4 this mixture of individual beta binomial distributions yields a good prediction of the observed distribution of excised nodules per person in both forest and savanna settings. Fig. 5 shows the predicted nodule size represented by the parametric and the individual-based fit. The logarithmic scale is added, to show the low frequencies of large nodule sizes. A χ^2-tests on the individual-based fit cannot be performed, because the number of q_i reduces the number of the degrees of freedom below zero. χ^2-tests on the other fits show significant results due to mixed influences from outliers,

underestimation of the observations (Fig. 5) and variability in the observations (Fig. 4).

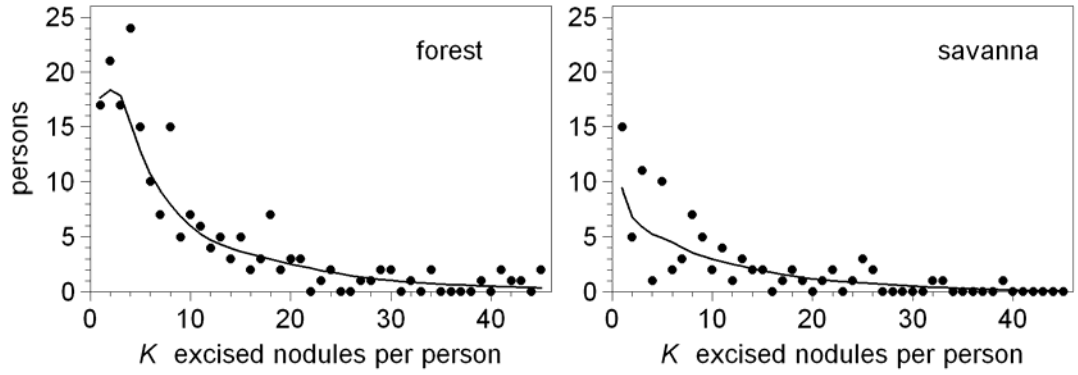

Fig. 4: Comparison of the observed distribution of nodule numbers per person (•) with the theoretically expected distribution (-) (the latter is the sum of beta binomial distributions (eq. (3)) of all individuals, calculated on the basis of α, β and the individual N_i).

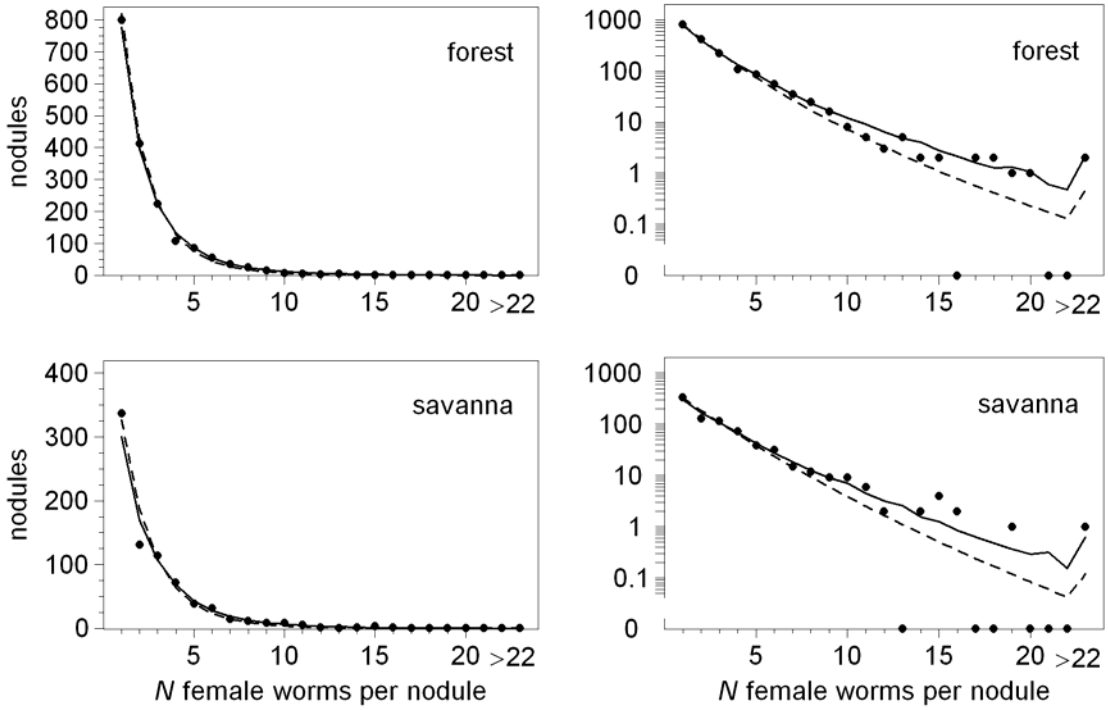

Fig. 5: Comparison of the observed distribution of nodule sizes (•) with the theoretically expected distribution (sum of the partition distributions). Dashed line: parametric fit, calculated on the basis of α, β and N_i (eq. (6a) with (3)). Solid line: individual-based fit, calculated on the basis of q_i and N_i (eq. (6c)). Graphs in the right column show the logarithmic representation of the same data as in the left column.

Predicting the number of female worms from palpation or surgery data

The quantiles shown in Fig. 6 demonstrate the expected variability if the numbers of live and dead female worms per person are deduced from surgery data. Using the chart requires consideration of the following three points:

1. To obtain the expected number of live female worms from the chart it is necessary to subtract the percentage of dead female worms. The data do not show a significant decline or increase in the proportion of dead females with increasing total female worm burden. Therefore for practical purposes the values can be set constant and they amount to 12.2% and 15.2% for the forest and savanna strains, respectively (Table 1).
2. If the chart is used to predict the number of live female worms from palpation data the number of palpated nodules must first be multiplied by 1.6 (forest strain) or 1.25 (savanna strain) to get the number of nodules expected in a nodulectomy (Albiez, 1983). However, it is important to note that in this case the variance given in the chart is only a lower estimate, because the variance caused by palpation is not considered.
3. It should be noticed that the numbers of female worms predicted from the chart refer to the number found in the nodulectomy trial, in which the presence of deep nodules was not examined. A crude approximation to the expected real number of parasites is given by multiplication with factor 3.5 (forest strain) (Duke, 1993), which is the only available figure for considering deep nodules.

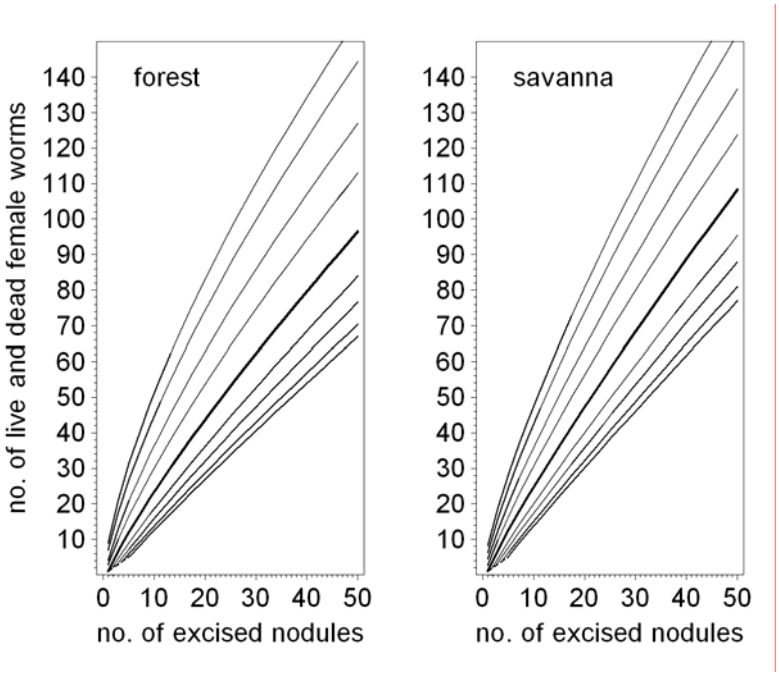

Fig. 6: Quantiles for the predicted number of live and dead female worms as based on the number of palpated nodules. Central, bold line: median, wrapped by the 50%, 75%, 90% and 95% regions of tolerance (thin lines). The discrete, stepwise functions were smoothed.

DISCUSSION

Biological implications

The results deduced from this model show an aggregation of female *O. volvulus* in nodules explained by a probabilistic process based on a single parameter, the formation probability *q*, or its counterpart, the invasion probability *p*=1-*q*. The estimates for the average formation probabilities μ_q=0.40 (forest strain) and μ_q=0.37 (savanna strain) clearly indicate that female infective larvae tend to join existing nodules rather than forming new ones. This suggestion is also supported by the small proportion of female worms found living solitary in a nodule, with 16% in forest and 18% in savanna localities of West Africa.

In 40% of the operated persons the total number of males exceeded the number of nodules, suggesting that the aggregation of females might facilitate mating due to the abovementioned necessity for repeated insemination (Schulz-Key & Karam, 1986). However, this is not the only possible explanation for worm aggregation. Bovine *O. ochengi*, living in intradermal nodules, is the closest relative of the human parasite, showing many morphological and genetic similarities. It is suggested that humans acquired the parasite when commencing cattle husbandry thousands of years ago (Bain, 1981). Both *Onchocerca* species still share the same vectors and have a similar reproductive biology such as repeated inseminations and migration of male worms (Schulz-Key & Karam, 1986). However, females of *O. ochengi* do not at all aggregate in nodules, being usually solitary (nevertheless nodules accumulate in a small area of the ventral part of the host). This inconsistency between the behaviour of *O. volvulus* and *O. ochengi* raises questions as to the role and formation of the nodule and as to the nature of the mechanism responsible for sexual attraction and for attraction of female larvae to already existing nodules.

It is supposed that intranodular species are more specialized and phylogenetically younger than those that do not form nodules (Bain, 1981). In addition, the morphology of these onchocercomata is not uniform. Mobile female worms are found in cystic nodules (e.g. *O. jakutensis,* Plenge-Bönig, Krömer & Büttner, 1995) or else closely and tightly embedded in connective tissues as in the human parasite. It is suggested that nodule formation is actively induced by still unknown stimuli from the parasite.

The natural host spectrum of the genus *Onchocerca* is principally represented by ungulates with humans (or primates) being atypical hosts. This fact supports the hypothesis of human onchocerciasis originating from a zoonosis. Since the parasite-host relationship of the human species seems to be evolutionarily much younger than that of its bovine counterpart, it is also suspected to be less balanced. Zoonoses often induce severe immune

reactions and pathologies. This might result in exceptionally strong and exaggerated nodule formation in human onchocerciasis.

There are several conceivable factors which might be responsible for the attraction of invading filarial larvae. For example, products secreted or released by the resident female worm might allure other worms; or less probably, the larva might be guided by a chemical gradient derived from the reactive tissue of the host. In contrast, sexual attraction should be caused by pheromones irrespective of the existence of a nodule. These products released by the female worms might be excreted or derived from the uterine fluid which extravasates during release of microfilariae. The actual reproductive state of the female is suspected to play an important role in signaling readiness to mate.

The degree of clustering of female parasites is increased by the formation of conglomerates of nodules with adherent young satellite nodules (Albiez, 1983; Albiez et al., 1988; Büttner et al., 1988). No relevant dependence of the average size of the nodules on the number of satellites was found. However, the distribution of formation probabilities for those persons who show only wheak conglomeration, has greater variance (analysis not shown, further aspects see below). A comparison of the aggregation patterns does not reveal striking differences between the forest and the savanna strain of *O. volvulus,* because of overlapping confidence limits for the average formation probability (see Fig. 2).

The assumptions of the model are that a developing female larva joins or invades a nodule independently of the sizes of existing nodules and independently of the total female worm burden of a host. The first assumption implies that the attraction effect of a nodule on a developing larva would not depend on the number of females located in it. With respect to chemotaxis, this would mean that a developing female larva recognizes females in a nodule qualitatively but not quantitatively. The model prediction suggests this as a plausible explanation for the observation of smaller nodule sizes. However, the lack of the fit for higher nodule sizes (Fig. 5) indicates that there should exist a factor that weakly supports the formation of large nodules. The model cannot descriminate between a more heterogeneous or a preferred invasion of large nodules. Decriptive analysis suggests the first of these two posibilities (see below). According to the second assumption, the aggregation pattern is not altered by *N*, the total worm burden of a host. The pattern seems to be stable as given by the model and its partition distribution. This is also in agreement with the findings of Albiez et al. (1988) that the number of live female worms per nodule does not depend on the endemicity level.

To explain the observed variability of the data, it was assumed that the average formation probability for developing larvae depends on the host. This dependence is interpreted as a more or less intense host-specific reaction to worm encapsulation. A possible factor for this heterogeneity is the time lag

before the parasite is encapsulated by the immunological response of the host. Analysis of covariance does not show the host age or sex to affect the formation probability, so that a plausible reason for this variability is the differing immunological states of the individual hosts. It would be worthwhile to verify experimentally these speculations in order to clarify the rationale underlying this parasite behavior.

Statistical considerations

The basic model with a binomially distributed number of nodules and the same parameter q for all individuals cannot result in an acceptable fit of the data. In Fig. 5, for example, nodule sizes would be predicted from this model by a geometric distribution (linear decrease in logarithmic representation), of which the variance is too low. Thus, it is essential to implement variance-increasing effects in the individual-based distributions of nodule sizes. This can be achieved either by introducing heterogeneity on the level of the population or by implementing the formation probability as a linearly increasing function of the nodule size. Since both approaches yield the same distribution, it is theoretically impossible to estimate their impact simultaneously (Duerr & Dietz, 2000). We therefore decided that the variance-increasing effect shall be attributed solely to heterogeneity, which is a fundamental and widespread characteristic of parasitic infections. Should there exist a dependency with respect to the nodule size, then this contribution is incorporated and compensated by the aspect of heterogeneity.

In comparison to the individual-based fit, the parametric fit in Fig. 5 shows an understimation of large nodule sizes. A χ^2-test shows a significant result which has to be attributed to mixed influences from outliers, variability in the observations and underestimation of the observations. To interpret the latter means that individual q_i's contribute a greater variance than the parametric beta distribution. This additional variance might be attributed to the data-based observation that persons who show only a weak degree of conglomeration have a greater variance in their distribution of q_i's. However, as stated before, a possible dependency from the nodule size cannot be excluded. The intention of this work focussed on modelling with a minimal set of parameters and, altough the derivation of the model requires some efforts, it does suggest only a simple, *plausible* explanation for the genesis of the data. Discrepancies between model prediction and observed data may provide a stimulus for further discussion of the aggregation behaviour of *O. volvulus.*

Acknowledgement

The authors are grateful to M. Eichner and H.H. Diebner for fruitful collaboration and to M.G. Basáñez for suggesting the use of the model to estimate worm burden from nodule palpation. This work was supported by the *f*ortüne grant no. 528 of the University Hospital, Tübingen, Germany and by a grant from the Deutsche Forschungsgemeinschaft, Graduiertenkolleg Lebensstile, soziale Differenzen und Gesundheitsförderung.

REFERENCES

ALBIEZ, E.J. (1983). Studies on nodules and adult *Onchocerca volvulus* during a nodulectomy trial in hyperendemic villages in Liberia and Upper Volta. I. Palpable and impalpable onchocercomata. *Tropenmedizin und Parasitologie* **34**, 54-60.

ALBIEZ, E.J., BÜTTNER, D.W.& SCHULZ-KEY, H. (1984). Studies on nodules and adult *Onchocerca volvulus* during a nodulectomy trial in hyperendemic villages in Liberia and Upper Volta. II. Comparison of the macrofilaria population in adult nodule carriers. *Tropenmedizin und Parasitologie* **35**, 163-166.

ALBIEZ, E.J., BÜTTNER, D.W. & DUKE, B.O.L. (1988). Diagnosis and extirpation of nodules in human onchocerciasis. *Tropical Medicine and Parasitology* **39** (Suppl. IV), 331-346.

BAIN, O. (1981). Le genre *Onchocerca*: hypothèses sur son évolution et clé dichotomique des espèces. *Annales de Parasitologie* **56**, 503-526

BÜTTNER, D.W., ALBIEZ, E.J., VON ESSEN, J.& ERICHSEN, J. (1988). Histological examination of adult *Onchocerca volvulus* and comparison with the collagenase technique. *Tropical Medicine and Parasitology* **39** (Suppl. IV), 390-417.

COLLINS, R.C., LUJAN, R., FIGUEROA H. & CAMPBELL, C.C. (1982). Early formation of the nodule in Guatemalan onchocerciasis. *American Journal of Tropical Medicine and Hygiene* **31** (2), 267-269.

DUERR, H.P. & DIETZ, K. (2000). Stochastic models for aggregation processes. *Mathematical Biosciences* **165**, 135-145.

DUKE, B.O.L (1993). The population dynamics of *Onchocerca volvulus* in the human host. *Tropical Medicine and Parasitology* **44**, 61-68.

PLENGE-BÖNIG, A., KRÖMER, M. & BÜTTNER, D.W. (1995). Light and electron microscopy studies on *Onchocerca jakutensis* and *O. flexuosa* of red deer show different host-parasite interactions. *Parasitology Research* **81**, 66-73

PRESS, W. H., TEUKOLSKY, S. A., VETTERLING, W. T. & FLANNERY, B. P. (1992). *Numerical recipes in C,* 2nd edn. Cambridge University Press, Cambridge.

SCHULZ-KEY, H. & ALBIEZ, A.J. (1977). Worm burden of *Onchocerca volvulus* in a hyperendemic village of the rain-forest in West Africa. *Tropenmedizin und Parasitologie* **28**, 409-560

SCHULZ-KEY, H., ALBIEZ, E.J. & BÜTTNER, D.W. (1977). Isolation of adult *Onchocerca volvulus* from nodules. *Tropenmedizin und Parasitologie* **28**, 428-430.

SCHULZ-KEY, H. & KARAM, M. (1986). Periodic reproduction of *Onchocerca volvulus*. *Parasitology Today* **2**, 284-286.

WIMMER, G. & ALTMANN, G. (1999). *Thesaurus of univariate discrete probability distributions*. Stamm, Essen, Germany.

The interpretation of age-intensity profiles and dispersion patterns in parasitological surveys[1]

SUMMARY

The present paper describes how age-intensity profiles of parasite burdens are affected by processes controlling the distribution of the parasites in the human host. In particular, we outline the concept of density-dependent parasite establishment which has recently been developed with respect to parasite species, especially helminths, which can induce a state of immunosuppression in their hosts. Properties and the impact of this process on age-intensity profiles are compared to other commonly known processes as i) age-dependent exposure, ii) parasite-induced host mortality, iii) heterogeneity within the host population, iv) clumped infection and v) density-dependent parasite mortality. For each of these processes we show typical patterns in the age-intensity profile and provide, if possible, explicit and simple solutions for the age-dependent mean parasite burden and the corresponding dispersion patterns. Emphasis is given on age-intensity profiles resulting from the superposition of different processes. By means of two examples we show that the interpretation of observed patterns can be ambiguous if more than one process takes place. These findings underline that age-intensity profiles should be interpreted on the basis of available *a priori* knowledge about the processes assumed to be involved. For purposes of testing different hypotheses, a simulation program is provided with which discrepancies between model prediction and data can be explored.

INTRODUCTION

The distribution of parasite numbers within the host population is the result of many regulatory processes interacting with each other and controlling the stability of the host-parasite relationship. The simulation study by Crofton (1971) has stimulated a variety of investigations regarding the impact of such processes on the density and the distribution of parasites. In particular, dispersion or aggregation patterns have attracted much attention and the corresponding parasite distributions for many regulatory processes are known. After a paper of Anderson & Gordon (1982) suggested that certain alterations in age-specific parasite distributions point at parasite-induced host mortality, it has become popular to infer processes from observed dispersion patterns. Although the mathematical literature provides explicit solutions for many of these processes, it seems that their predictive capacity has rarely been used to test different hypotheses.

---

[1] eingereicht bei Parasitology: H.P. Duerr, K. Dietz, M. Eichner, The interpretation of age-intensity profiles and dispersion patterns in parasitological surveys

Here, we investigate how various processes regulating the acquisition of parasites and the survival of hosts and parasites influence the shape of age-intensity profiles as obtained from cross-sectional surveys. Extending the classification given by Hudson & Dobson (1982), we discriminate four types of age-intensity profiles as shown in Fig. 1. Representing the age-specific parasite distributions by means of their quantiles, age-intensity profiles can also illustrate dispersion patterns, i.e. the variability of parasite burdens over host age. Dispersion, usually represented by the standard deviation or the variance, is in the parasitological context often measured by the variance to mean ratio (*VMR*). This is an appropriate measure if dispersion is compared to the Poisson distribution (as a nullmodel, see below), for which the variance equals the mean, hence *VMR*=1. Values greater than one (variance>mean) are the most common dispersion pattern, indicating an overdispersed parasite distribution, often called aggregated distribution (Anderson & May 1991; Shaw et al. 1998). The *VMR* is also an important parameter with respect to the stability of the host-parasite relationships. (Adler & Kretzschmar 1992; Kretzschmar & Adler 1993).

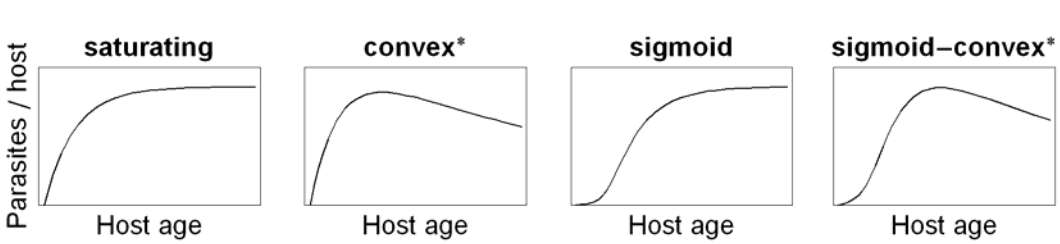

Fig. 1 : Four types of age-intensity profiles (* the term "convex" is used here as in the parasitological literature; in the mathematical literature this type of curve is called "concave").

This paper has two main intentions: Firstly, we will describe the properties and consequences of density-dependent parasite establishment, which has recently been suggested to be a main determinant of the age-intensity profiles found for cross-sectional data on parasite burdens of onchocerciasis patients (Duerr et al., submitted). Modelling other processes of parasite acquisition or regulation could not explain the observed data satisfactorily. Since the parasite *Onchocerca volvulus* is also known to induce an immunocompromised status in the human host (see for example Cooper et al. 2001; Soboslay et al. 1997), this kind of density-dependence has been implemented into the model which then yielded a good fit to the data. The influence of density-dependent parasite establishment on the age-specific parasite burdens in the host population can best be illustrated when compared to the other commonly known processes regulating the parasite density. Therefore the second intention is, to compare these regulatory processes, which are i) age-dependent exposure, ii) parasite-

induced host mortality, iii) heterogeneity within the host population, iv) clumped infection and v) density-dependent parasite mortality.

The most basic mathematical model describing the acquisition of parasites which do not multiply within the host (macroparasites, Anderson & May 1991) is an immigration-death process. In the following, we call it the "null"model. It describes the rate of change in the mean parasite burden *w* over host age *a* by the differential equation

$$\frac{dw}{da} = \lambda - \mu\, w\,, \tag{1}$$

where λ denotes the immigration rate (number of parasites establishing in the host per unit of time) and μ the death rate of parasites (with $1/\mu$ being the life expectancy of the parasite). In aged hosts, parasite acquisition and parasite mortality become balanced, hence the parasite burden does not change over age any more and we obtain the equilibrium parasite burden from *dw*/*da*=0 as

$$w^* = \frac{\lambda}{\mu}. \tag{2}$$

The age-dependent mean parasite burden *w*(*a*) is obtained by integrating equation (1), yielding

$$w(a) = \frac{\lambda}{\mu}\left(1 - e^{-\mu\, a}\right) = w^*\left(1 - e^{-\mu\, a}\right), \tag{3}$$

a saturating function which asymptotically approaches the equilibrium parasite burden.

A stochastic formulation of the nullmodel leads to parasite burdens which are Poisson distributed at any age (Cox & Miller 1965, p. 168) so that the probability of having *n* parasites is given by

$$P(n) = \frac{w^n}{n!}\, e^{-w}\ . \tag{4}$$

Here, *w* denotes the mean parasite burden, which can be taken from the deterministic model (3) and thus, we obtain the age-specific distribution of parasite numbers as shown in Fig. 11-a1. The Poisson distribution implies that the variance equals the mean and hence the variance to mean ratio is one, constantly over all host ages. Implicit assumptions of the nullmodel are that i) parasites infect the host randomly (homogeneous host-parasite encounter), ii) infection is not clumped (i.e. one parasite is transmitted per infectious contact) and iii) there is no density-dependence, neither in the acquisition nor in the survival of the parasites.

This paper is structured in four sections. The first three sections describe the six processes under investigation, classifying them into three categories according to their impact on the age-intensity profile: i) processes which affect only the mean (age-dependent exposure, parasite-induced host mortality), ii) processes which affect only the variance (heterogeneity, clumped infection) and iii) processes which affect both, mean and variance in the age-intensity profile (density-dependent parasite mortality and establishment). The fourth section shows by means of two examples that the superposition of different processes can produce similar dispersion patterns and that the same process can produce differing dispersion patterns depending on the processes involved in superposition. These examples show that the association between process and pattern is ambiguous and that the complex nature of several processes in superposition makes it difficult to infer processes from observed patterns.

METHODS

Simulations were performed where explicit solutions are not available. The simulation algorithm is designed such that it is a stochastic equivalent of the differential equations given in the particular sections. Parameters were taken as listed there, operating in a population of 100.000 individuals. The time step Δ is variable because it is determined by random numbers R_Δ according to $\Delta = -\ln(R_\Delta / \Sigma)$, where Σ represents the sum of all rates involved in the current evaluations. Each step results from sampling two random numbers, where the first one (R_Δ) determines the exponentially distributed time step Δ and the second one (R_S) determines the type of step S according to a multinomial distribution.

RESULTS

1 Processes which affect only the mean of the parasite distributions

1.1 Age-dependent exposure

Certain age groups may be only partly exposed to infection and consequently acquire only a proportion of infections per unit of time. The exposure factor can increase (children are less exposed) or decrease with age (the elderly are less exposed).

Model: Age-dependent exposure is modelled by multiplying the acquisition rate λ with an age-dependent exposure factor $p(a)$ within the intervall $[0,1]$. The rate of change in the parasite burden over age is then

$$\frac{dw}{da} = \lambda\ p(a) - \mu w\,. \tag{5}$$

It is useful to assume an exposure function of the form

$$p(a) = \frac{1}{1+\exp\left(-\beta\,(a-A)\right)}, \tag{6}$$

where A denotes the age of 50% exposure and β is proportional to the slope of the exposure function at this age. Positive values for β yield an increasing exposure function and negative values yield a decreasing function. Accordingly, for positive β (yielding $p(\infty)=1$) the equilibrium parasite burden is the same as in the nullmodel (equation (3)) and for negative β (yielding $p(\infty)=0$) it is zero. With $A \approx 10$ years and $\beta \approx 0.55$ per year the function approximates an exposure which increases proportional to the body surface during growth in childhood (Dietz 1982b). A function of this form is flexible enough to cover many patterns of age-dependence and it allows to solve the differential equation (5) (see Appendix 1).

Tendency of the mean: The impact of the exposure function can be seen in Fig. 2: If exposure increases with age, the age-intensity profile becomes sigmoid because of the delayed parasite acquisition during the first years of life; if it decreases, the age-intensity profile becomes "convex" because of the reduced parasite acquisition during later life. Similar patterns in the mean parasite burden can result from acquired, protective host immunity, which controls parasite establishment after accumulated experience of infection (see Discussion).

Dispersion patterns: Age-dependent exposure affects only the mean in the age-intensity profile; parasite burdens are Poisson distributed at any age and hence the variance equals the mean, resulting in *VMR*=1 (Fig. 11-b).

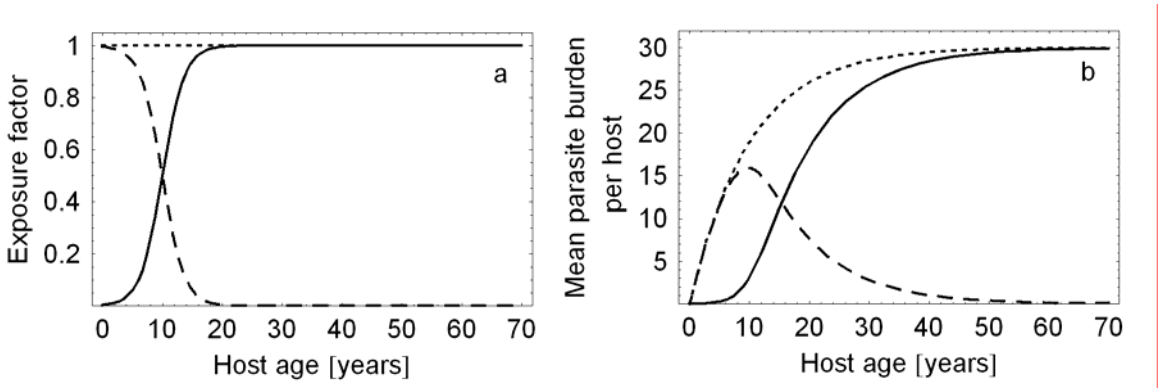

Fig. 2: Two cases of age-dependent exposure with an immigration rate of λ=3 parasites/year and a parasite life expectancy of $1/\mu$=10 years. The dotted lines show the immigration death process (nullmodel) for comparison. **a**: Exposure functions (equation (6)). Solid line: Increasing exposure with parameters *A*=10 years, β=0.55 per year. Dashed line: Symmetrically decreasing exposure with parameters *A*=10 years, β=-0.55 per year. **b**: Age-intensity profiles (equations see Appendix 1).

1.2 Parasite-induced host mortality

Some parasites increase directly or indirectly the mortality of their hosts and a linear relationship between parasite burden and host mortality has been proposed (Hudson & Dobson 1982). Assuming such a linear relationship, parasite-induced host mortality affects only the mean and parasites are Poisson distributed among hosts of a given age (Dietz 1982a; Hadeler & Dietz 1982; Isham 1995). This process affects the variance only if interacting with variance-increasing processes such as heterogeneity in exposure among hosts or clumped infection (see section 2). There are two exceptions where parasite-induced host mortality may alter the dispersion pattern; however, since these exceptions are rather theoretically interesting than biologically relevant, we have placed this process in section 1. Firstly, underdispersed parasite distributions may result from a threshold parasite burden above which hosts immideately die. In this case, the variance is reduced due to the removal of heavily parasitized hosts, i.e. the parasite distributions are truncated (Crofton 1971b). Secondly, overdispersed parasite distributions may result from an excess mortality which is constant, i.e. independent of the parasite burden (Barbour & Pugliese 2000). However, our simulations performed for a wide range of parameter values did not yield any relevant degree of overdispersion in this case (i.e. *VMR*s did hardly exceed values of 1.1).

Model: In the following, the degree of parasite-induced host mortality is denoted by parameter α, which is the rate at which hosts die per parasite and year. This excess mortality operates in the same way as the natural parasite death rate μ, so that we can add both parameters in the differential equation as follows:

$$\frac{dw}{da} = \lambda - (\alpha + \mu)\, w\,, \tag{7}$$

yielding a mean parasite burden of

$$w_\alpha(a) = \frac{\lambda}{\alpha + \mu}\left(1 - e^{-(\alpha+\mu)a}\right), \tag{8}$$

(Dietz 1982a; Hadeler & Dietz 1982). From $dw/da=0$, we find the excess mortality in the equilibrium parasite burden of very old hosts ($a \to \infty$) as

$$w^*_\alpha = \frac{\lambda}{\alpha + \mu}\,. \tag{9}$$

Tendency of the mean: As can be seen in Fig. 3, parasite-induced host mortality, which increases linearly with the parasite burden, can practically not be detected in the age-intensity profile: one would rather find a population dying out than finding a reduction in the mean parasite burden over age. In this context, the proportion of hosts having survived parasite infection is given by Dietz (1982a) with

$$S_\alpha(a) = \exp\left[-\frac{\alpha\lambda}{(\alpha+\mu)^2}\left\{a(\alpha+\mu) - 1 + \exp\left[-a(\alpha+\mu)\right]\right\}\right]. \tag{10}$$

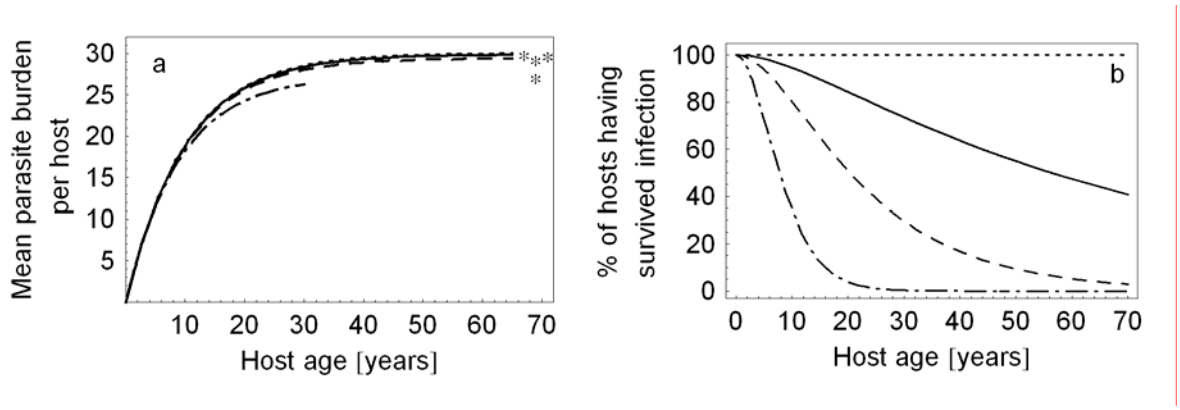

Fig. 3: The effect of parasite-induced host mortality on the mean parasite burden in an age-intensity profile and on host survival. The dotted line shows the nullmodel for comparison. For all four curves the immigration rate is λ=3 parasites/year and the parasite life expectancy is $1/\mu$=10 years, conditioned on host survival. **a**: Age-intensity profiles according to equation (8); asterisks in the right margin of the graph indicate the equilibrium given by equation (9). **b**: Host survival (only deaths caused by the parasite are considered, i.e. the natural host mortality is omitted). Solid line: α=0.0005 per parasite and year, dashed line: α=0.002 per parasite and year, dash-dot line: α=0.01 per parasite and year.

To illustrate the effect of parasite-induced host mortality on the age-intensity profile, we introduce parameter *p* denoting the relative reduction in the equilibrium parasite burden with excess mortality, w^*_α, which is compared with the equilibrium of the nullmodel, w^*, without excess mortality, i.e. we set $p = (w^* - w^*_\alpha)/w^*$. After solving for α, this relation is independent of the immigration rate λ and we obtain

$$\alpha = \mu \frac{p}{1-p}. \tag{11}$$

If, for example, we expect parasite-induced host mortality to reduce the mean parasite burden by 10% (p=0.1), assuming the life expectancy of the parasite to be $1/\mu$=10 years, then the excess host mortality rate must amount to α=0.01 additional host deaths per parasite and year. This value, however, yields an implausible host survival because 97% of the population would have died from infection before reaching the age of 20 years (Fig. 3b, $S_{0.01}(20)$=0.97, assuming an immigration rate of λ=3 parasites/year). This example shows the importance of verifying an hypothesis on parasite-induced host mortality with the survival function of the hosts.

2 Processes which affect only the variance in parasite distributions

2.1 Heterogeneity within the host population

Heterogeneity in exposure or susceptibility is the most commonly known process to cause overdispersed parasite distributions and its interpretation is often associated with the negative binomial distribution (NBD). This is because the NBD can be generated from a Poisson distribution, of which the mean varies according to a gamma distribution (Greenwood & Yule 1920). In the parasitological context, this means that we can regard the infection with parasites as an immigration-death process (which yields Poisson distributed parasite burdens), assuming that the immigration rate λ varies among hosts according to a gamma distribution.

Model and tendency of the mean: Heterogeneity does only affect the dispersion pattern in the age-intensity profile; the mean parasite burden is identical to the nullmodel with a saturating profile. We introduce parameter h_i , which denotes a host-specific exposure factor. The annual acquisition rate of a host is then multiplied with this factor and we assume that it remains constant throughout the host's life. The age-dependent mean parasite burden of an individual host *i* of age *a* is then

$$w_i(a) = h_i\, w^* (1 - e^{-\mu a}), \tag{12}$$

where *w** denotes the equilibrium parasite burden according to the nullmodel (equation (2)). In the following, we consider cases where h_i varies according to a gamma distribution because (i) of the association to the NBD, (ii) it is a distribution which is continuous and defined only for nonnegative values, and (iii) it is capable of covering many patterns of host heterogeneity. Since the exposure factor averaged over the population must equal one, we can restrict ourselves to a gamma distribution with mean=1, so that its density can be written as

$$\phi(h) = \frac{e^{-k\,h}\, k^k\, h^{k-1}}{\Gamma(k)}, \tag{13}$$

where $\Gamma(.)$ denotes the gamma function; the variance of the gamma distribution is given in this case by $\sigma^2_{\text{gamma}}=1/k$.

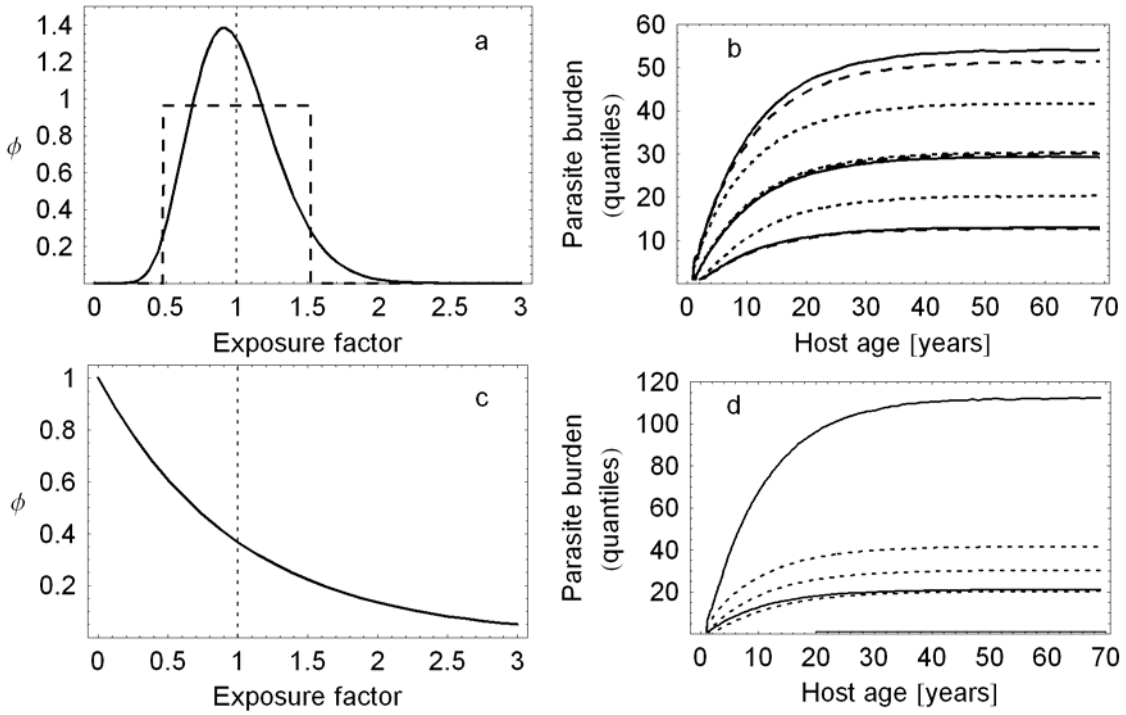

Fig. 5: The effect of heterogeneity in exposure or susceptibility on the variance in parasite burdens. **a,c**: Distributions of the exposure factor (each with mean=1); the dotted line shows the assumption in the nullmodel for comparison. **a**: Solid line: Gamma distribution with σ^2_{gamma}=0.1 (i.e. *k*=10). Dashed line: Uniform distribution with σ^2=0.1 (intervall [0.49;1.51]); **c**: Gamma distribution with σ^2_{gamma}=1 (i.e. *k*=1). **b,d**: Simulated age-intensity profiles represented by median and quantiles 2.5% and 97.5% (the 2.5% quantile in d with *k*=1 (solid line) is almost zero). The dotted quantiles show the nullmodel for comparison. For all curves the immigration rate is λ=3 parasites/year and the parasite life expectancy is $1/\mu$=10 years.

Dispersion patterns: If heterogeneity is introduced by mixing the acquisition rate λ according to a gamma distribution, then the parasite burdens are negative binomial distributed and the probability of having *n* parasites is

$$P(n) = \frac{\Gamma(k+n)}{\Gamma(n+1)\Gamma(k)} \quad \frac{(w/k)^n}{(1+w/k)^{k+n}}, \tag{14}$$

where $k=1/\sigma^2_{gamma}$ as mentioned before and *w* denotes the mean parasite burden. Since in this case parasite burdens have a negative binomial distribution at all ages (Dietz 1982a; Isham 1995), we can replace *w* by the deterministic solution of the nullmodel (equation (3)) and obtain the age-specific distributions of parasite burdens as shown in Fig. 5b,d. The variance in these distributions is proportional to the variance of the heterogeneity-introducing distributions whereby the type of the mixing distribution is less important

(compare uniform with gamma distribution in Fig. 5a,b). Increasing the variance of the mixing distribution shifts the median towards lower parasite burdens due to the skewness introduced by the mixing distribution. For a mixing distributions with mean=1 and variance σ^2, the age-specific dispersion of parasite distributions is given by

$$\begin{aligned} \sigma_h^2(a) &= w(a)\left(1+w(a)\sigma^2\right) \\ VMR_h(a) &= 1+w(a)\sigma^2, \end{aligned} \tag{15}$$

where $w(a)$ denotes the mean parasite burden of the nullmodel. Fig. 11-f illustrates these properties for the case where heterogeneity is implemented by the NBD, where the variance in the parasite distributions increases quadratically with the mean and the *VMR* increases linearly with the parasite burden.

2.2 Clumped infection

Infection is always a discrete event, i.e. parasites infect hosts in doses of 1, 2, 3 or more parasites per infectious contact. Clumping affects only the dispersion pattern of parasite distributions, not the mean.

Model and tendency of the mean: Let m_c be the mean package size, i.e. the mean number of parasites transmitted to the host per infectious contact and φ the contact rate. Then, $\lambda = \varphi m_c$ and the age-dependent mean parasite burden is

$$w_m(a) = \frac{\varphi m_c}{\mu}(1-e^{-\mu a}) \tag{16}$$

with an equilibrium parasite burden of $w_m^* = \varphi m_c / \mu$.

Dispersion patterns: The effect of clumped infection on the age-specific variance to mean ratios (*VMR*s) is opposite to the pattern caused by heterogeneity: overdispersion is high in children and it decreases asymptotically to a constant value at ages where the equilibrium is approached (Grenfell et al. 1995) (compare Fig. 11-g2 with f2). Higher overdispersion at young ages results from the dispersed parasite input which is - relatively seen - larger for low parasite burdens than for high ones. The age-specific variances in parasite distributions can be obtained from Dietz (1982a):

$$\sigma_m^2(a) = \frac{\varphi m_c}{\mu}(1-e^{-\mu a})\left(1+\frac{\sigma_c^2+m_c^2-m_c}{2}\right)(1+e^{-\mu a}), \tag{17}$$

where m_c and σ_c^2 denote the mean and the variance of the distribution of package sizes, respectively.

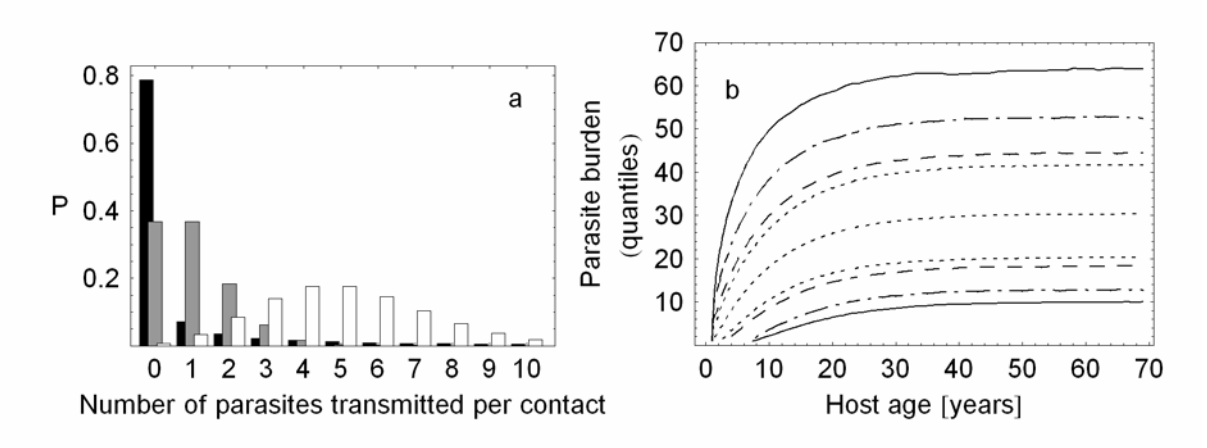

Fig. 6: The effect of clumped infection on the distributions of parasite burdens. **a**: Underlying distributions. **b**: Simulated age-intensity profiles represented by quantiles 2.5% and 97.5% each. The dotted quantiles show the nullmodel for comparison, additionally with median. Black bars in a and solid lines in b: Negative binomial distribution with mean m_c=1 and k=0.1 (equation (14) with w=m_c). Grey bars in a and dashed lines in b: Poisson distribtution with mean m_c=1. White bars in a and dash-dot lines in b: Poisson distribution with mean m_c=5. For all four distributions in b the immigration rate is λ=3 parasites/year and the parasite life expectancy is $1/\mu$ =10 years.

The type and shape of the package size distribution strongly depends on the parasite, its transmission mode and the endemicity level. Whereas the Poisson distribution noteworthily contributes only with a large mean package size to overdispersed parasite burdens, the NBD can, depending on the value of the dispersion parameter k, yield an extent of overdispersion comparable to the influence of heterogeneity. As in the case of heterogeneity, high variances in the package sizes (small k) yield a median lying considerably below the mean, i.e. the parasite distribution becomes more and more skewed.

3 Processes which affect both mean and variance in parasite distributions

3.1 Density-dependent parasite mortality

Parasite mortality can increase with increasing parasite burden (parasite density), for example due to limited host resources or immunological host defence.

Model: For purposes of interpretation, it is useful to assume that each parasite enhances the natural mortality rate μ of the parasite population in the host by a factor q (e.g. for q=0.1 each parasite enhances μ by 10%). With this factor, we denote the age-specific rate of change in the parasite burden as

$$\frac{dw}{da} = \lambda - \mu(1+qw)\,w\,. \tag{18}$$

This is a Riccati differential equation for which the solution yields the age-dependent parasite burden as

$$w_q(a) = 2\lambda\left(\mu\sqrt{\Delta}\,\frac{1+e^{-a\mu\sqrt{\Delta}}}{1-e^{-a\mu\sqrt{\Delta}}}+\mu\right)^{-1}, \tag{19}$$

where Δ =1+ 4λq /μ ; the equilibrium parasite burden in very old hosts ($a \to \infty$) is

$$w_q^* = \frac{\sqrt{\Delta}-1}{2q}\;;\;\; q>0\,. \tag{20}$$

For q=0 we get the equilibrium parasite burden of the nullmodel (2).

Tendency of the mean: We see in Fig. 7a that the age-intensity profile with density-dependent parasite mortality is still saturating, having a reduced equilibrium parasite burden according to the value of q. Although equation (20) is nonlinear in μ, the equilibrium parasite burden increases - for relevant values of μ - almost linearly with the life expectancy of the parasite (Fig. 7b), as it is the case in the nullmodel.

Dispersion patterns: Density-dependent parasite mortality produces slightly underdispersed parasite distributions (Anderson & Gordon 1982; Barbour & Pugliese 2000), i.e. the variance is lower than in the nullmodel and the variance to mean ratio is less than one. We see in Fig. 11-d that this underdispersion develops until the equilibrium is reached. For the sake of completeness, we note that negative density-dependence in parasite mortality produces opposite effects, i.e. it yields overdispersion comparable to positive density-

dependence in parasite establishment (see end of paragraph 3.2). A biological example for such a negative correlation between parasite burden and parasite mortality is not known and, therefore, we do not consider it further.

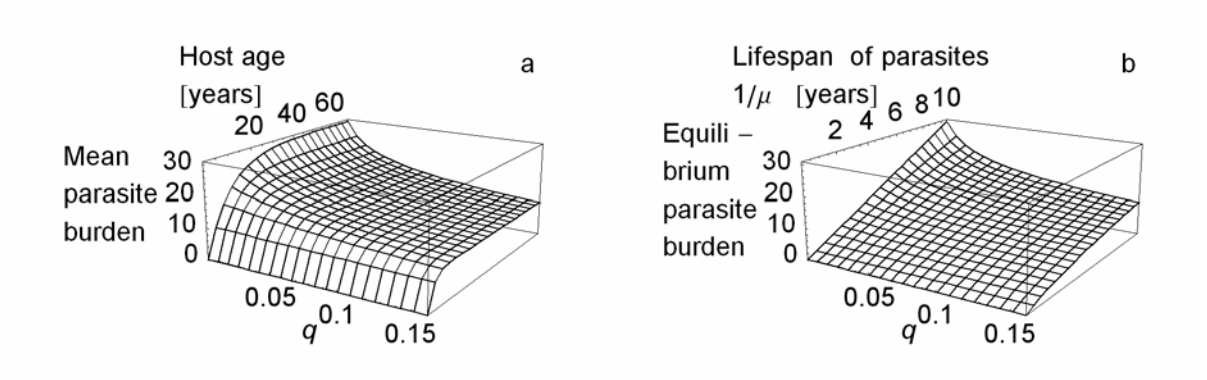

Fig. 7: The effect of density-dependent parasite mortality under an immigration rate of λ=3 parasites/year. **a**: Age-intensity profiles according to equation (19) for a parasite life expectancy of $1/\mu$=10 years and varying mortality factor *q*. **b**: Equilibrium parasite burden depending on the parasite life expectancy and *q* (equation (20)).

3.2 Density-dependent parasite establishment

The concept of density-dependent parasite establishment has emerged from a modelling approach describing age-intensity profiles of onchocerciasis data (Duerr et al., submitted). Our data show an almost linear increase in parasite burdens over host age. Such a profile can be produced either by an unrealistically high life expectancy of the parasite (*L*>100 years) in combination with an unrealistically low immigration rate or, alternatively, by age-dependent exposure increasing almost linearly with age. Both assumptions seemed inacceptable and moreover, experimental knowledge pointed at immunosuppressive processes which are likely to regulate the density of this parasite in the hosts (Cooper et al. 2001; Elkhalifa et al. 1991; Soboslay et al. 1997). Parasite-induced immunosuppression leads to an autocatalytic parasite establishment with positive feedback, such that parasites, which have already established in the host, increase the hosts susceptibility with respect to the infection with further parasites. To avoid an uncontrollable self-enhancement, this positive feedback must be limited by an upper boundary in the parasite burden which results in a maximum establishment rate.

Model: As modelled for the other processes, the rate of change in the age-specific parasite burden can be described by an immigration-death process:

$$\frac{dw}{da} = \lambda(w) - \mu w\,, \tag{21}$$

in which the immigration (establishment) of parasites $\lambda(w)$ depends on the parasite burden w present in the host. We introduce an establishment function of the form

$$\lambda(w) = \frac{\lambda_0 + s\,\lambda_\infty\, w}{1 + s\, w}, \tag{22}$$

where λ_0 is the number of parasites establishing per year in non-infected hosts, ($\lambda(0)=\lambda_0$) and λ_∞ is the rate of infection in most heavily infected hosts ($\lambda(\infty)=\lambda_\infty$). The parameter s controls the "speed" with which the establishment rate $\lambda(w)$ changes from λ_0 to λ_∞. Therefore, s phenomenologically represents the degree of immunosuppression caused per parasite (high values of s lead to an establishment function where λ_∞ is reached "fast", indicating that few parasites are sufficient to induce the status of maximum immunosuppression). Modelling immunosuppression assumes that $\lambda_0<\lambda_\infty$, i.e. the establishment rate increases with increasing parasite burden. By choosing $\lambda_0>\lambda_\infty$ we can consider gain in immunocompetence (this case, however, is only shown for purposes of comparison; it is not investigated further because this model assumes that immunity results only from the current parasite burden and not from the past experience of infection). The special cases of s=0 or $\lambda_0=\lambda_\infty$ lead to the nullmodel with λ=constant.

Tendency of the mean: An explicit solution to the age-dependent parasite burden can only be given for the inverse function (not shown) of age for a given number of parasites. From dw/da=0 we can derive the equilibrium parasite burden

$$w^* = \frac{1}{2\,s\,\mu}\left(s\,\lambda_0 - \mu + \sqrt{(s\,\lambda_\infty - \mu)^2 + 4\,s\,\lambda_0\,\mu}\right). \tag{23}$$

In the following, we restrict ourselves to explaining the dynamics of this process qualitatively (see also Fig. 8). Density-dependent parasite establishment which increases with increasing parasite burden (positive density-dependence) has a sigmoid age-intensity profile. Children, still immunocompetent due to low parasite burdens, acquire only few parasites per year so that the initial increase in the age-intensity profile occurs very slowly. But, as soon as some parasites have managed to establish in the host, immunosuppression takes place and facilitates further infections; this appears as an increase in the age-intensity profile. In the course of developing a high parasite burden, this process gradually leads to an immunocompromised host status, where additionally establishing parasites cannot further enhance the extent of immunosuppression. Consequently, the age-intensity profile saturates and the host acquires the maximum number of parasites per year (λ_∞). Whereas a positive density-dependence prominently affects the age-intensity profile, negative density-dependence, leads to rather unspectacular results: the para-

site burden saturates as in the nullmodel; however, the equilibrium is reached earlier in life because of a higher λ_0 being necessary to yield a comparable equilibrium.

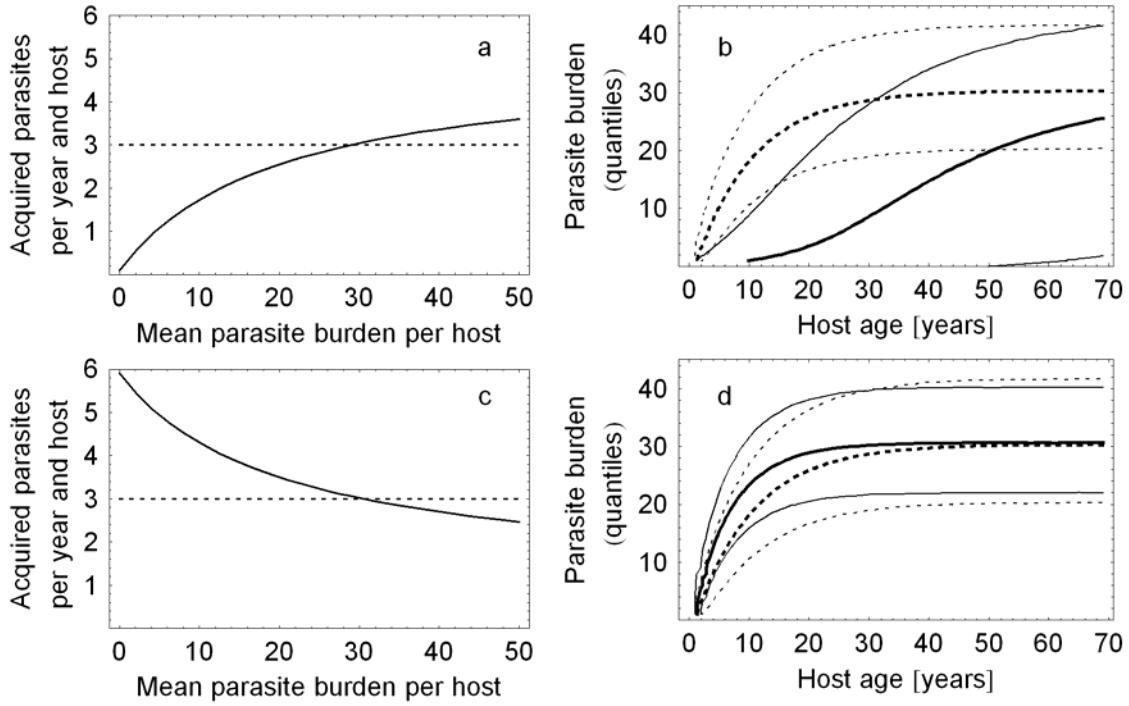

Fig. 8: The effect of density-dependent parasite establishment on the age-specific parasite distributions. The dotted lines show the nullmodel (λ=3 parasites/year) for comparison. All three age-intensity profiles lead to an equilibrium parasite burden of 30 parasites/host using a parasite life expectancy of $1/\mu$=10 years. **a,c**: Establishment functions (equation (22)); **b,d**: Simulated age-intensity profiles, represented by median (bold lines) and the quantiles 2.5% and 97.5% (thin lines). **a**: Data based function of an increasing parasite establishment (positive density-dependence) with parameters λ_0=0.1 par/yr, s=0.05, λ_∞=5.0 par/yr, resulting in a sigmoid profile with strong overdispersion (**b**). The distribution is right-skewed and consequently capable of explaining very low parasite burdens (see 2.5% quantile which is almost zero until the age of 50 years). **c**: Hypothetically decreasing parasite establishment (negative density-dependence) with parameters λ_0=5.9 par/yr, s=0.05, λ_∞=1.1 par/yr (chosen for purposes of symmetry to curve in a), resulting in a saturating profile with slight under-dispersion (**d**).

Dispersion patterns: Positive density-dependence in parasite establishment leads to highly overdispersed parasite distributions. Since an explicit solution is only available for the equilibrium distribution (Appendix 2), we explain the age-specific impact of the establishment function on the dispersion pattern by means of the two extreme cases, i.e. the almost linear increase at low parasite burdens and the almost constant parasite establishment at high parasite burdens. If the immigration rate increases linearly with the parasite burden, then, the corresponding parasite distribution is negative binomial (McKendrick 1997). This is the prevailing dispersion pattern for young hosts, illustrated in

Fig. 11-e3 by the fact that the variance initially increases almost quadratically with the mean. The variance to mean ratio increases steeply until early adulthood (Fig. 11-e2). As hosts acquire more and more parasites and, therefore, as the establishment function moves towards saturation, overdispersion decreases and in the extreme case, if the establishment rate becomes constant, the parasite distribution approaches a Poisson distribution.

We deduce from the preceding paragraph that the degree of overdispersion does not depend on the *current absolute value* of the establishment function but on its *slope* at a specific parasite burden. The parasite distribution needs not necessarily approach a Poisson distribution: if the establishment function exhibits a still noteworthy slope in the region of the equilibrium parasite burden, then there is still an influence causing overdispersion. A further property of positive density-dependence in parasite establishment concerns the skewness of the distribution: We note in the parasite distributions of old hosts in Fig. 11-e1 that there is more variance below than above the median, i.e. this process causes a right-skewed distribution which is capable of explaining a great proportion of low parasite burdens.

We complete this paragraph with two remarks on negatively density-dependent parasite establishment: a decreasing establishment function causes underdispersed parasite distributions as shown in Fig. 8d. This is comparable to (positive) density-dependence in parasite mortality and for the special case of $\lambda_\infty=0$ we note that both processes have an identical equilibrium where $q=s$ (cf. equations (20) and (23)). This equality may seem somehow artificial, but it points at common principles in density-dependence if it is based on the current parasite burden (and not on the past experience of infection which may be relevant for acquired immunity). In the case where $\lambda_\infty=0$, we see that negative density-dependence in parasite establishment produces the same effect on the equilibirum as positive density-dependence in parasite mortality.

4 Complex processes - simple patterns, and vice versa

The previous paragraphs show that the different processes influencing the parasite distribution produce very distinct dispersion patterns (Fig. 11). However, in a biological context, it is not likely that these processes act isolated. Therefore, we now consider two examples of combined processes, showing that the superposition can alter dispersion patterns profoundly and that inferring a process from an observed pattern can very easily lead to erroneous conclusions.

4.1 Example 1: Host mortality combined with heterogeneity

We have shown in section 1.2 that parasite-induced host mortality can hardly be detected in the age-intensity profile if considered in isolation. We know furthermore that it does not affect the variance in parasite burdens, whereas heterogeneity does not affect the mean but only the variance (section 2.1). The superposition of these processes leads to a situation where not only both, mean and variance are affected, but where also the shape of the age-intensity profile changes from a saturating profile to a "convex" one (Fig. 9). Assuming heterogeneity within the host population, this pattern in the age-dependent variance to mean ratio has been shown by Anderson & Gordon (1982) who speculated that parasite-induced host mortality may be assumed if such a pattern is found concomitant with a "convex" mean in the age-intensity profile. Considering other processes, we can see that the same pattern in the variance to mean ratio arises from (positive) density-dependence in parasite establishment (Fig. 11-e2), showing that inferring process from pattern suffers from ambiguities. This example demonstrates that the superposition of processes may cause delicate effects and that very different processes can lead to the same dispersion pattern.

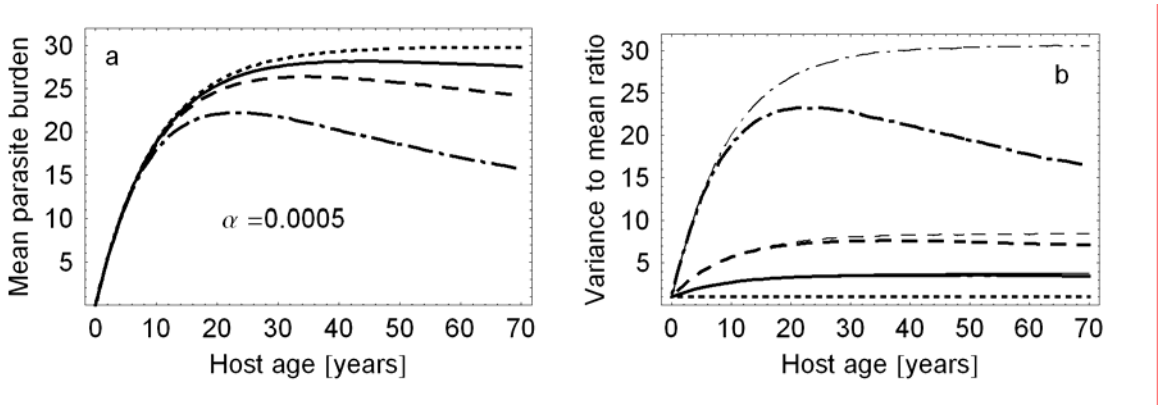

Fig. 9: The combined effect of heterogeneity within the host population and parasite-induced host mortality on the mean parasite burdens and the dispersion patterns. The dotted lines show the nullmodel for comparison. **a**: Simulated age-intensity profiles. **b**: Age-specific variance to mean ratios (thin lines allow comparing the dispersion pattern without excess host mortality). For all four curves, the immigration rate is λ=3 parasites/year, the excess host mortality rate is α=0.0005 per parasite and year and the parasite life expectancy is $1/\mu$=10 years. Heterogeneity is implemented as follows (see also equation (13)): Solid lines: gamma distribution with σ^2_{gamma}=0.1 (k=10). Dashed lines: gamma distribution with σ^2_{gamma}=0.25 (k=4). Dash-dot lines: gamma distribution with σ^2_{gamma}=1.0 (is identical to an exponential distribution with mean=1).

4.2 Example 2: Host mortality combined with clumped infection

From the preceding example, we may also suspect that not heterogeneity in particular but overdispersion in general is a prerequisite for a "convex" age-profile of the variance to mean ratio (*VMR*). In order to test this hypothesis, we let, in this example, overdispersed parasite distributions not result from heterogeneity but from clumped infection.

Identical dispersion patterns in the equilibrium can be found such that the *VMR* caused by heterogeneity is of the same extent as caused by clumped infection. To bring both processes into relation with each other, we set

$$VMR_h^* = VMR_m^*, \tag{24}$$

The left-hand side results from (15) in the equilibrium, i.e. $VMR^*_h=1+w^*/k_h$, where $k_h=1/\sigma^2_{gamma}$. The right-hand side results from the variance (17) in the equilibrium, divided by the equilibrium parasite burden w_m^*. By assuming a mean package size of $m_c=1$, equation (17) reduces to $VMR_m^* = \frac{\varphi m_c}{\mu w_m^*}\left(1+\frac{\sigma_c^2}{2}\right)$ and with $w_m^* = \varphi m_c/\mu$ (16) we obtain $VMR_m^* = (3+1/k_c)/2$, where k_c is the dispersion parameter of a negative binomial distribution (12) assumed to underly the distribution of package sizes. With these rearrangements, equation (24) simplifies to

$$k_c = 1 \Big/ \left(\frac{2\lambda}{\mu k_h} - 1\right), \tag{25}$$

a relation with which we can find an identical *VMR* in the equilibrium for both processes.

We see in Fig. 10 that the same extent of parasite-induced host mortality produces different age-intensity profiles, although operating within the same degree of overdispersion. Whereas clumped infection retains a saturating age-intensity profile as in the nullmodel, this is turned into a "convex" one in the case of heterogeneity. Moreover, the degree of overdispersion is only slightly reduced in clumped infection, whereas this reduction is profound in the case of heterogeneity. This profound effect of heterogeneity can be attributed to the assumption that the exposure factor is individual-specific and does not change throughout an individual's lifetime. Consequently, parasite-induced host mortality selectively removes those individuals form the population who are heavily parasitized due to their exposure factor. The selective removal of heavily parasitized indiviuals lowers the mean parasite burden in the population more strongly than in case of a "homogeneous" removal.

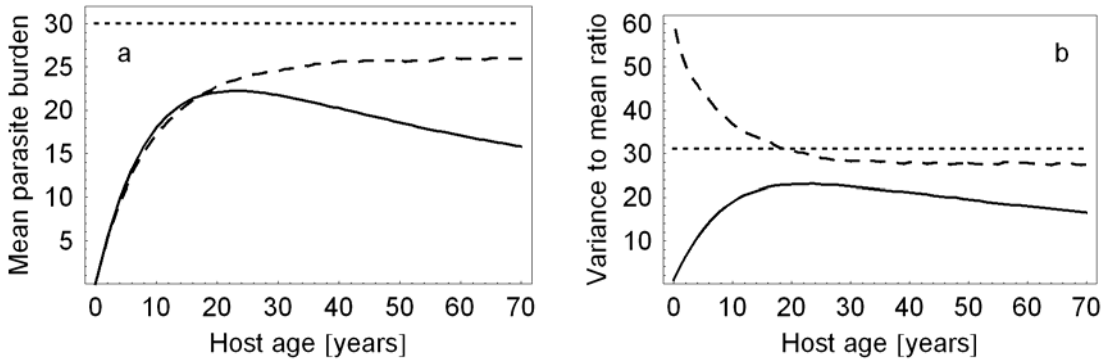

Fig. 10: The combined effect of parasite-induced host mortality and heterogeneity or clumped infection on the mean parasite burden and the dispersion pattern. **a**: Simulated age-intensity profiles showing the mean parasite burden. **b**: Age-specific variance to mean ratios (*VMR*s). Solid lines: overdispersion caused by heterogeneity, using a gamma distribution with σ^2_{gamma}=1 (cf. section 2.1). Dashed lines: overdispersion caused by clumped infection, sampling the package size from a negative binomial distribution with a mean package size of m_c=1 and dispersion parameter k_c=0.017. Both processes yield an equilibrium *VMR** =31 and an equilibrium parasite burden of *w** =30, if considered without parasite induced host mortality (α=0, dotted lines). The immigration rate is λ=3 parasites/year, the excess host mortality rate is α=0.0005 per parasite and year and the parasite life expectancy is $1/\mu$=10 years.

This example shows that similar processes can yield different outcomes if combined with other processes. Together with the preceding example, showing that different processes can yield similar outcomes, it must be stated that dispersion patterns in parasite distributions alone do not allow to draw clear conclusions with respect to the underlying processes.

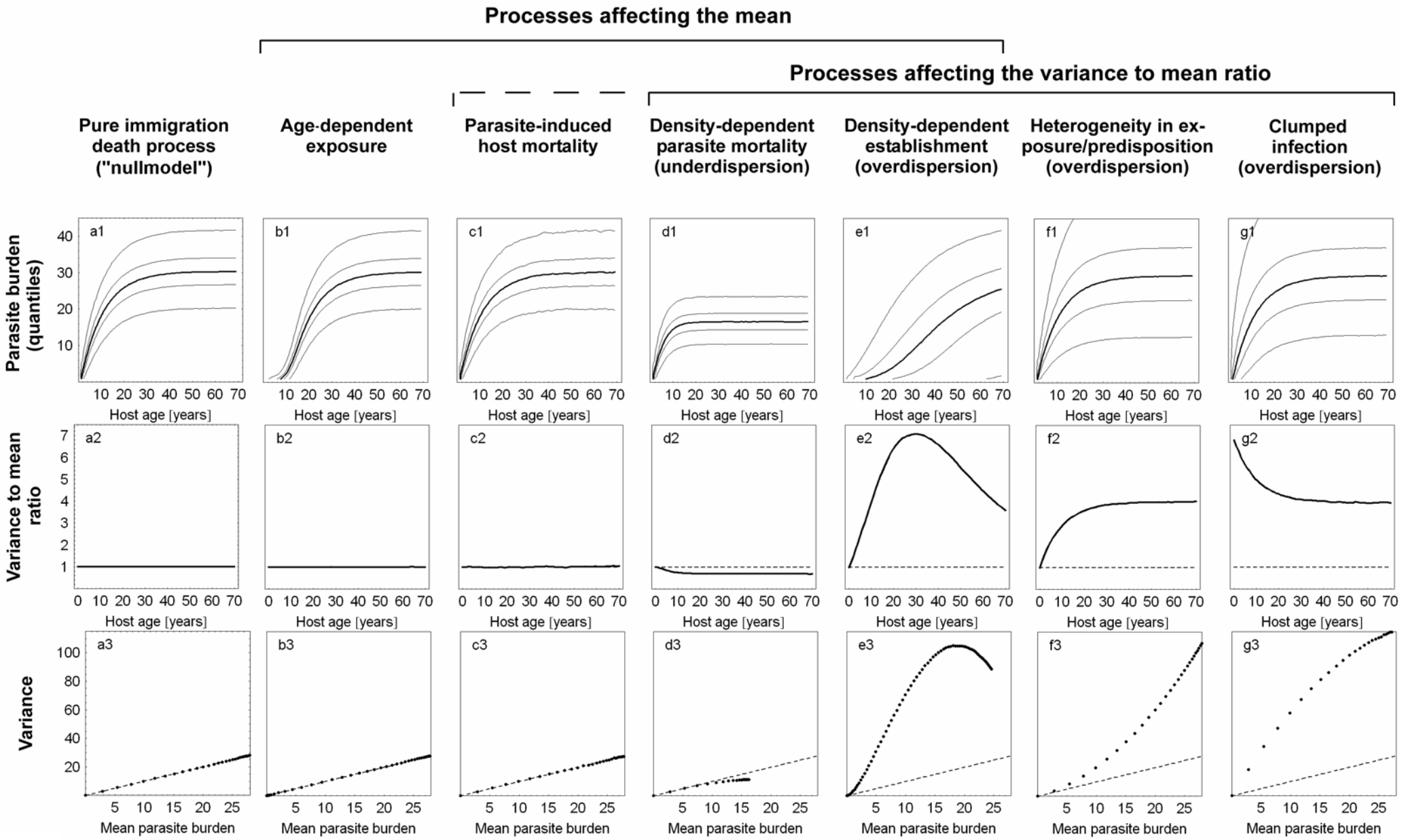
Processes affecting the mean
Processes affecting the variance to mean ratio
Pure immigration death process ("nullmodel")
Age-dependent exposure
Parasite-induced host mortality
Density-dependent parasite mortality (underdispersion)
Density-dependent establishment (overdispersion)
Heterogeneity in exposure/predisposition (overdispersion)
Clumped infection (overdispersion)
Parasite burden (quantiles)
Variance to mean ratio
Variance
a1
b1
c1
d1
e1
f1
g1
a2
b2
c2
d2
e2
f2
g2
a3
b3
c3
d3
e3
f3
g3
Host age [years]
Mean parasite burden

Fig.11: Dispersion patterns of processes influencing the distribution of parasites in the host population. Row **1**: Age-intensity profiles with quantiles 2.5%, 25%, median (bold line), 75% and 97.5%. Row **2**: Age-dependent variance to mean ratios (*VMR*s). Row **3**: Density-dependent variance in parasite burdens. Points represent - in years - the age-specific values of the mean and the variance. The dashed line indicates the dispersion pattern of the pure immigration-death process, i.e. the nullmodel with Poisson distributed parasite burdens where the variance equals the mean (row 3) and the *VMR* equals one at every age (row 2). Parameters: The immigration rate is λ=3 parasites/year (**a-g**, except **e,** see there) and the parasite lifespan is $1/\mu$=10 years (**a-g**). **a**: Pure immigration-death process (nullmodel), involving no parameters other than λ and μ. (equation(3)) **b**: The parameters A=10 and β=0.55 (equation (6)) yield an age-dependent exposure function which is proportional to the increasing body surface during growth in childhood; 95% of exposure are achieved in the 15 year olds. **c**: Parameter α=0.0005 per parasite and year introduces host mortality such that 60% of the 70 year old hosts have died as a consequence of infection with the parasite (equation (10), survival function see Fig. 3b; although this implies a very strong impact of the infection on host mortality, the age-intensity profile hardly differs from the nullmodel). Parasite-induced host mortality does only affect the mean, but not the *VMR* of parasite burdens (the dashed line above the graphs indicates the exceptions listed in section 1.2). **d**: The density-dependent excess mortality of parasites is q=0.05 (equation (18)), i.e. one parasite increases the mortality rate μ of all parasites in the host by 5%. **e**: λ_0=0.1 parasites/year, s=0.05, λ_∞=5 parasites/year (equation (22)). Density-dependent parasite establishment can lead to highly overdispersed parasite burdens and to sigmoid age-intensity profiles. **f**: Heterogeneity in exposure or susceptibility is implemented by a gamma distributed exposure factor with mean=1 and variance=0.1. **g**: The infection dose is negative binomial distributed with a mean of m_c=1 transmitted parasites per infective contact and k_c=0.2 (equation (25), see also Fig. 6).

DISCUSSION

The present paper summarizes the impact of different processes regulating the distribution of parasites on age-intensity profiles as obtained from cross-sectional surveys. Special emphasis is given to density-dependent parasite establishment, which may be relevant for parasite species, especially helminths, which have been suggested to suppress the immunological responsiveness of their hosts (King & Nutman 1991; Maizels et al. 1993). Comparing six processes, we note that only two of them (age-dependent exposure and density-dependent parasite establishment) can produce a shape of the age-intensity profile different than the saturating one given by the nullmodel (Fig. 11). Although density-dependent parasite mortality and parasite-induced host mortality influence also the equilibrium parasite burden, the saturation in the age-intensity profile is still conserved and it is thus not easy to identify these processes from cross-sectional data. On the other hand, heterogeneity within the host population and clumped infection affect only the variance but not the mean of parasite distributions.

At first glance, dispersion patterns seem to be more promising if one wishes to interpret age-intensity profiles with respect to possibly underlying processes. For example, the variance to mean ratios (*VMR*s) in Fig 11 (e2-g2) suggest that dispersion patterns over age differ so profoundly that they might be used as a diagnostic tool. However, one must bear in mind that these dispersion patterns were obtained from processes acting in isolation. Considering the superposition of two processes (see section 4) reveals that the interpretation of *VMR*s is subject to a high degree of ambiguity, which will further increase when taking more processes into account (see below).

Age-intensity profiles which are "convex" either in their tendency of the mean or in their dispersion pattern have attracted most attention, assuming an informative structure in these patterns. However, "convex" age-intensity profiles may be the most easily produced type of artefact: the sample size in cross-sectional data sets usually decreases with host age, simply because of the naturally decreasing survival function of the host population. Since both the mean parasite burden and the degree of dispersion are systematically underestimated in low sample sizes (Gregory & Woolhouse 1993), we can *expect* to find a "convex" profile in a study of limited sample size. The patterns observed in old hosts are, therefore, less informative. The simulation studies of these authors have also shown that splitting the total sample into age groups of equal sample size cannot solve this problem, instead contradictory conclusions are likely to be found.

The previous paragraphs have indicated that the reliability of interpreting dispersion patterns is strongly reduced when taking the superposition of processes or differing sample sizes into account. We want to complete this point of view by two more aspects, namely the influence of the number of processes under investigation and of the used dispersion index. As shown in

section 4, parasite-induced host mortality acting within highly overdispersed parasite burdens can produce dispersion patterns similar to those resulting from density-dependent parasite establishment. Having found a new process resulting also in a "convex" dispersion pattern, the number of possible interpretations for this pattern has doubled and we note that the success rate of "inferring process from pattern" decreases with the number of processes we know. Similar difficulties arise from the choice of the dispersion index: Besides the *VMR*, which may not be the "best" index but a convenient and most commonly used one, there are also the coefficient of variation (standard deviation / mean), the index of discrepancy (Poulin 1993) or the corrected moment k' of the negative binomial distribution (Elliot 1977, described in Woolhouse et al. 1994) (k' is adjusted to the sample size as opposed to the unadjusted moment k, which is highly biased by the sample size). These measures do not necessarily lead to a congruent evaluation of the dispersion pattern because they are differently biased by their dependence on the mean, the sample size and the type of distribution underlying the data.

Opposed to dispersion patterns, the informative capacity of the mean seems to be underestimated, especially in young hosts where we usually obtain large sample sizes. Explaining again the properties of the nullmodel shall illustrate this: We usually have "guesstimates" about the approximate lifespan $L=1/\mu$ of the parasite under investigation and the equilibrium parasite burden w^* in the hosts. Then, from the relation $w^*=\lambda/\mu$ we obtain a "guesstimate" about the parasite acquisition rate λ so that we can easily plot the deterministic solution of the nullmodel (3) together with the data. Discrepancies between predicted and observed parasite burdens, especially during the increasing part of the curve, may point at other processes involved. To explore these discrepancies, the nullmodel is, naturally, the most informative model. The explicit solutions given here provide some more tools for testing other hypotheses and predicting the outcome of additional processes assumed to be involved.

The most appropriate way to infer processes from observed patterns may be given by testing different models which incorporate characteristic processes in a hierarchical comparison (see, for example Woolhouse et al. 1994). *A priori* knowledge about involved processes is often available and it can be used to predict the corresponding age-intensity profile. Discrepancies between model prediciton and data may then point at additional processes necessary to explain the data. For such hypotheses testing, we offer to share the simulation program and its source code (C++) used for the present investigations. Age-intensity profiles can be simulated for any combination of processes, with variable sample size or specific parameter values. This may help to examine the predictive capacity of different hypotheses or to explore how the reliability of intended interpretations depends on the sample size.

This paper shows only six processes which focus on the acquisition of parasites, their establishment within and their interaction with the host. Other impor-

tant processes regulating the parasite distribution include spatial factors and acquired immunity. Geographical clustering usually results in overdispersed parasite distributions, even if the assumptions of homogeneous host-parasite interactions are retained (Leung 1998). The impact of acquired immunity on the age-intensity profile has been described by various authors (for example, see Anderson & May 1985; Grenfell et al. 1995; Jose 1989; Woolhouse 1992). Acquired immunity usually leads to a "convex" tendency in the age-intensity profile due to the enhanced immunological defence after experience of infection, either against the invading stage of the parasite or the longevity of established parasites. The effects of these mechanisms are similar either to age-dependent exposure and negative density-dependence in parasite establishment or to positive density-dependence in parasite mortality, respectively. Differences arise from taking immunological memory into account, which is based on the cumulative experience of infection, opposed to the density-dependent processes shown here, which refer to the current parasite burden.

As shown in section 1.2, parasite-induced host mortality can hardly be detected from age-intensity profiles (see also Grenfell et al. 1995). This conclusion was illustrated for specific parameter values, i.e. λ=3 parasites per year and an excess host mortality of α<0.01 per parasite and year. These parameter values are "guesstimates" chosen with reference to an investigation into age-intensity profiles on onchocerciasis. Exceptions to the drawn conclusion arise from extreme values for these parameters and we refer to equations (9) and (10) if specific hypotheses need to be tested. The relevance of parasite-induced host mortality seems to emerge only from the combination with processes introducing overdispersion (Anderson & Gordon 1982; Pacala & Dobson 1988). In particular, "convex" age-intensity profiles resulting from parasite-induced host mortality seem to be specifically associated with heterogeneity within the host population. Yet, other processes, as for instance spatial heterogeneity, remain to be tested. Simulations have revealed that a "convex" age-intensity profile cannot result from overdispersion introduced by density-dependent parasite establishment (results not shown).

Among the processes considered here, positive density-dependent parasite establishment is the most complex one, yielding a sigmoid age-intensity profile and a "convex" dispersion pattern over age. This process is capable of introducing much overdispersion which is, opposed to host heterogeneity and clumped infection, right-scewed and consequently accounts for a great proportion of low parasite burdens (compare quantile plots, row 1, in Fig 11). This process has been suggested in the context of parasite-induced immunosuppression or immunotolerance which assumes that parasites can suppress the host's defence mechanisms, and, therefore, increase the susceptibility of the host and the rate at which subsequent infections are acquired. Density-dependent parasite establishment has complex consequences for the dynamics within the transmission cycle (Duerr et al., submitted) and will be investigated further, in particular with respect to its impact on control programmes.

APPENDIX

Deterministic solution for parasite burdens if exposure depends on age.

The solution of

$$\frac{dw}{da} = \frac{\lambda}{1+\exp\big(-\beta(a-A)\big)} - \mu w\,.$$

is given by

$$w(a) = \frac{\lambda e^{-(A\beta + a\mu)}}{\beta+\mu}\left(e^{a(\beta+\mu)}\ {}_2F_1\left[1,1+\frac{\mu}{\beta},2+\frac{\mu}{\beta},-e^{(a-A)\beta}\right] - {}_2F_1\left[1,1+\frac{\mu}{\beta},2+\frac{\mu}{\beta},-e^{-A\beta}\right]\right)$$

where the hypergeometric function ${}_2F_1(a,b,c,z)$ has the series expansion

$${}_2F_1[a,b,c,z] = \sum_{k=0}^{\infty} \frac{(a)_k\,(b)_k}{(c)_k}\frac{z^k}{k!}\,.$$

(Gradshteyn & Ryzhik 1980) with $(x)_k = \prod_{i=0}^{k-1}(x+i)$ and $(x)_0$=1.

Equilibrium distribution of parasite burdens if parasite establishment is density-dependent

In the following, we proceed according to (Karlin 1966, pp. 194). The age-dependent transitions to move from a status with parasite burden j to the status j+1 are given by

$$P_0'(a) = -\lambda_0 P_0(a) + \mu_1 P_1(a)$$
$$P_j'(a) = \lambda_{j-1}P_{j-1}(a) - (\lambda_j + \mu_j)P_j(a) + \mu_{j+1}P_{j+1}(a);\quad j \geq 1.$$

In the equilibrium, we have $P_0'(a) = 0$ and $P_j'(a) = 0$ and by starting with π_0=1, the solution can be obtained by induction as

$$\pi_w = \prod_{j=0}^{w-1}\lambda_j \ \Big/ \prod_{j=1}^{w}\mu_j$$

For density-dependence in the parasite acquisition rate λ but not in the parasite mortality rate μ, we define the transition rates as follows,

$$\lambda_j = \frac{\lambda_{\min} + s\,\lambda_{\max}\,j}{1+s\ j}$$
$$\mu_j = \mu\, j\,.$$

With these, the solution is given by

$$\pi_w = \frac{\Gamma\left(\frac{\lambda_0}{s\,\lambda_\infty} + w\right)\ \Gamma\left(\frac{1}{s}\right)}{\Gamma\left(\frac{1}{s} + w\right)\ \Gamma\left(\frac{\lambda_0}{s\,\lambda_\infty}\right)\ w!}\ \left(\frac{\lambda_\infty}{\mu}\right)^w .$$

π_w still depends on the definition of π_0 and for purposes of normalization we compute $\sum \pi_k$, yielding the confluent hypergeometric function ${}_1F_1(c_1, c_2, c_3)$:

$$\sum_{k=0}^{\infty} \pi_k = {}_1F_1\left(\frac{\lambda_0}{s\,\lambda_\infty}, \frac{1}{s}, \frac{\lambda_\infty}{\mu}\right).$$

Normalizing π_w with this term yields the distribution, so that the probability of having *w* parasites at equilibrium is

$$P(w) = \frac{\pi_w}{{}_1F_1(c_1, c_2, c_3)}$$

This is the confluent hypergeometric distribution (Wimmer & Altmann 1999), which has the probability generating function

$$f(x) = \frac{{}_1F_1(c_1, c_2, c_3\,x)}{{}_1F_1(c_1, c_2, c_3)}$$

from which we obtain the mean and the variance as

$$E(W) = f'(1) = \frac{\lambda_{\min}}{\sigma}\,\frac{{}_1F_1(1+c_1, 1+c_2, c_3)}{{}_1F_1(c_1, c_2, c_3)}$$

$$Var(W) = f'(1) - (f'(1))^2 + f''(1)$$

$$= E(W) - (E(W))^2 + \frac{\lambda_{\min}\left(\lambda_{\max} + \frac{\lambda_{\min}}{s}\right)}{\sigma^2\left(1 + \frac{1}{s}\right)}\,\frac{{}_1F_1(2+c_1, 2+c_2, c_3)}{{}_1F_1(c_1, c_2, c_3)} .$$

Acknowledgement

This work was supported by the *f*ortüne grant no. 528 of the University Hospital, Tübingen, Germany and by a grant from the Deutsche Forschungsgemeinschaft, Graduiertenkolleg Lebensstile, soziale Differenzen und Gesundheitsförderung, Germany.

REFERENCES

Adler, F. R. & Kretzschmar, M. 1992 Aggregation and stability in parasite-host models. *Parasitology* **104**, 199-205.

Anderson, R. M. & Gordon, D. M. 1982 Processes influencing the distribution of parasite numbers within host populations with special emphasis on parasite-induced host mortalities. *Parasitology* **85**, 373-398.

Anderson, R. M. & May, R. M. 1985 Herd immunity to helminth infection and implications for parasite control. *Nature* **315**, 493-6.

Anderson, R. M. & May, R. M. 1991 *Infectious diseases of humans*. Oxford: Oxford University Press.

Barbour, A. D. & Pugliese, A. 2000 On the variance-to-mean ratio in models of parasite distributions. *Adv Appl Prob* **32**, 701-719.

Cooper, P. J., Mancero, T., Espinel, M., Sandoval, C., Lovato, R., Guderian, R. H. & Nutman, T. B. 2001 Early human infection with *Onchocerca volvulus* is associated with an enhanced parasite-specific cellular immune response. *J Infect Dis* **183**, 1662-1668.

Cox, D. R. & Miller, H. D. 1965 *The theory of stochastic processes*. Methuen's monographs on applied probability and statistics. London: Methuen & Co Ltd.

Crofton, H. D. 1971a A model of host-parasite relationships. *Parasitology* **63**, 343-364.

Crofton, H. D. 1971b A quantitative approach to parasitism. *Parasitology* **62**, 179-193.

Dietz, K. 1982a Overall population patterns in the transmission of infectious diseases. In *Population biology of infectious diseases*, vol. Dahlem Workshop on population biology of infectious diseases agents (ed. R. M. Anderson & R. M. May), pp. 87-102. Berlin: Springer.

Dietz, K. 1982b The population dynamics of onchocerciasis. In *The population dynamics of infectious diseases: theory and applications* (ed. R. M. Anderson), pp. 209-241. London, New York: Chapman and Hall.

Elkhalifa, M. Y., Ghalib, H. W., Dafa'Alla, T. & Williams, J. F. 1991 Suppression of human lymphocyte responses to specific and non-specific stimuli in human onchocerciasis. *Clin Exp Immunol* **86**, 433-439.

Elliot, J. M. 1977 Statistical analysis of samples of benthic invertebrates. *Freshwater Biological Association*, Scientific Publication No. 25.

Gradshteyn, I. S. & Ryzhik, I. M. 1980 *Table of integrals, series, and products*. New York: Academic Press.

Greenwood, M. & Yule, G. U. 1920 An inquiry into the nature of frequency distributions representative of multiple happenings with particular reference to the occurrence of multiple attacks of disease or of repeated accidents. *Journal of the Royal Statistical Society. Series A* **83**, 255-279.

Gregory, R. D. & Woolhouse, M. E. 1993 Quantification of parasite aggregation: a simulation study. *Acta Trop* **54**, 131-9.

Grenfell, B., Dietz, K. & Dobson, A. 1995 Modelling the immuno-epidemiology of macroparasites in wildlife host populations. In *Ecology of infectious diseases in natural populations* (ed. B. Grenfell & A. Dobson): Cambridge University Press.

Hadeler, K. P. & Dietz, K. 1982 Nonlinear hyperbolic partial differential equations for the dynamics of parasite populations. *Comp Math Appl* **9**, 415-430.

Hudson, P. J. & Dobson, A. 1982 Overall population patterns in the transmission of infectious diseases. In *Population biology of infectious diseases*, vol. Dahlem Workshop on population biology of infectious diseases agents (ed. R. M. Anderson & R. M. May). Berlin: Springer.

Isham, V. S. 1995 Stochastic models of host-parasite interaction. *Ann App Prob* **5**, 720-740.

Jose, M. V. 1989 On the solution of mathematical models of herd immunity in human helminth infections. *J Math Biol* **27**, 707-15.

Karlin, S. 1966 *A first course in stochastic processes*. New York, London: Academic Press.

King, C. L. & Nutman, T. B. 1991 Regulation of the immune response in lymphatic filariasis and onchocerciasis. *Immunol Today* **12**, A54-A58.

Kretzschmar, M. & Adler, F. R. 1993 Aggregated distributions in models for patchy populations. *Theor Popul Biol* **43**, 1-30.

Leung, B. 1998 Aggregated parasite distributions on hosts in a homogeneous environment: examining the Poisson null model. *Int J Parasitol* **28**, 1709-12.

Maizels, R. M., Bundy, D. A., Selkirk, M. E., Smith, D. F. & Anderson, R. M. 1993 Immunological modulation and evasion by helminth parasites in human populations. *Nature* **365**, 797-805.

McKendrick, A. G. 1997 Applications of mathematics to medical problems. Reprint of McKendrick's paper (1926) with an introduction by K. Dietz. In *Breakthroughs in Statistics*, vol. III (ed. S. Kotz & N. L. Johnson), pp. 17-57: Springer.

Pacala, S. W. & Dobson, A. P. 1988 The relation between the number of parasites/host and host age: population dynamic causes and maximum likelihood estimation. *Parasitology* **96**, 197-210.

Poulin, R. 1993 The disparity between observed and uniform distributions: a new look at parasite aggregation. *Int J Parasitol* **23**, 937-44.

Shaw, D. J., Grenfell, B. T. & Dobson, A. P. 1998 Patterns of macroparasite aggregation in wildlife host populations. *Parasitology* **117**, 597-610.

Soboslay, P. T., Geiger, S. M., Weiss, N., Banla, M., Lüder, C. G., Dreweck, C. M., Batchassi, E., Boatin, B. A., Stadler, A. & Schulz-Key, H. 1997 The diverse expression of immunity in humans at distinct states of *Onchocerca volvulus* infection. *Immunology* **90**, 592-599.

Wimmer, G. & Altmann, G. 1999 *Thesaurus of univariate discrete probability distributions*. Essen: Stamm.

Woolhouse, M. E. 1992 Immunoepidemiology of intestinal helminths: pattern and process. *Parasitology Today* **8**, 111.

Woolhouse, M. E., Ndamba, J. & Bradley, D. J. 1994 The interpretation of intensity and aggregation data for infections of Schistosoma haematobium. *Trans R Soc Trop Med Hyg* **88**, 520-6.

Density-dependent parasite establishment suggests infection-associated immunosuppression as an important mechanism for parasite density regulation in onchocerciasis[1]

SUMMARY

The modulation of human immune response by filarial parasites has yielded contradictory experimental findings and attracted much controversy. We address the unresolved question of acquisition, establishment and accumulation of *Onchocerca volvulus* by using a modelling approach that relates computer simulations to cross-sectional data concerning parasite burdens in 913 West African onchocerciasis patients. The results strongly emphasise the importance of immunosuppressive processes in man, associated with the presence of adult parasites or microfilariae. It is suggested that these processes suppress immunity against incoming infective larvae (L3), which themselves act as an immune modulating component once they have successfully passed the barrier of concomitant immunity. Suppression of parasite-specific immunity leads to parasite establishment rates which increase along with the parasite burden, but which hardly depend on hyperendemic annual transmission potentials (ATP). Children, still immunocompetent due to low parasite burdens, acquire 0.1-0.5 adult female parasites per year, whereas aged people, immunosuppressed due to high burdens, acquire adult female 2-4 parasites per year. Differences in parasite establishment between the forest and the savanna strains of *O. volvulus* are quantified and dynamic aspects of density-dependent parasite establishment discussed.

INTRODUCTION

Age-related immunological investigations into filarial infections yielded contradictory results ranging from acquired immunity increasing with age to immunity decreasing in adults due to parasite-associated immunosuppression. Information on the parasite *Onchocerca volvulus* is sparse and must sometimes be inferred from what is known about the related filariae *Wuchereria bancrofti* and *Brugia malayi*, the infectious agents of lymphatic filariasis. Differences in the transmitting vectors and in the macro- and microfilarial life cycle, however, serve to complicate analogical considerations. Investigations into immunity to lymphatic filariasis (reviewed in King & Nutman 1991) have suggested age dependence in parasite acquisition, as assessed either by levels of circulating

[1] eingereicht bei den Proceedings of the Royal Society of London, Series B. H.P. Duerr, K. Dietz, H. Schulz-Key, D.W. Büttner, M. Eichner. Density-dependent parasite establishment suggests infection-associated immunosuppression as an important mechanism for parasite density regulation in onchocerciasis.

filarial antigen (Day et al. 1991b), by cytokine profiles (Sartono et al. 1997), or by a modelling approach (Vanamail et al. 1989). In chronic parasitic diseases, however, age is strongly correlated with permanent parasite acquisition, and the resulting confounding makes causative considerations problematic. Further complications arise from the fact that immunological markers may only specify cells or molecules, but do not describe protective immunity as a whole.

The present investigation is an immunoepidemiological approach using mathematical modelling for purposes of extracting information about the establishment of adult parasites from cross-sectional onchocerciasis surveys of parasite burdens as recorded by nodule ectomy. This represents a great gain over comparing to data on lymphatic filariasis, for which the burden of adult parasites cannot be determined directly. Throughout this paper the main point of interest is the parasite establishment rate, i.e. the number of *O. volvulus* acquired per person and year. By relating it to the adult reproductive filarial stages we can consider effective parasite establishment, this being a net measurement of both infection and immunological defence. In particular, we pay attention to density-dependent immunity, which, in terms of immunosuppression, has been shown to occur in infection with *O. volvulus* (Cooper et al. 2001; Elkhalifa et al. 1991; Soboslay et al. 1994) as well as in the specific mouse model (Hoffmann et al. 2001). In the following, the term "parasite" is used primarily as a short form for the live adult female *O. volvulus*.

Description of the establishment and survival of parasites which do not replicate in the host must be based on the concept of a general "immigration-death process", which assumes, in its simplified form, that parasite establishment (immigration) occurs constantly throughout life. It describes changes in the parasite burden w over age a by the differential equation $dw/da = \lambda - \sigma w$, where λ denotes the establishment rate and σ the death rate of parasites. The equilibrium parasite burden results from $dw/da = 0$ and is given by $w^* = \lambda/\sigma$, where parasite life expectancy is $1/\sigma \cong 10$ years for adult *O. volvulus*. If, for example, the equilibrium parasite burden in adults is $w^* \cong 20$ parasites, the parasite establishment rate must be $\lambda \cong 2$ parasites per year. Problems become evident when plotting the model prediction, given by the solution $w(a) = w^* (1-e^{-\sigma a})$, against cross-sectional data on age-specific parasite burdens. The observed parasite burdens reach the equilibrium much later than predicted (assuming parasite life expectencies below 20 years). Furthermore, the age-specific curve of the population's parasite burden seems shifted to the right, i.e. children have much less and adults more parasites than expected when assuming a constant establishment rate.

Lower parasite burdens in children, also confirmed by a low prevalence of antibodies against the adult parasite (Weiss & Karam 1987), suggest the existence of protective factors, which can generally be attributed to (1) an age-related decline in the host defence mechanisms (assuming strong resistance in young individuals), (2) a density-dependent decline accompanying an

increasing parasite burden, or (3) changes in age-dependent exposure. The latter is subject to controversy and is, at least in our data set of forest onchocerciasis, a very unsatisfactory hypothesis (see Discussion). The age- or density-dependent decline of host resistance opposes the concept of acquired immunity, which assumes immune reactivity to increase with continuing parasite exposure. Although a recent study on lymphatic filariasis suggests a purely age-dependent decrease in specific immunological markers (Terhell et al. 2001), we restrict our model to density-dependence because parasite-associated immunosuppression or tolerance has been demonstrated as a wide-spread phenomenon in chronic helminthic diseases (reviewed in Maizels et al. 1993; Ottesen 1995; Urquhart 1970).

In regarding immunity against filarial parasites, we must specify the immunological targets, i.e. the different stages of the parasite. These are the invading parasite (infective larva L3; reviewed for *Brugia* in Devaney & Osborne 2000), the stage following infection (L4), the adult parasite and, finally, the offspring (microfilariae). A crude immunological classification is given by the terms (1) innate immunity, which is thought to be mainly unspecific and cellular, (2) acquired immunity, in which the action of specific antibodies dominates and (3) a subterm of the latter, concomitant immunity, which is a specific immune response against the invasive stage of the parasite.

The primary intention of this investigation is to determine the density-*dependent* and consequently age-*related* establishment rate of adult female *O. volvulus*. We shall examine, from this perspective, the most basic process in filarial infection and provide a basis for research and discussion of immunological questions. Using a simulation-based stochastic model, we uncover an important pattern of infection with *O. volvulus*, whereby the causality suggested should be the object of further investigation.

METHODS

Sources of data

Our data derive from two pre-control nodule ectomy campaigns in villages of the West African countries Liberia (rain forest) and Burkina Faso (savanna), conducted in 1976/77 and 1977/78 respectively. Both regions were hyperendemic for onchocerciasis at the time of nodule ectomy. After extirpation, the nodules were digested with collagenase so that the number of worms per nodule could be assessed precisely (Schulz-Key et al. 1977). Descriptive aspects of these data sets, the worm burdens, the relation of palpable to impalpable nodules and the incidence of different worm stages have been published elsewhere (Albiez 1983; Albiez et al. 1984; Duerr et al. 2001; Schulz-Key & Albiez 1977). Included in our analysis are the Liberian villages

Mauwa (6°52'N, 10°26'W), Sungbeta (6°53'N, 10°21'W), Wodee (6°38'N, 10°31'W), Yeahmeah (6°45'N, 10°18'W) and Meningee (6°38'N, 10°31'W), all located east of St. Paul River in Southern Bong and in Montserrado counties, also the Burkina Faso villages Kourougbele, Hemkoa, and Yabar (all located 10°41'N, 3°1'W, south of the Bougouriba River in the region of Gaoua). For all 913 patients, the following variables are considered: 1) age, 2) country, 3) the number of palpated nodules obtained by pre-examination, 4) the number of excised nodules obtained by nodule ectomy from 629 patients and 5) the number of live adult female parasites isolated from the nodules. For sample sizes per village see Table 1. ATP values for the Liberian villages were obtained from published data (Garms 1983).

Statistical methods

The methodical part of this work consists of a simulation to produce a frequency distribution of adult female worms, given the host's age in years (example see Fig. 1), an adjustment procedure to adapt the simulation results to the study design, and a minimization routine to estimate model parameter values based on the maximum likelihood method.

The simulation algorithm operates in yearly steps following an individual's life history from age a=1...A, where A denotes the age of a patient in the data set. The establishment of parasites $\lambda(w_a)$ during the year starting with age a is simulated recursively using the sigmoid, density-dependent establishment function $\lambda(w_{a+1}) = (\lambda_{\min} + \lambda_{\max} s w_a)/(1 + s w_a)$, where w_a denotes the parasite burden at age a. Newborns are free of infection (w_0=0) so that the parasite establishment rate during the first year of life is equal to λ_{min}. The annually acquired number of parasites is sampled with random numbers from a negative binomial distribution (NBD) with mean $\lambda(w_a)$. The life span of each newly acquired parasite is sampled from a Weibull distribution with survival function $S(t)$=exp(-0.0001185 $t^{3.76}$), yielding a life expectancy of 10 years (Duke 1993; Karam et al. 1987; Plaisier et al. 1991) with a standard deviation of 3.0 years. During simulation, the life span of each parasite is registered in an individual's age array, which contains the parasite burden w_a and allows the density-dependent establishment to be determined in the course of iteration over the following years. Repeating age-specifically the steps of 1) sampling the acquired number of parasites per year and 2) sampling and registering the survival time of each new parasite yields the parasite burden of an individual at age A. Simulating many individuals yields a distribution of parasite burdens for individuals at age A and simulating all host ages A=1...75 yields age-specific distributions of parasite burdens, $P_a(w)$, as illustrated by Fig. 1. With a view to computing time, simulating N_{sim}=300,000 individuals per age was chosen as likely to provide satisfactorily high precision during parameter estimation.

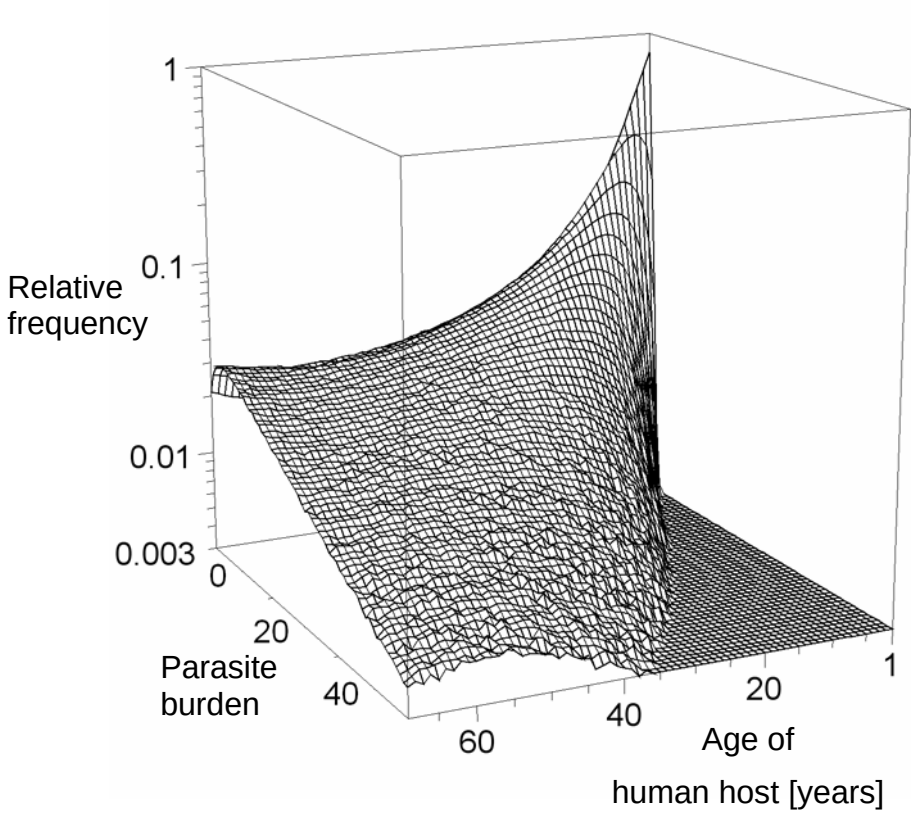

Figure 1: Frequency distribution of age-specific parasite burdens obtained from a simulation with 300,000 individuals (corresponds to the study-adjusted quantiles in Fig. 2a, Mauwa). The shape of the distribution depends on the parameters to be estimated, i.e. *s* (village-specific), λ_{min} and λ_{max} (strain-specific) and *k* (global dispersion parameter of the negative binomial distribution). For the purpose of illustration, parasite burdens >60 are omitted.

In contrast to ordinary maximum likelihood estimations, which are based on explicit parametric distributions, our approach uses simulated distributions. The simulated frequency of appearing in the study and having *w* adult female parasites at age *a* is $P_a(OP^+, w_a) = P_a(w_a)\,P_a(OP^+ \mid w_a)$, i.e. the product of the (simulated) frequency of having w_a parasites and a term which adjusts our simulations to the study design. The latter pays special attention to the study-related selection of patients. Simulating the study rather than cross-sectional data in general allows unbiased estimates to be obtained. The adjustment procedure is described in detail in the Appendix. Operated patients ($n=N_{OP+}$) individually contribute $P_a(OP^+, w_a)$ to the total likelihood and non-operated patients ($n=N_{OP-}$) individually contribute $P_a(OP^-) = 1 - P_a(OP^+) = 1 - \sum_{w=1}^{\infty} P_a(OP^+, w)$. Maximizing the product of all likelihood contributions

$$L = \left[\prod_{i=1}^{N_{OP^+}} P_{a_i}\left(OP^+, w_i\right) \right] \left[\prod_{i=1}^{N_{OP^-}} P_{a_i}\left(OP^-\right) \right]$$

leads to the parameter vector which maximises the probability of all observations occurring. Powell's algorithm (Press et al. 1996) was used to minimise the negative log-likelihood, where convergence was defined to a precision of 10^{-3} and confirmed by starting with different sets of initial values.

The estimated parameters consist of 7 village-specific parameters (shape parameters ***s*** of the establishment functions), 4 strain-specific parameters ($\lambda_{\min}$ and $\lambda_{\max}$ for savanna and forest) and the overall dispersion parameter *k* of the NBD. Different hypotheses were tested by likelihood ratio tests based on $N_{sim}=10^8$ simulations (demanding one week of computing time at 750 MHz), with each using the estimated parameter vectors of the particular hypotheses.

The age-related establishment rate (Fig. 3b) is derived from the density-dependent establishment rate (Fig. 3a) by using the simulated, unbiased frequency distribution: density-dependent establishment rates are averaged (geometric mean) over all age-specific parasite burdens, taking into account the weights as given by the frequency distribution. Village-specific mean establishment rates (Table 1) were calculated from the age-related establishment rates, averaging over an OCP standard population (Dietz 1982).

RESULTS

Fig. 2a shows the cross-sectional data of two villages comparable in parasite burdens and sample sizes, together with the simulation results represented by the medians and by four quantiles for each village. The village Kourougbele (Burkina Faso) represents the savanna strain of *O. volvulus* while Mauwa (Liberia) represents the forest strain. In contrast to the forest data set, where the median burden of adult female parasites increases almost linearly with age (unadjusted fit in Fig. 2b), parasite burdens in the savanna increase faster and attain saturation pointing at an equilibrium situation in old individuals. The decline of the curves in both diagrams in Fig 2a is a consequence of adjusting the simulation to study characteristics and must not be mistaken for parasite-induced mortality among aged human hosts. An impression of the "true" parasite burdens is provided by Fig. 2b, which shows the simulation result without adjustment, i.e. without study bias. For young individuals, the unadjusted parasite burdens are below those obtained in the study. Over-represented parasite burdens found in the study result from the fact that highly-infected patients were more likely to be recognised by palpation and so were more often selected for surgery.

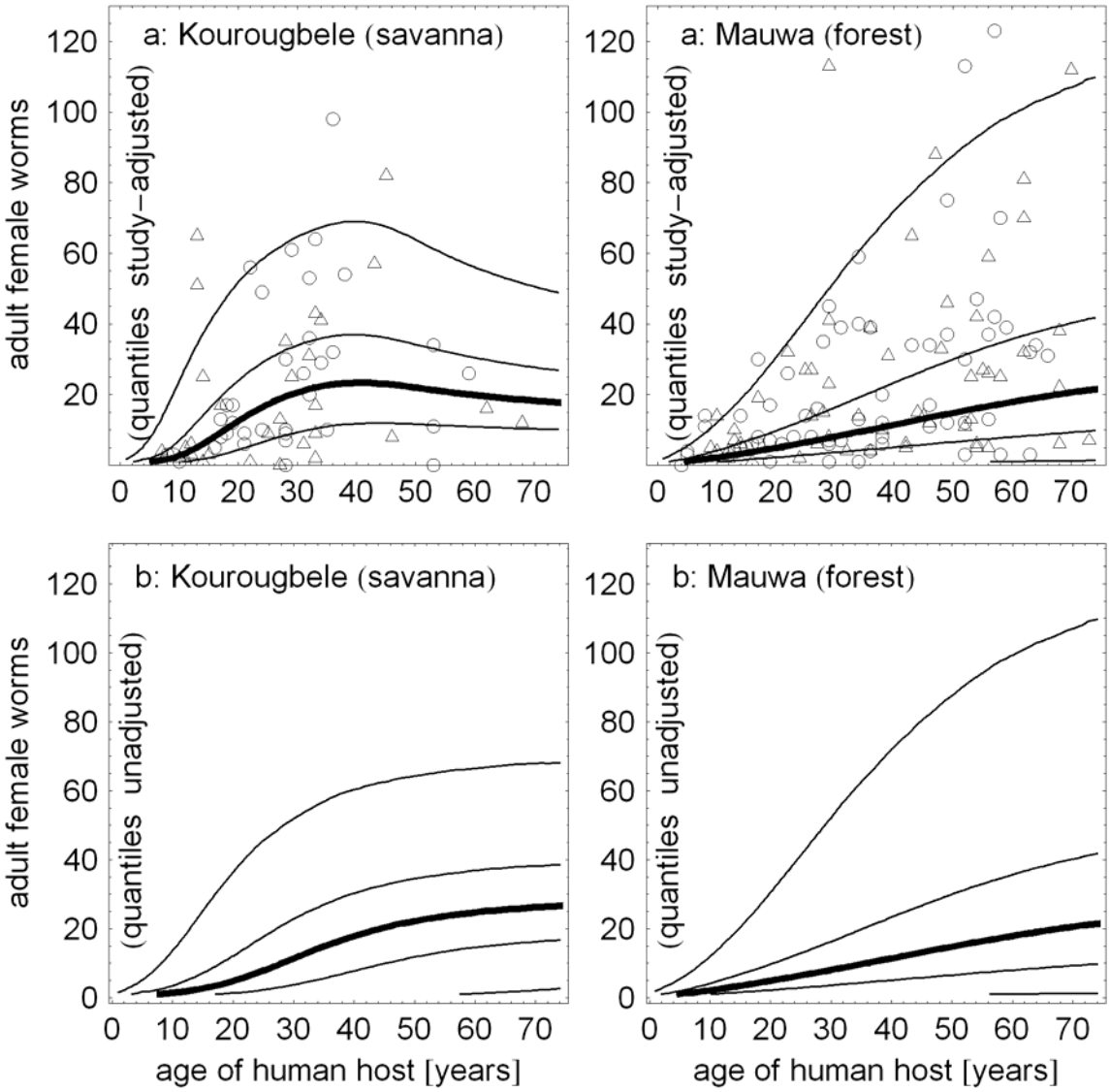

Figure 2. a: Model validation. Quantiles derived from the study-adjusted simulation related to data of individual parasite burdens found by nodule ectomy; circles: females, triangles: males. b: Unadjusted simulation. Age-related parasite burdens without study-biased influences, represented by quantiles of the simulated frequency distribution. Bold line: median. Thin lines: quantiles 2.5%, 25%, 75%, 97.5%.

Parameter values of the maximum likelihood estimation are shown in Table 1 and differences between savanna and forest strains can be described as follows: a smaller value of the shape parameter *s*, which indicates the intensity of immunosuppression caused by the parasite, produces a slower increase of the parasite burden in the forest as compared to the savanna region. Thus, immunosuppression by the forest strain of *O. volvulus* is weaker than by the savanna strain; however it hardly saturates, as is indicated by the saturation

parameter λ_{max}=19.1 parasites/year (this establishment rate refers to hosts with extremely high parasite burdens and is practically never achieved in the forest region). The low increase in the forest establishment function (*s*=0.0065) compensates for higher establishment rates during childhood as indicated by parameter λ_{min}=0.16 parasites/year. In contrast to the findings for the forest strain of *O. volvulus*, the establishment of parasites in the savanna reaches higher parasite burdens by a 4-10 fold degree of immunosuppression (*s*=0.05). This enhanced establishment compensates for the lower rate during early childhood (λ_{min}=0.10 parasites/year), but allows a maximum rate of only λ_{max}=4.8 parasites/year.

Country (strain)	Village (N_{OP}; N_{nonOP})	ATP	Estimated parameters			Derived parameters	
			s	λ_{min}	λ_{max}	mean λ	P(L3→W)
Burkina Faso (savanna)	Kourougbele (132 ; 67)	-	0.0500	0.10	4.8	0.89	-
	Hemkoa (92 ; 14)	-	0.0450			0.78	-
	Yabar (96 ; 6)	-	0.0273			0.37	-
Liberia (forest)	Yeahmeah (43 ; 18)	440*	0.0043	0.16	19.1	0.40	0.00091
	Mauwa (139 ; 120)	~1000*§	0.0065			0.80	0.00080
	Meningee Woodee (93 ; 47)	2062*	0.0067			0.86	0.00042
	Sungbeta (34 ; 12)	3582*	0.0054			0.56	0.00016

Table 1: Parameter values. N_{OP} : number of patients who underwent nodule ectomy. N_{nonOP}: number of patients who did not undergo nodule ectomy. Dispersion parameter *k* of the negative binomial distribution equals 0.6. Establishment rates (ER) in units of live adult female parasites per year; λ_{min}: ER in the parasite-free state; λ_{max}: ER in the state of maximum infection; mean λ: mean ER in the villages, using an age distribution of a standard population. *s*: shape parameter of the density-dependent establishment function. P(L3→W): probability of an infective larva to develop into an adult female worm. * Values taken from Garms, 1983 (Table 4; Gaingema=Sungbeta, Mine Ninge=Meningee, §Mawua=Mauwa is published with ATP=437, which is probably underestimated, see Discussion).

Graphical representations of the density-dependent establishment functions are given in Fig. 3a for both strains. Whereas a saturation in the density-dependent parasite establishment is clearly visible for the savanna strain, the almost linear increase in the forest function indicates almost no density dependence in the forest strain. The age-related parasite establishment, which is calculated as the geometric mean of all density-dependent establishment

rates per age class, is shown in Fig. 3b. Whereas up to the age of 20 years the establishment rates of both strains increase similarly, the parasite establishment in hosts older than 20 years is considerably higher in the savanna. Thus, adults in the savanna acquire more parasites per year than do adults in forest villages.

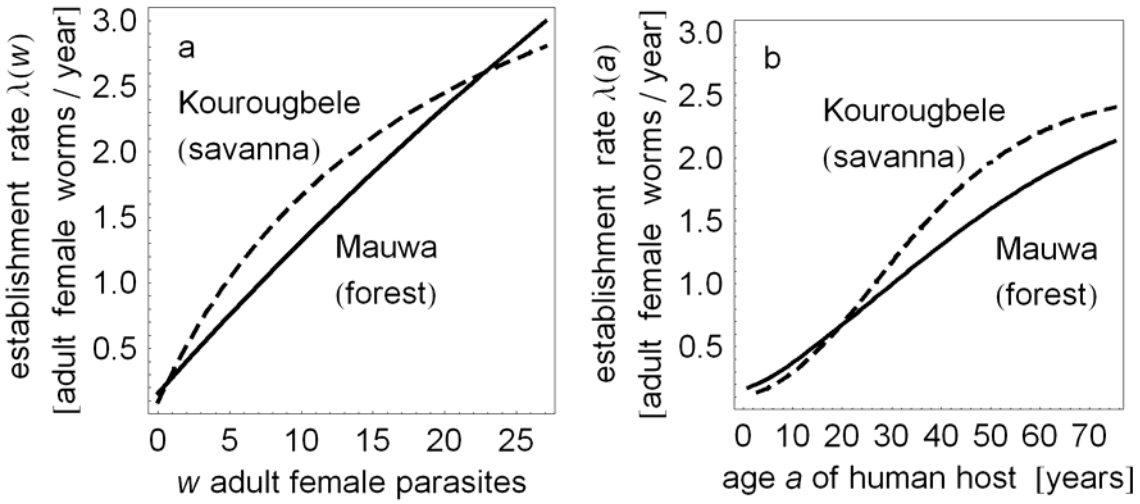

Figure 3. a: estimated density-dependent establishment rates $\lambda(w)$. b: derived age-related establishment rates $\lambda(a)$.

In forest villages for which transmission data are available, immunosuppression as measured by parameter ***s*** can be related to the annual transmission potential (ATP) (Table 1). The value of ***s*** seems to be nearly constant (***s*** $\approx$0.006) for high ATPs. A similar relationship holds for the average establishment rates (for details see statistical methods), which increase to a rate of mean $\lambda \approx 0.8$; however a unimodal relationship in the transmission-related parasite establishment may occur due to a decline at very high ATPs. Dividing mean λ by the ATP gives the theoretical proportion of L3, which develop into adult female parasites. The figures given in Table 1 (P(L3$\rightarrow$W)) indicate that this proportion decreases almost linearly with the ATP.

Fitting the high variability of parasite data is often achieved by means of the NBD, which is overdispersed. The value of the dispersion parameter k=0.6, as estimated by our stochastic simulations, indicates that a variance-increasing contribution is necessary to explain the variability. The presented model parametrisation is validated by several hierarchical models, with these being related to the best hypothesis (with a negative log-likelihood of -lnL=1324.6) by likelihood ratio tests. The alternative models, investigating whether village- or strain-specific parameters can be partly or totally merged to form a common

establishment functions, lead to significantly inferior fits. The tested hypotheses can be summarised as follows:

A: a common parameter λ_{min} for both strains yielding –lnL=1327.2 (p=0.018).
B: a common parameter λ_{max} for both strains yielding –lnL=1330.9 (p=0.0003).
C: common parameters λ_{min} and λ_{max} for both strains: –lnL=1333.3 (p=0.0001).
D: a common slope parameter *s* for all forest villages: –lnL=1332.2 (p=0.0004).
E: a common slope parameter *s* for all savanna villages: –lnL=1335.2 (p=0.0001).

After applying a Bonferroni-Holm correction for multiple testing, hypothesis *A* can no longer be considered as differing significantly from the best hypothesis (using a significance level of α=5%). The establishment of parasites during early childhood may therefore be similar in both subtypes of onchocerciasis. Neither a common slope parameter *s* for both strains nor an establishment function identical in all parameters for all villages yielded acceptable fits.

DISCUSSION

The present investigation shows by simulation-based mathematical modelling that the establishment of *O. volvulus* must depend on either age or parasite burden to explain the age-specific parasite burdens shown in our cross-sectional onchocerciasis data (Fig. 2a). This is in accordance with other modelling approaches which, for purposes of data fitting, assume density-dependent parasite establishment in the vector (Basanez & Boussinesq 1999) or age-dependent exposure of the host (Dietz 1982). Constant parasite establishment as implemented in a simple immigration-death process excessively overestimates parasite burdens in children and leads to an equilibrium occuring much too early in life. We show that the establishment rate of *O. volvulus* must increase with age, but suggest that the reason for this is density-dependent parasite establishment due to infection-associated immunosuppression.

Modifying parasite establishment

Of the three processes which can serve to modify parasite establishment (see Introduction), age-dependent exposure was first tried out to see if it fitted the data. For the savanna data, fits became acceptable by implementing a formerly suggested (Dietz 1982) sigmoid function given by $f(age)=1/(1+\exp(-0.55(age-10)))$ for savanna regions, starting at age zero with almost zero exposure and with 95% of exposure being achieved at the age of 15 years. The almost linearly increasing parasite burdens in forest onchocerciasis data, however, made it necessary to assume that age-dependent exposure in turn increased linearly with age, which seems inacceptable. With the exception of seasonal differences in transmission (see below), it can be assumed that the exposure of people living in both areas is similar. Thus, age-dependent exposure cannot serve solely as a source for modifying the parasite establishment.

Moreover, the assumption of a purely age-related decline in the host's defence mechanisms seems not suitable due to contrary experimental results for lymphatic filariasis: the suggestion that children acquire more parasites than adults, as assessed by levels of circulating filarial antigen (Day et al. 1991b), is contradicted by a recent transmigrant study, which used levels of specific IgG4 as an indirect marker for the parasite burden (Terhell et al. 2001). A modelling approach suggested an intermediate result: an unimodal age profile of the "rate of gain of infection", peaking in the 16-20 year age-class (Vanamail et al. 1989). These results demonstrate that the role of age-dependent parasite establishment needs further clarification, that indirect measurements for parasite burdens must be interpreted carefully and that considering the intensity of infection as a potential source of confounding must not be neglected.

Modifying parasite establishment by density-dependence appears to be necessary, especially when looking at the various approaches that have identified parasite-associated immunosuppression or tolerance as playing a major role in the parasite-host relationship (Maizels & Lawrence 1991). In lymphatic filariasis, lymphocyte proliferation could be suppressed *in vitro* by sera of microfilariae-positive patients (Piessens et al. 1980). Examining the effects of secretory/excretory products of different nematodes have on proliferation of T-cells from patients infected with lymphatic filariasis has led to the assumption that down-regulating the host's immune response might be a common feature among nematodes (Allen & MacDonald 1998). Identifying the parasite stages which act as a source of immunosuppression is difficult and multiple influences may exist. *In vitro* experiments showed the lymphocyte proliferative response to be inhibited either by live microfilariae or by secretory/excretory products of both adult female parasites and microfilariae (Elkhalifa et al. 1991). The incidence of ivermectin-facilitated immunity (reviewed in Schulz-Key et al. 1992) in human onchocerciasis argues for microfilariae contributing immunosuppressive substances. Since the adult parasite population is hardly affected by ivermectin, improved immunocompetence in treated individuals can be attributed to microfilariae (Soboslay et al. 1992; Soboslay et al. 1994). On the other hand, recent experiments in the mouse model of onchocerciasis underline the impact of adult parasites by showing that one adult female of *Litomosoides sigmodontis* is sufficient to make mice susceptible to microfilariae (Hoffmann et al. 2001).

Modelling density-dependent parasite establishment

In the present model, we attributed density-dependent parasite establishment to the parasite burden of adult live female *O. volvulus*. If we assume that the microfilarial load is proportional to the number of reproductive females, the impact of both parasite stages becomes indistinguishable. Our establishment function operates within the boundaries of the minimum establishment rate λ_{min}, representing the mean annual number of parasites acquired in the parasite-free state, and the maximum establishment rate λ_{max}, which is achieved by hosts with very high parasite burdens.

Modelling a parasite establishment as regulated by immunosuppressive influences may be described as in Fig. 4. An infectious larva (L3) which has successfully passed the host defence develops via the intermediate stage L4 into a reproductive parasite. The stimulus to establish a specific response is assumed to arise from those L3 which develop into adult worms (assuming that all incoming larvae stimulate a specific immune response poses the logical problem that continuous infection could not occur equally well for high and low ATPs - the immense boosting as provided by ATP values of several hundreds or thousands of L3 should lead either to a state of full protection or to a parasite establishment proportional to the ATP). Developing L3 induce an

immune response which prevents subsequent infections with L3 (concomitant immunity). This defence mechanism, however, is short-lived so that occasional infections during early childhood occur according to the minimum establishment rate λ_{min}. The slowly increasing parasite burden, however, is capable of suppressing these immune mechanisms in the host and consequently, the number of successfully developing L3 increases with an increasing parasite burden. This facilitated or self-enhancing infection process cannot grow indefinitely, as it is restricted in our model by the maximum establishment rate λ_{max}.

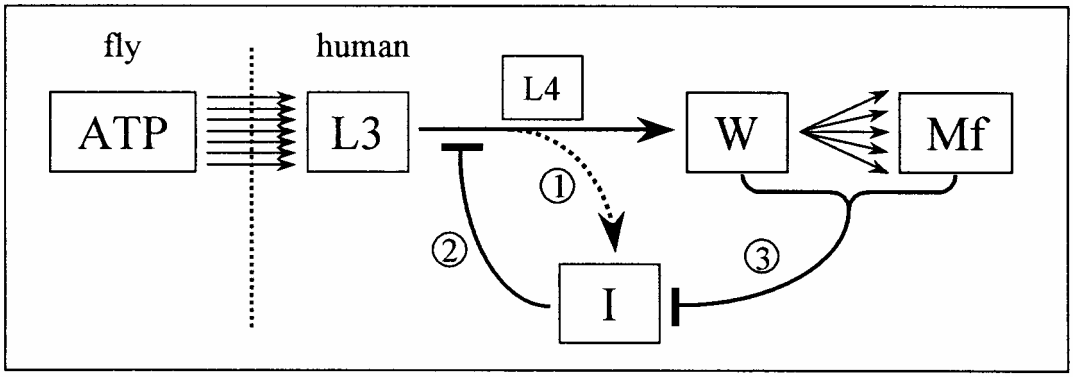

Figure 4: Model of density dependent parasite establishment in hyperendemic transmission. ATP: annual transmission potential. L3: infectious larva. L4: intermediate larval stage. W: adult female parasite. Mf: microfilariae. I: immunity with short-lived memory assumed. 1: specific immune stimulus by a developing L3. 2: concomitant immunity suppresses development of L3. 3: adult female worms and/or microfilariae suppress the capacity of the immunological response.

The host defence must be extremely efficient in its unsuppressed state: if we consider, for example, an ATP of 1000 L3/year and the minimum establishment rate of λ_{min}=0.1 adult parasites/year, then the proportion of successfully developing L3 is only 0.01%. Although the majority of L3 is neutralised by the host, those parasites which develop into adults can initiate immunosuppressive processes leading to facilitated parasite establishment during later years in life. Such a density-dependent decline in the immunological defence might be attributed to the cellular immune response, which seems to play a major role in immunity to filarial infections (reviewed in Ottesen 1995). It may also confirm the recent finding that cellular reactivity is vigorous during early stages of infection, becoming down-regulated in the progression into the chronic state (Cooper et al. 2001; Soboslay et al. 1991). The very low proportion of successfully developing L3 underlines the importance of concomitant immunity. This immune defence, however, is not necessarily antibody-mediated as was indicated by very low or absent antibody titres against *Wuchereria bancrofti* L3 in individuals under the age of 20 years (Day et al. 1991a). In this case, innate immunity, which has become of great interest in recent years

(Fearon & Locksley 1996), might act as a first-line defence mechanism. Simple model considerations estimated that a cumulative infection with approximately ten thousand L3 is necessary before antibodies against L3 can be detected (Day et al. 1991a).

Significant differences exist between the establishment functions of the savanna and forest strains (see Results, hypothesis C). The maximum establishment rate λ_{max} seems to be a major influence (hypothesis B), whereas the minimum establishment rate λ_{min} is probably identical for both strains (hypothesis A). It must be noted that λ_{min} affects the overall fit of the data and thus, is not only estimated from the data of weakly infected patients or children. The specific impact of the minimum establishment rate is, therefore, difficult to examine and differences between both strains should be assessed by the whole establishment function. In contrast to the establishment of parasites of the forest strain, which increases almost proportionally to relevant parasite burdens, establishment in the savanna is enhanced at low parasite burdens and becomes saturated when infections become severe (Fig. 3a). Enhanced parasite establishment in the savanna must be regarded in a cumulative way, as is apparent when looking at the derived, age-related establishment rate (Fig. 3b). Whereas the establishment rates of both strains increase to a comparable extent up to the age of 20 years, the establishment rate for adults living in the savanna continuously exceeds the establishment rate of adults living in the forest zone. Assuming similarity in age-related exposure and in age-related immunological changes between the host populations of both parasite strains, the differences in parasite establishment may be attributed to strain-specific immunogenicity, strain-specific immunosuppression, or to seasonal transmission in the savanna. Referring to the latter requires the assumption of a short-lived immunological memory in the host defence, which becomes lost during the transmission-free season and consequently leads to enhanced parasite establishment during the next period of infection. Such strain-specific considerations, which could also explain the enhanced pathology observed in savanna onchocerciasis (Duke 1990), strongly require experimental research focusing on immunological differences between both strains.

The question remains why children seem to be enormously competent in controlling their developing parasite burden. Summarising the previous paragraphs leads to the simple assumption that the parasite-free state is the one offering the best protection against parasite establishment. This point of view, however, is incomplete if the host defence mechanisms are only induced by infection. It is known that specific defence mechanisms also imply the loss of immunological resistance during intervention campaigns in which a specific immune stimulus in the host is missing (see below).

Density-dependence and control

Immunosuppression, which decreases along with reduction of the population's parasite burden, should influence the control of filarial infections positively. As in the case of ivermectin-facilitated immunity (see above) improved immunocompetence in the population should help to reduce reinfection in a self-enhancing manner. The Onchocerciasis Control Programme (OCP), which has been conducted in several West African countries since the mid-1970s, led to some observations being made that might be ascribed to control-associated immunocompetence. A re-activation of parasite-specific immune responses in patients under transmission control (Soboslay et al. 1997) may affect the residual parasites and could be one of factors behind the reduction of their reproductive activity (Karam et al. 1987). It could also explain the unexpectedly rapid decline in the community microfilarial load during control (Remme et al. 1990) as well as the sustained endemicity-free state in the post-control situation (Hougard et al. 2001).

Surprisingly, the mean establishment rate (mean λ in Table 1) is quite unrelated to ATPs higher than 400, indicating that parasite establishment is weakly affected by hyperendemic transmission. Unfortunately, we have no data from villages with a very low ATP; also the ATP value of 437 for the village Mauwa is probably underestimated, because the corresponding catching site was located near a small creek 4 kilometers from the village and not at St. Paul River which comes as close as 300 meters to Mauwa. Since in Sungbeta, which is also very close, a much higher ATP of 3582 was found, it can be assumed that most of the inhabitants of Mauwa were exposed to ATPs of one thousand or more. This may point at a proportionality between the mean establishment rate and the ATP in hypo- and mesoendemic transmission.

Transmission dynamics at very low ATPs depend on whether concomitant immunity is specific or unspecific. If we assume (as suggested in Fig. 4 by arrow 1) that developing L3 generate protective immunity against incoming L3, then hosts are fully susceptible when infection is completely eliminated. This control-induced loss of immunocompetence may be disadvantageous when infections are imported from non-controlled or incompletely controlled areas. If occasional infections are imported into controlled areas, the concept of parasite-induced immunosuppression raises this question: will *enhanced* immunocompetence (due to reduced parasite burdens) or *reduced* immunocompetence (due to missing booster infection) dominate the infection dynamics? The answer, however, is intuitively difficult to find so that further quantitative modelling should be undertaken for predicting the outcome of such antagonism. In cases where a specific mechanism is involved, cross-protection by the nearest relative of *O. volvulus*, the cattle parasite *O. ochengi*, may provide a natural source of booster immunisations (Wahl et al. 1998). Severe consequences from imported infections are not to be expected if the host is protected by unspecific immunity. Considering the outcome of these differing

assumptions shows that clarification of the origin of concomitant immunity strongly requires further immunological experiments and that future developments in OCP areas very much depend on the mode of concomitant immunity.

Methodical considerations

The establishment rate is estimated from the parasite burden of live adult female *O. volvulus* found by nodule ectomy. Since nodules located in deep tissue layers cannot be recognised in a nodule ectomy (Albiez 1983; Duke 1993), our values for the establishment rate underestimate the true rate. Nodule ectomy data are, however, our best source for investigating the parasite burden. Our results are further based on the assumption that parasite burdens found by nodule ectomy reliably represent a constant proportion of the true parasite burdens. Parasite establishment is not attributed to male worms, which have been shown not to provide immunosuppressive influences (Elkhalifa et al. 1991), nor is it to dead female worms, which we believe to play no role in this context.

There are significant differences within the villages of each country. In the present model, such village-specific characteristics are compensated by the parameter ***s*** in the establishment functions. Village-specific influences could also be compensated by the other parameters of the establishment function, i.e. λ_{min} and λ_{max}. At the current state of knowledge, however, it is not possible to decide which of these three parameters should preferably compensate for village- or ATP-specific influences, nor which one may provide the best biological interpretation. After comparing minimisation outcomes for these three possibilities, parameter ***s*** was chosen because it yielded the best likelihoods.

The strength of the present investigation lies in the determination of parasite establishment from data on parasite burdens by means of a flexible simulation approach. This approach permits us to consider both heterogeneity in the transmission and Weibull distributed survival of the parasites. No analytical approach to considering these two important features is known. The price of this flexibility is stochastic noise, inevitable when random numbers are used in the optimisation algorithm. Although such an approach (first described by Diggle & Gratton 1984) cannot claim to specify very precisely the parameter vector for the best estimate, we have raised accuracy to a high level - by simulating $3x10^5$ individuals during optimization, by simulating 10^8 individuals for purposes of comparing different hypotheses, and by confirming estimates through optimisation with differing initial values. A further feature of this approach is that it simulates the study outcome rather than theoretically models the underlying processes. Although adjusting the simulation to specific study characteristics (see Appendix) may demand some effort, our comparison of the adjusted and unadjusted fits in Fig. 2 illustrates the extent to which a

study bias can alter the model outcome. We hope that the approach will stimulate future developments in the field of adjusted estimation techniques.

APPENDIX

Adjustment of the simulations to the study design and data collection process: Female *O. volvulus* are surrounded by capsule-like host tissue, the onchocercoma or nodule, this being most frequently located in the subcutis and often palpable. The probability $P(k_e \mid w)$ that w worms form k_e nodules as found by nodule ectomy can be described by the beta binomial distribution

$$P(k_e \mid w) = \frac{1}{B(\alpha,\beta)} \binom{w-1}{k_e-1} B(k_e - 1 + \alpha, w - k_e + \beta) \quad (1)$$

with parameter vector (α, β) = (11.80, 19.80) and (6.35, 9.47) for savanna and forest, respectively (Duerr et al. 2001), where $B(\alpha,\beta)$ denotes the beta function.

The probability for palpating k_p out of k_e nodules is given by the binomial distribution

$$P(k_p \mid k_e) = \binom{k_e}{k_p} p^{k_p} (1-p)^{k_e - k_p} \quad (2)$$

of which the parameter was estimated by maximum likelihood as p=0.50 (95% CI 0.46-0.53) and 0.42 (95% CI 0.40-0.44) for savanna and forest respectively.

The probability of a patient undergoing nodule ectomy depended on age a and the number of palpated nodules k_p, this being determined during a pre-examination study conducted several months before nodule ectomy. The results of a second and decision-making palpation, which was performed right before nodule ectomy, were not recorded. The fact that a few additional nodules were found in the second palpation is seen in individuals included in nodule ectomy, although no nodules were found in the pre-examination. On the other hand, some patients with positive palpation did not undergo nodule ectomy due to, for example, a critical state of health. To account for a possible bias due to patient selection, we fitted the probability of patients undergoing nodule ectomy, given pre-palpation result k_p and age a, by logistic regression, yielding

$$\begin{aligned} P_a(\mathrm{OP}^+ \mid k_p) &= 1/(1+\exp(2.75 - 0.015\, a - 0.35\, k_p + 0.012\,(a-20.2)(k_p-2.4))) \\ P_a(\mathrm{OP}^+ \mid k_p) &= 1/(1+\exp(1.75 - 0.009\, a - 0.62\, k_p + 0.015\,(a-27.1)(k_p-2.1))) \end{aligned} \quad (3)$$

for savanna and forest respectively.

The probability of an individual of age a with worm burden w undergoing nodule ectomy can be derived from equations (1) to (3) by summing up the

probabilities of all possible combinations of excised and palpated nodules, which yield a worm burden *w*:

$$P_a(OP^+ \mid w_a) = \sum_{k_e=1}^{w_a} P(k_e \mid w_a) \sum_{k_p=0}^{k_e} P(k_p \mid k_e)\; P_a(OP^+ \mid k_p)\,. \qquad (4)$$

The probability of an individual of age ***a*** not undergoing nodule ectomy is then

$$P_a(OP^-) = 1 - \sum_{w=1}^{\infty} P_a(OP^+ \mid w)\,. \qquad (5)$$

To adjust the simulation result to the data collection design, a random number must be drawn after each simulation run, with the result of having *w* worms at age ***a*** being assigned either to a patient who undergoes surgery (at probability $P_a(OP^+ \mid w)$) or to a patient who does not undergo surgery (at probability $P_a(OP^-)$). To avoid unnecessary simulations, the probabilities are added directly to the age-specific distribution (instead of drawing a random number and adding either one or zero) and are normalised by the number of performed simulations.

Acknowledgement

The authors are grateful to P. Soboslay and W. H. Hoffmann for helpful discussions about the immunological context. R. Garms kindly provided ATP values for Liberia and S. Zehnder gave valuable technical support. This work was supported by the *f*ortüne grant no. 528 of the University Hospital, Tübingen, Germany and by a grant from the Deutsche Forschungsgemeinschaft, Graduiertenkolleg Lebensstile, soziale Differenzen und Gesundheitsförderung.

REFERENCES

Albiez, E. J. 1983 Studies on nodules and adult *Onchocerca volvulus* during a nodulectomy trial in hyperendemic villages in Liberia and Upper Volta. I. Palpable and impalpable onchocercomata. *Tropenmed Parasitol* **34**, 54-60.

Albiez, E. J., Büttner, D. W. & Schulz-Key, H. 1984 Studies on nodules and adult Onchocerca volvulus during a nodulectomy trial in hyperendemic villages in Liberia and Upper Volta. II. Comparison of the macrofilaria population in adult nodule carriers. Tropenmed Parasitol 35, 163-166.

Allen, J. E. & MacDonald, A. S. 1998 Profound suppression of cellular proliferation mediated by the secretions of nematodes. *Parasite Immunol* **20**, 241-247.

Basanez, M. G. & Boussinesq, M. 1999 Population biology of human onchocerciasis. Philos Trans R Soc Lond B Biol Sci 354, 809-826.

Cooper, P. J., Mancero, T., Espinel, M., Sandoval, C., Lovato, R., Guderian, R. H. & Nutman, T. B. 2001 Early human infection with Onchocerca volvulus is associated with an enhanced parasite-specific cellular immune response. J Infect Dis 183, 1662-1668.

Day, K. P., Gregory, W. F. & Maizels, R. M. 1991a Age-specific acquisition of immunity to infective larvae in a bancroftian filariasis endemic area of Papua New Guinea. Parasite Immunol 13, 277-290.

Day, K. P., Grenfell, B., Spark, R., Kazura, J. W. & Alpers, M. P. 1991b Age specific patterns of change in the dynamics of Wuchereria bancrofti infection in Papua New Guinea. Am J Trop Med Hyg 44, 518-527.

Devaney, E. & Osborne, J. 2000 The third-stage larva (L3) of Brugia: its role in immune modulation and protective immunity. Microbes Infect 2, 1363-1371.

Dietz, K. 1982 The population dynamics of onchocerciasis. In The population dynamics of infectious diseases: theory and applications (ed. R. M. Anderson), pp. 209-241. London, New York: Chapman and Hall.

Diggle, P. J. & Gratton, R. J. 1984 Monte Carlo methods of inference for implicit statistical methods. J R Stat Soc [Ser B] 46, 193-227.

Duerr, H. P., Dietz, K., Büttner, D. W. & Schulz-Key, H. 2001 A stochastic model for the aggregation of Onchocerca volvulus in nodules. Parasitology 123, 193-201.

Duke, B. O. 1990 Human onchocerciasis - an overview of the disease. Acta Leiden 59, 9-24.

Duke, B. O. 1993 The population dynamics of Onchocerca volvulus in the human host. Trop Med Parasitol 44, 61-68.

Elkhalifa, M. Y., Ghalib, H. W., Dafa'Alla, T. & Williams, J. F. 1991 Suppression of human lymphocyte responses to specific and non-specific stimuli in human onchocerciasis. Clin Exp Immunol 86, 433-439.

Fearon, D. T. & Locksley, R. M. 1996 The instructive role of innate immunity in the acquired immune response. Science 272, 50-53.

Garms, R. 1983 Studies of the transmission of Onchocerca volvulus by species of the Simulium damnosum complex occurring in Liberia. Angew Zool 70, 101-117.

Hoffmann, W. H., Pfaff, A. W., Schulz-Key, H. & Soboslay, P. T. 2001 Determinants for resistance and susceptibility to microfilaraemia in Litomosoides sigmodontis filariasis. Parasitology 122, 641-649.

Hougard, J. M., Alley, E. S., Yameogo, L., Dadzie, K. Y. & Boatin, B. A. 2001 Eliminating onchocerciasis after 14 years of vector control: a proved strategy. J Infect Dis 184, 497-503.

Karam, M., Schulz-Key, H. & Remme, J. 1987 Population dynamics of Onchocerca volvulus after 7 to 8 years of vector control in West Africa. Acta Trop 44, 445-457.

King, C. L. & Nutman, T. B. 1991 Regulation of the immune response in lymphatic filariasis and onchocerciasis. Immunol Today 12, A54-A58.

Maizels, R. M., Bundy, D. A., Selkirk, M. E., Smith, D. F. & Anderson, R. M. 1993 Immunological modulation and evasion by helminth parasites in human populations. Nature 365, 797-805.

Maizels, R. M. & Lawrence, R. A. 1991 Immunological tolerance: the key feature in human filariasis? Parasitol Today 7, 271-276.

Ottesen, E. A. 1995 Immune responsiveness and the pathogenesis of human onchocerciasis. J Infect Dis 171, 659-671.

Piessens, W. F., Ratiwayanto, S., Tuti, S., Palmieri, J. H., Piessens, P. W., Koiman, I. & Dennis, D. T. 1980 Antigen-specific suppressor cells and suppressor factors in human filariasis with Brugia malayi. N Engl J Med 302, 833-837.

Plaisier, A. P., van Oortmarssen, G. J., Remme, J. & Habbema, J. D. 1991 The reproductive lifespan of Onchocerca volvulus in West African savanna. Acta Trop 48, 271-284.

Press, W. H., Teukolsky, S. A., Vetterling, W. T. & Flannery, B. P. 1996 Numerical recipes in C. Cambridge: Cambridge University Press.

Remme, J., De Sole, G. & van Oortmarssen, G. J. 1990 The predicted and observed decline in onchocerciasis infection during 14 years of successful control of Simulium spp. in West Africa. Bull World Health Organ 68, 331-339.

Sartono, E., Kruize, Y. C., Kurniawan, A., Maizels, R. M. & Yazdanbakhsh, M. 1997 Depression of antigen-specific interleukin-5 and interferon-gamma responses in human lymphatic filariasis as a function of clinical status and age. J Infect Dis 175, 1276-1280.

Schulz-Key, H. & Albiez, E. J. 1977 Worm burden of Onchocerca volvulus in a hyperendemic village of the rain-forest in West Africa. Tropenmed Parasitol 28, 431-438.

Schulz-Key, H., Albiez, E. J. & Büttner, D. W. 1977 Isolation of living adult Onchocerca volvulus from nodules. Tropenmed Parasitol 28, 428-430.

Schulz-Key, H., Soboslay, P. T. & Hoffmann, W. H. 1992 Ivermectin-facilitated immunity. Parasitol Today 8, 152-153.

Soboslay, P. T., Dreweck, C. M., Hoffmann, W. H., Lüder, C. G., Heuschkel, C., Gorgen, H., Banla, M. & Schulz-Key, H. 1992 Ivermectin-facilitated immunity in onchocerciasis. Reversal of lymphocytopenia, cellular anergy and deficient cytokine production after single treatment. Clin Exp Immunol 89, 407-413.

Soboslay, P. T., Dreweck, C. M., Taylor, H. R., Brotman, B., Wenk, P. & Greene, B. M. 1991 Experimental onchocerciasis in chimpanzees. Cell-mediated immune

responses, and production and effects of IL-1 and IL-2 with Onchocerca volvulus infection. J Immunol 147, 346-353.

Soboslay, P. T., Geiger, S. M., Weiss, N., Banla, M., Lüder, C. G., Dreweck, C. M., Batchassi, E., Boatin, B. A., Stadler, A. & Schulz-Key, H. 1997 The diverse expression of immunity in humans at distinct states of Onchocerca volvulus infection. Immunology 90, 592-599.

Soboslay, P. T., Lüder, C. G., Hoffmann, W. H., Michaelis, I., Helling, G., Heuschkel, C., Dreweck, C. M., Blanke, C. H., Pritze, S., Banla, M. & Schulz-Key, H. 1994 Ivermectin-facilitated immunity in onchocerciasis; activation of parasite-specific Th1-type responses with subclinical Onchocerca volvulus infection. Clin Exp Immunol 96, 238-244.

Terhell, A. J., Haarbrink, M., Abadi, K., Syafruddin, Maizels, R. M., Yazdanbakhsh, M. & Sartono, E. 2001 Adults acquire filarial infection more rapidly than children: a study in Indonesian transmigrants. Parasitology 122, 633-640.

Urquhart, G. M. 1970 Immunological unresponsiveness in parasitic infections. J Parasitol 56, 547-551.

Vanamail, P., Subramanian, S., Das, P. K., Pani, S. P., Rajagopalan, P. K., Bundy, D. A. & Grenfell, B. T. 1989 Estimation of age-specific rates of acquisition and loss of Wuchereria bancrofti infection. Trans R Soc Trop Med Hyg 83, 689-693.

Wahl, G., Enyong, P., Ngosso, A., Schibel, J. M., Moyou, R., Tubbesing, H., Ekale, D. & Renz, A. 1998 Onchocerca ochengi: epidemiological evidence of cross-protection against Onchocerca volvulus in man. Parasitology 116, 349-362.

Weiss, N. & Karam, M. 1987 Humoral immune responses in human onchocerciasis: detection of serum antibodies in early infections. *Ciba Found Symp* **127**, 180-188.

Danksagung

Die vorliegende Doktorarbeit ist interdisziplinär zwischen Biologie und Mathematik entstanden und sie wäre ohne die Unterstützung aus beiden Fachbereichen nicht möglich geworden.

Mein größter Dank gilt daher meinen Doktorvätern und Betreuern. Prof. Dr. K. Dietz[1] (Institut für Medizinische Biometrie) hat das Projekt von Anfang an in die richtige Richtung geführt und sehr vorausschauend betreut. Prof. Dr. H. Schulz-Key[2] (Institut für Tropenmedizin) hat durch seine Arbeiten zur Onchozerkom-Analyse die wesentliche Voraussetzung für das Thema geschaffen und das Projekt angeregt. Dr. M. Eichner[3] war in allen Fragen ein überaus hilfreicher Ansprechpartner und geduldiger Betreuer. Alle drei haben mit Freude das Wachsen meiner Arbeit begleitet und ich danke ihnen für eine lehrreiche Zeit, die auch in persönlicher Hinsicht sehr bereichernd war.

Dr. H. H. Diebner[4] danke ich für die gemeinsame Zeit im Büro und Stefan Zehnder[5] für die Wiederbelebung unwilliger Computer. W. Hoffmann und PD Dr. P. Soboslay (beide Institut für Tropenmedizin) waren hilfreiche Diskussionspartner zur Immunologie der Onchozerkose. Meine Geschwister haben ermunternd nach dem Stand der Dinge gefragt, und meinen Eltern danke ich für die Unterstützung im Studium.

Prof. Dr. Dr. D. W. Büttner (Bernhard-Nocht-Institut Hamburg) danke ich für die Bereitstellung der Daten und für die wichtigen Informationen zu deren Erhebung. Prof. Dr. D. Ammermann (Zoologisches Institut, Abteilung für Zellbiologie) und Prof. Dr. K. - P. Hadeler (Lehrstuhl für Biomathematik) haben sich freundlicherweise für die Erstellung der Zweitgutachten bereiterklärt.

Prof. Dr. W. Schlicht und Prof. Dr. M. Diehl haben durch die Gründung bzw. Weiterführung des DFG-Graduiertenkollegs "Lebensstile, soziale Differenzen und Gesundheitsförderung" den finanziellen Rahmen für das Projekt geschaffen.

Allen danke ich herzlich.

Dieses Projekt wurde durch das *f*ortüne-Programm des Universitätsklinikums Tübingen und durch das o.g. DFG-Graduiertenkolleg gefördert.

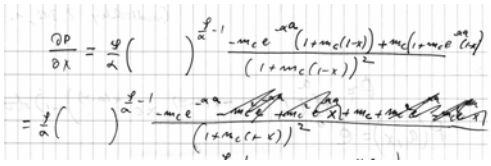

[1] "Das kann man ganz einfach hinschreiben: ....." ..."

[2] "Magst 'nen Schnaps?"

[3] "Was tun wir da eigentlich?"

[4] ...und die Sehnsucht nach einem Gabelstapler

[5] "...ja und dann könnte man da noch..."

Lebenslauf

geboren	am 20.06.1967 in Calw (Schwarzwald)
1983	Mittlere Reife
1983 - 85	Berufsausbildung als Biologisch-Technischer Assistent in Überlingen (Bodensee)
1985 - 87	Berufstätigkeit als BTA am Institut für Neurobiologie der Universität Heidelberg
1987 - 88	Zivildienst, Epilepsiezentrum Kehl-Kork, Kehl/Rhein
1988 - 90	Technische Oberschule Freiburg: Abitur
1990 - 92	Berufstätigkeit als BTA, Institut für Labormedizin, Dr. Salinger, Offenburg
1992 - 97	Universität Tübingen: Studium der Biologie Diplomarbeit: "Charakterisierung von *Drosophila*-cDNAs, die *Exuperantia*-interagierende Proteine kodieren", MPI für Entwicklungsbiologie, Tübingen
1997 - 98	Institut für Medizinische Biometrie, Tübingen: Wissenschaftliche Hilfskraft, Mitarbeit an Malaria-Projekt
Nov. 1998 bis März 2002	Promotion an der Eberhard-Karls-Universität in Tübingen Institut für Medizinische Biometrie, Institut für Tropenmedizin Stipendiat des Graduiertenkollegs Lebensstile, soziale Differenzen und Gesundheitsförderung

Im Selbstverlag herausgegeben von:

Hans-Peter Dürr
Sindelfingerstr. 41
72070 Tübingen, Germany